1.1.1 Heterocyclic compounds

A heterocyclic compound is one which possesses a cyclic structure with at least one different kind of an atom in the ring. Nitrogen, oxygen and sulfur are considered the most hetero atoms known [1,2]. If at least one ring atom is a C-atom, then the molecule is an organic heterocyclic compound. In this case, all the ring atoms which are not carbon are called heteroatoms, e.g.:

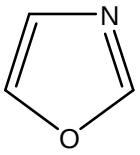

Oxazole

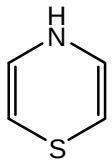

4 - *H* -1,4 - thiazine

In principle, all elements except the alkali metals can act as ring hetero atoms. Along with the type of ring atoms, their total number is important since this determines the ring size. The smallest possible ring is three-membered. The most important rings are the five- and six membered heterocycles. There is no upper limit; there exist seven-, eight-, nine- and larger-membered heterocycles [3].

Heterocyclic compounds are considered one of important types of organic compounds due to their applications in drug and industrial studies for monocyclic rings, the proper nomenclature is derived from combining an appropriate prefix and suffix to a given stem, where the suffix (-ole) and (-ine) are given for unsaturated five and six membered rings containing nitrogen atom[4].

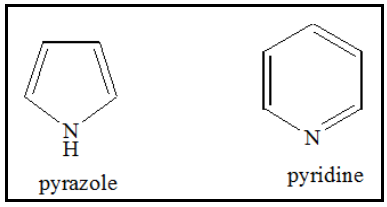

1.1.2 Heteroaromatic systems

This includes heteroannulenes, which comply with the HÜCKEL rule, i.e. which possess *(4n* + 2) π-electrons delocalized over the ring. The most important group of these compounds derives from [6] annulene (benzene). They are known as heteroarenes, e.g. furan, thiophene, pyrrole, pyridine, and pyrylium and thiinium ions. As regards stability and reactivity, they can be compared to the corresponding benzenoid compounds [(5)]. The anti-aromatic systems, i.e. systems possessing 4n delocalized electrons, e.g. oxepin, azepine, thiepin, azocine, and 1,3-diazocine, as well as the corresponding annulenes , are, by contrast, much less stable and very reactive.

The classification of heterocycles as heterocycloalkanes, heterocycloalkenes, heteroannulenes and heteroaromatics allows an estimation of their stability and reactivity. In some cases, this can also be applied to inorganic heterocycles. For instance, borazine, a colorless liquid, is classified as a heteroaromatic system.

1.2 Hydrazide derivatives

Hydrazide and thiosemicarbazide derivatives attracted a lot of attention because they are considered as intermediates to synthesize several compounds such as Schiff bases, thiadiazole [(6)], oxadiazole [(7)] and triazole [(8)] derivatives which all were reported to possess different

interesting applications. The structural formula for this type of compounds is (RCONHNH-).

Thiosemicarbazides are easily cyclized by the action of acids, bases or oxidants; therefore they are useful versatile building blocks for the preparation of heterocyclic ring systems. Some time ago, chemist investigated the reactions of thiosemicarbazides with π-deficient compounds. As a result, they synthesized many heterocyclic ring systems such as thiazoles, thiazines, thiadiazoles, thiadiazines, pyrazines and indazoles [9,10].

1.2.1 Hydrazide derivatives uses

Hydrazides and derivatives have been described as useful building blocks for the assembly of various heterocyclic compounds. A large number of aliphatic, alicyclic, aromatic and heterocyclic carbohydrazides, their derivatives and related compounds are reported to have a plethora of biological activities [11]. Mycobacterium tuberculosis infects over one-third of world's population and causes almost three million deaths every year. Isonicotinic acid hydrazide (isoniazid) is one of the primary drugs used in the treatment of tuberculosis [12]. Thus, different carbohydrazides were found to be useful as medicaments especially in the treatment of inflammatory and autoimmune disease, osteoarthritis, respiratory diseases, tumors, cachexia, cardiovascular diseases, fever, hemorrhage and sepsis [13].

Some hydrazinecarbothioamide derivatives are useful as corrosion inhibitors for mild steel in H_2SO_4 [14]. Other hydrazinecarbothioamides of fatty acid hydrazides from nontraditional oils have been synthesized and

evaluated as corrosion inhibitors for mild steel in hydrochloric acid (HCl) solution [15].

1.3 Thiadiazoles

Thiadiazole is five-membered diunsaturated ring composed of two nitrogen atoms and one sulfur atom. There are four isomeric types: 1,2,3-thiadiazole (I); 1,3,4-thiadiazole (II); 1,2,4-thiadiazole (III) and 1,2,5-thiadiazole (IV).

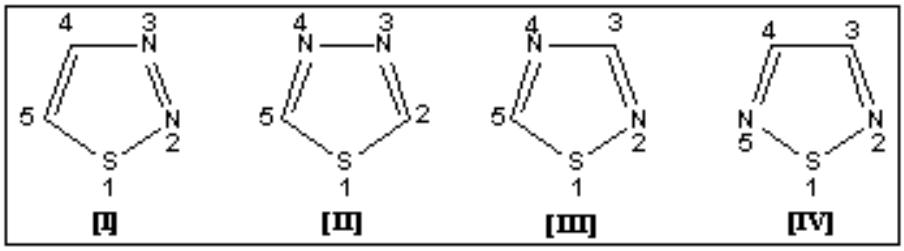

A glance at the standard references show that more studies have been carried out on the 1,3,4-thiadiazoles. Members of this ring system have found their ways into such diverse applications as pharmaceutical, oxidation inhibitors, cyanine dyes and metal complexing agents [16].

1.3.1 Synthesis of 1,3,4-thiadiazoles and their derivatives

1,3,4 - Thiadiazoles are available by a number of convenient general routes including cyclization of *N,N ′* -diacyl - hydrazines, or 1,3,4 - oxadiazoles, with phosphorus sulfides[17]. 2 - Amino - 1,3,4 - thiadiazoles are prepared via acylation of thiosemicarbazides [18] and the parent compound is easily obtained from hydrogen sulfide and dimethylformamide azine [19].

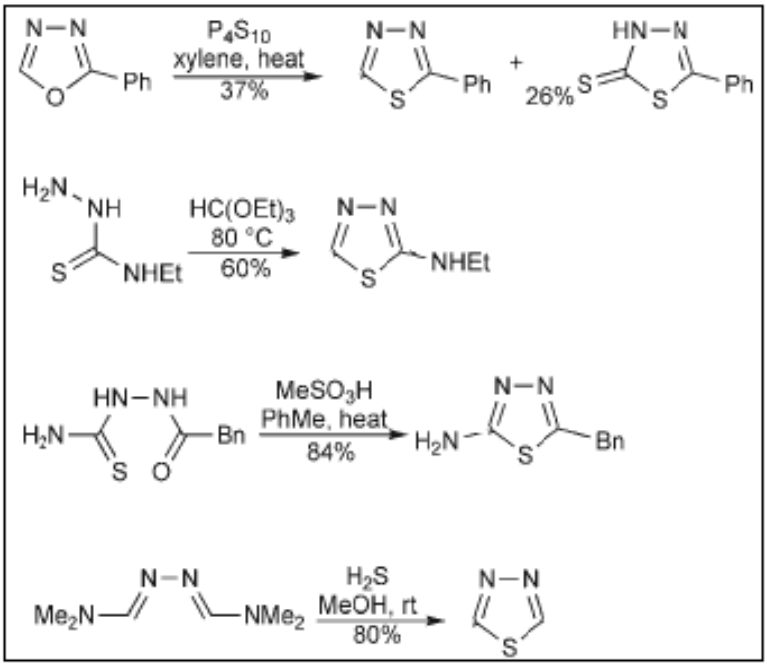

N. Demirbas [20] synthesized derivatives of 1,3,4-thiadiazole from the reaction of (4-amino-3-substituted-5-oxo-4,5-dihydro-1H-1,2,4-triazol-1-yl) acetic acid hydrazide with phenyl isothiocyanate and the resulting thiosemicarbazide derivatives were cyclized using sulfuric acid.

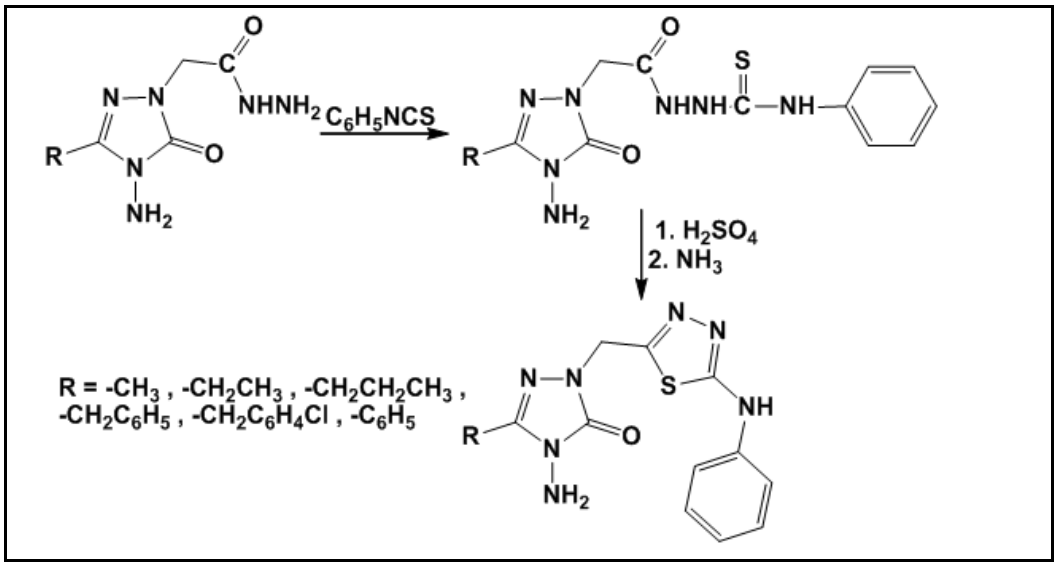

N. Demirbas [21] also synthesized derivatives of 2-amino-1,3,4-thiadiazole from the reaction of (4-amino-3-substituted-5-oxo-4,5-dihydro-1H-1,2,4-triazole-1-yl) acetic acid with thiosemicarbazide in phosphorus oxychloride to give 1,3,4-thiadiazole ring.

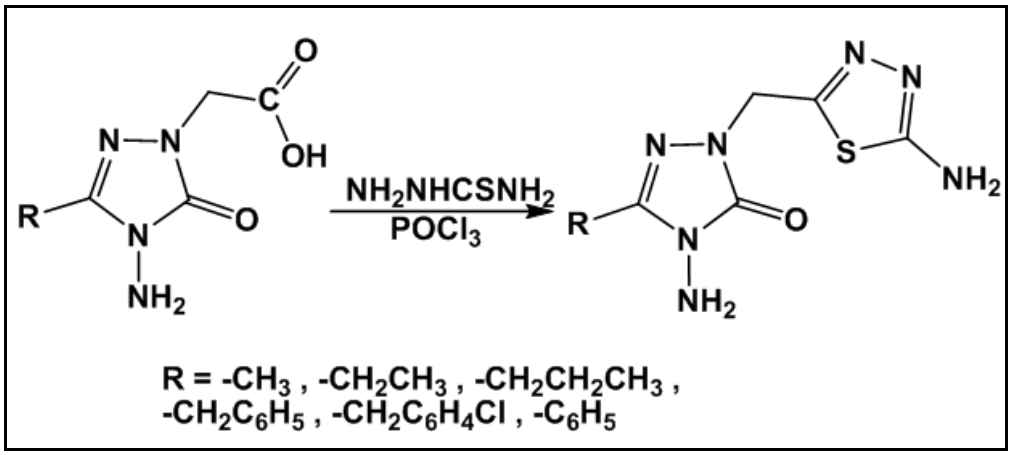

Aly and El-Sayed [22] have synthesized 2-amino-5-(3-chlorobenzo [b]thiophen-2-yl)-1,3,4-thiadiazole through condensation of 3-chlorobenzo[b]thiophene-2-carboxylic acid with thiosemicarbazide by using phosphorous oxychloride as condensing agent:

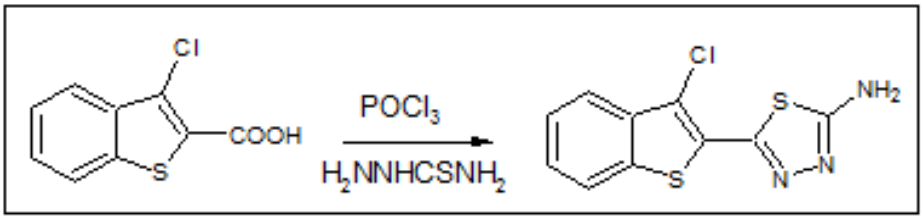

Petrow and coworkers [23] found that 5-amino-1,3,4-thiadiazole-2-thiol is formed with excellent yield when thiosemicarbazide is heated with carbon disulfide and equivalent potassium hydroxide in ethanol .

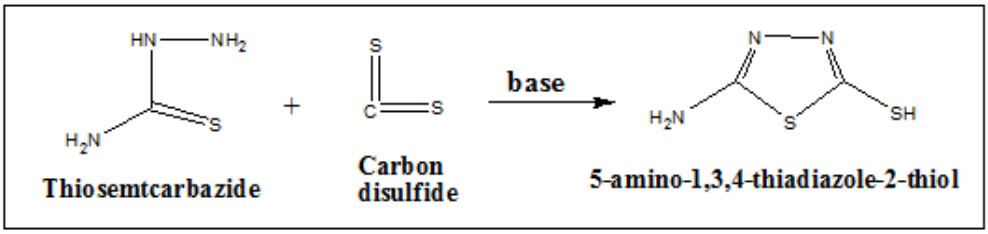

1.4 Schiff bases (SB)

The term Schiff base (SB) is used to define those organic compounds which contain the functional imine group (-C=N-) and can be designated structurally as(R''R'C=NR). The nature of group is limited to alkyl or aryl substituents or hydrogen at the point of attachment to the imino (C=N) carbon or nitrogen. The Schiff bases (SB) were first prepared by (Schiff) in 1864 [24,25] from the condensation reaction of aldehyde or ketones with primary amines by refluxing the mixture in absolute ethanol, benzene, or any other suitable solvent for one hour or few hours some times, the reaction may be catalyzed by acid[26,27]. The addition of proton to the carbonyl group yields the conjugated acid in which the carbon of the carbonyl group is more electrophilic, thus facilitating the attack of the amine on the carbonyl group. The added acid will enhance elimination of water molecule to give the final product (SB).

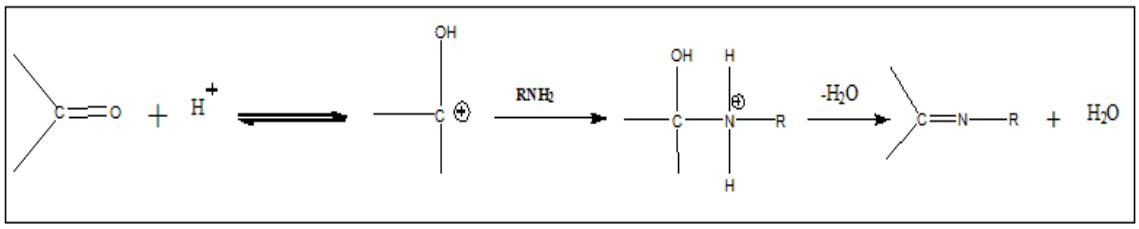

These bases can also be prepared by refluxing of equimolar quantities of aldehyde or ketone with primary amine without solvent or by slow melting for 10 minutes and then isolating and purifying the product by recrystallization or sublimation under reduced pressure [28].

Staab and coworker [29] prepared Schiff bases derivatives by removing water which is formed by condensation of aldehyde with the amine by reflux in benzene, this done by mixing the amine and the aldehyde in benzene and then the residual solution is distilled under vacuum.

A large number of Schiff bases and their complexes have been studied for some interesting and important properties. IR spectra show that 2-furancarboxaldehyde and o-phenylenediamine ligand is coordinated to the metal ions (Fe(III), UO_2(II), Co(II), Ni(II), Cu(II), Zn(II))in a tetradentate manner, with ONNO donor sites of azomethine–N and furan-O, whereas the 2-thiophenecarboxaldehyde and 2-aminothiophenol ligand is coordinated to the metal ions in a terdentate manner with SNS donor sites of azomethine–N, thiophene-S, and thiol-S[30].

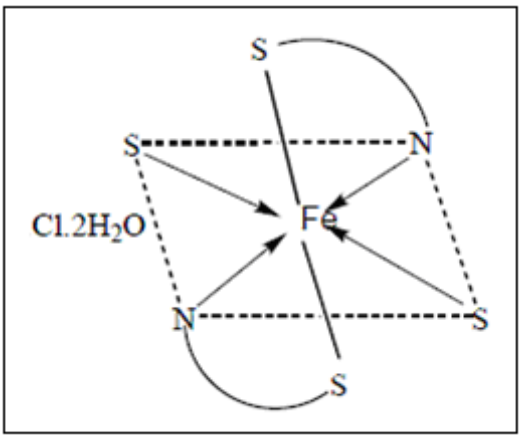

Terdentate manner

Transition metal complexes of Co(II),Ni(II),Cu(II) and Zn(II) with the tetradentate ligands [1,2-bis-(benzimidazole-2-thio) ethane, 1,3-bis-(benzimidazole-2-thio) propane, 4-bis-(benzimidazole-2-thio)butane] were behaved as bi dentate with N,N or S,S or S,S,N,N donor [31].

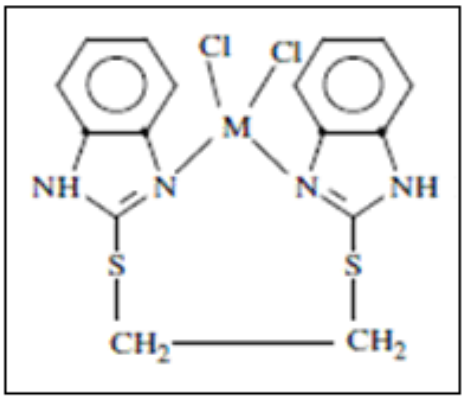

Complex of [1,2-bis-(benzimidazole-2-thio] ethane

The Schiff bases namely MIMFMA, MIMTMA and MIPMA have been prepared by reacting 3-amino-5-methyl isoxazole with 5-methyl furan-2-carboxyaldehyde, 5-methyl thiphene-2-carboxaldehyde and pyridine-2-carboxaldehyde act as neutral and bidentate and coordinate with ions [Cu(II), Ni(II), Co(II), Zn(II) and VO(IV)] through the azomethine nitrogen and furfural oxygen, thiophene sulphur and pyridine nitrogen, respectively[32].

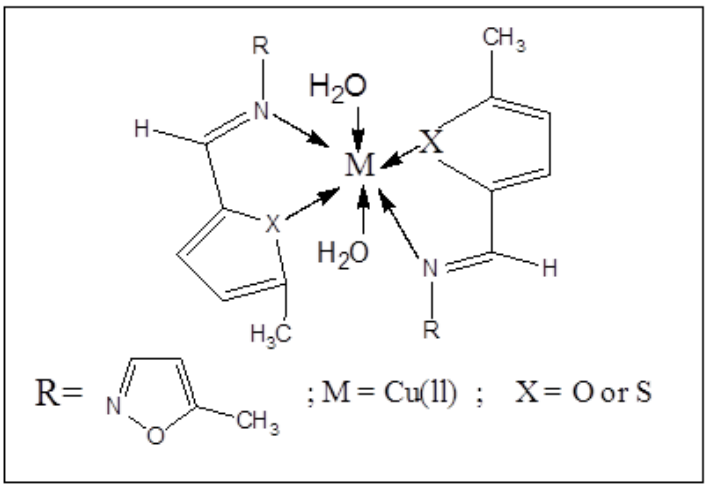

Proposed structures of Cu (II) complexes

1.5 The basic facts about sulfur and its compounds

Sulfur is a p-block element in group VI immediately below oxygen and between phosphorus and chlorine. It is natural for us to compare sulfur with oxygen but we will, strangely, compare it with carbon as well. Sulfur is much less electronegative than oxygen; in fact, it has the same electronegativity as carbon, so it is no good trying to use the polarization of the C–S bond to explain anything!

It forms reasonably strong bonds to carbon—strong enough for the compounds to be stable but weak enough for selective cleavage in the presence of the much stronger C–O bonds.

Sulfur In the periodic table (electronegativity)			
C (2.5)	N (3.0)	O (3.5)	F (4.0)
Si (1.8)	P (2.1)	S (2.5)	Cl (3.0)

Bond strength, KJ/mol				
	X = C	X = H	X = F	X = S
C–X	376	418	452	362
S–X	362	349	384	301

It also forms strong bonds to itself. Sulfur has d orbitals so it can have oxidation states of 2, 4, or 6 and coordination numbers from 0 to 7. Sulfur is a very versatile element: As well as this variety of oxidation states, sulfur shows a sometimes surprising versatility in function. Simple S(II) compounds are good nucleophiles as you would expect from the high-energy nonbonding lone pairs [33]. The greater reactivity of nucleophiles with large nucleophilic atoms is not entirely related to solvation. Larger atoms have greater polarizability (their electron clouds are more easily distorted); therefore, a larger nucleophilic atom can donate a greater degree of electron density to the substrate than a smaller nucleophile whose electrons are more tightly held [34]. Sulfides are easily synthesized by the Williamson ether synthesis, using a thiolate ion as the nucleophile [35].

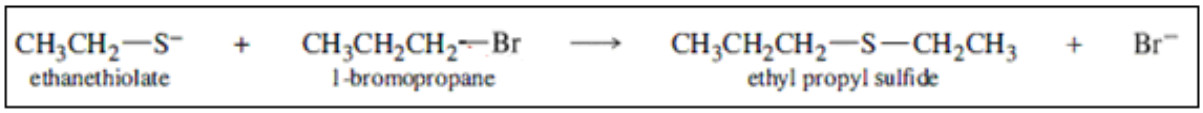

Thiols are more acidic than water. Therefore, thiolate ions are easily generated by treating thiols with aqueous sodium hydroxide.

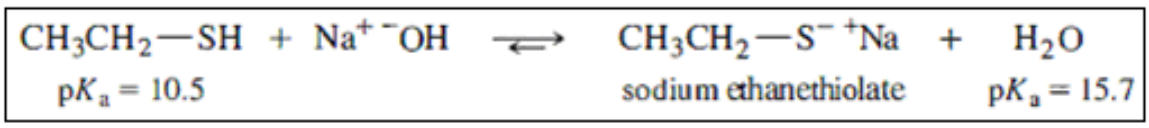

A mixture of a thiol (RSH) and NaOH reacts with an alkyl halide to give the sulfide alone by nucleophilic attack of RS^- [33].

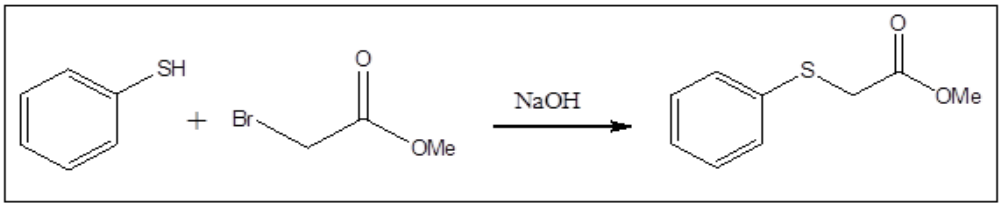

The first step is a rapid proton exchange between the thiol and hydroxide ion. The thiolate anion then carries out a very efficient S_N2 displacement on the alkyl bromide to give the sulfide.

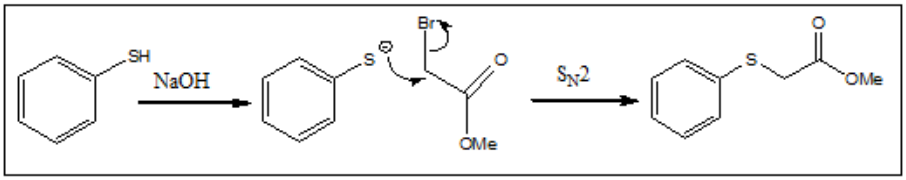

Notice that the thiolate anion does not attack the carbonyl group. Small basic oxyanions have high charge density and low-energy filled orbitals—they are hard nucleophiles that prefer to attack protons and carbonyl groups. Large, less basic thiolate anions have high-energy filled orbitals and are soft nucleophiles. They prefer to attack saturated carbon atoms. Thiols and thiolates are good soft nucleophiles [33].

1.6 Corrosion of metals [36]

Corrosion is the destructive attack of a metal by chemical or electrochemical reaction with its environment. Deterioration by physical causes is not called corrosion, but is described as erosion, galling, or wear. In some instances, chemical attack accompanies physical deterioration, as described by the following terms: corrosion-erosion, corrosive wear, or fretting corrosion. Nonmetals are not included in this definition of corrosion. Plastics may swell or crack, wood may split or

decay, granite may erode, and Portland cement may leach away, but the term corrosion, is restricted to chemical attack of metals. “Rusting” applies to the corrosion of iron or iron - base alloys with formation of corrosion products consisting largely of hydrous ferric oxides. Nonferrous metals, therefore, corrode, but do not rust. The three main reasons for the importance of corrosion are: economics, safety, and conservation.

1.6.1 Types of corrosion

Corrosion process has mainly (more or less implicitly) assumed that [36]:

1) Electrochemical corrosion is the only deterioration mechanism.

2) Anodic and cathodic reactions take place all over the electrode surface.

3) There are no significant macroscopic concentration differences in the electrolyte along the metal surface, and the metal is fairly homogeneous.

These three assumptions lead to uniform (general) corrosion. But this is only one of several corrosion forms that occur under different conditions. The other forms of corrosion depend on the deviations from the mentioned assumptions. Such deviations may be due to [37]:

a) Design (the macro–geometry of the metal surfaces).

b) Combination of metal and environment.

c) State of the surface (particularly cleanliness and roughness).

d) Other deterioration mechanisms.

On this basis, the following corrosion forms can be defined [38]:

- Uniform (general) corrosion
- Galvanic (two–metal) corrosion
- Thermo galvanic corrosion

- Crevice corrosion (including deposit corrosion)
- Pitting, pitting corrosion
- Selective attack, selective leaching (de–alloying)
- Intergranular corrosion (including exfoliation)
- Erosion corrosion
- Cavitation corrosion
- Fretting corrosion
- Corrosion fatigue

A simple illustration of the various forms of corrosion is shown in Figure 1-1.

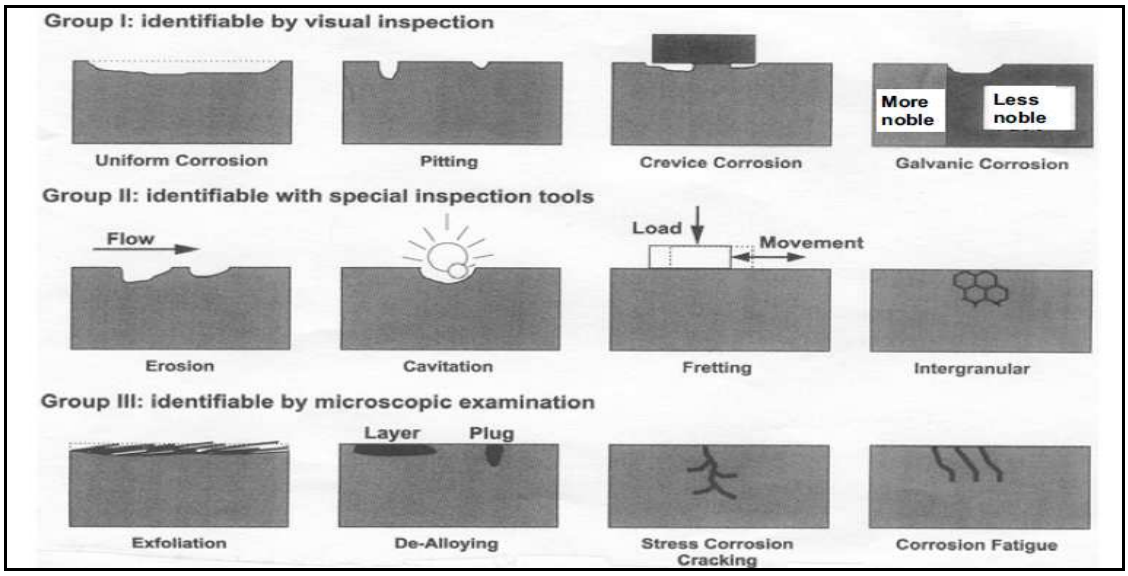

Figure 1-1. Main forms of corrosion grouped by their ease of recognition [39].

1.6.2 Uniform (General) Corrosion [40]

By definition, attacks of this type are quite evenly distributed over the surface, and consequently it leads to a relatively uniform thickness reduction (Figure 1-2). The necessary conditions for uniform corrosion

have already been presented. Homogeneous materials without a significant passivation tendency in the actual environment are liable to this form of corrosion.

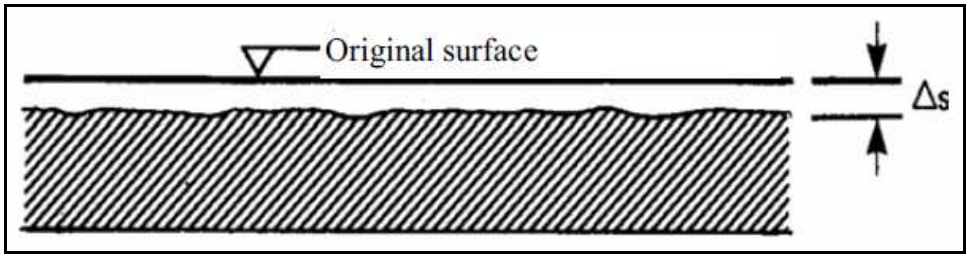

Figure 1-2. Uniform (general) corrosion.

Uniform corrosion is assumed to be the most common form of corrosion and particularly responsible for most of the material loss. Traditionally, however, it is not recognized as a dangerous form of corrosion, because:

1. Prediction of thickness reduction rate can be done by means of simple tests. Corresponding corrosion allowance can be added, taking into account strength requirements and lifetime.
2. Available protection methods are usually so efficient that the corrosion rate is reduced to an acceptable level. Actual methods are application of coatings, cathodic protection or possibly change of environment or material.

1.6.3 Corrosion cell of rusting of iron [41]

Consider the rusting that occurs when a drop of water is in contact with iron. The edge of the water drop exposed to the air becomes one pole of a voltaic cell (see Figure 1-3). At this edge, molecular oxygen from air is reduced to hydroxide ion in solution.

$$O_2(g) + 2H_2O(l) + 4e^- \longrightarrow 4OH^-(aq) \qquad \text{(cathode)}$$

The electrons for this reduction are supplied by the oxidation of metallic iron at the center of the drop, which acts as the other pole of the voltaic cell.

$$Fe(s) \longrightarrow Fe^{2+}(aq) + 2e^- \qquad \text{(anode)}$$

These electrons flow from the center of the drop through the metallic iron to the edge of the drop. The metallic iron functions as the external circuit between the cell poles. Ions move within the water drop, completing the electric circuit. Iron (II) ions move outward from the center of the drop, and hydroxide ions move inward from the edge. The two ions meet in a doughnut-shaped region, where they react to precipitate iron(II) hydroxide.

$$Fe^{2+}(aq) + 2OH^-(aq) \longrightarrow Fe(OH)_2(s)$$

This precipitate is quickly oxidized by oxygen to rust (approximated by the formula $Fe_2O_3.H_2O$).

$$4Fe(OH)_2(s) + O_2(g) \longrightarrow 2Fe_2O_3 \cdot H_2O(s) + 2H_2O(l)$$

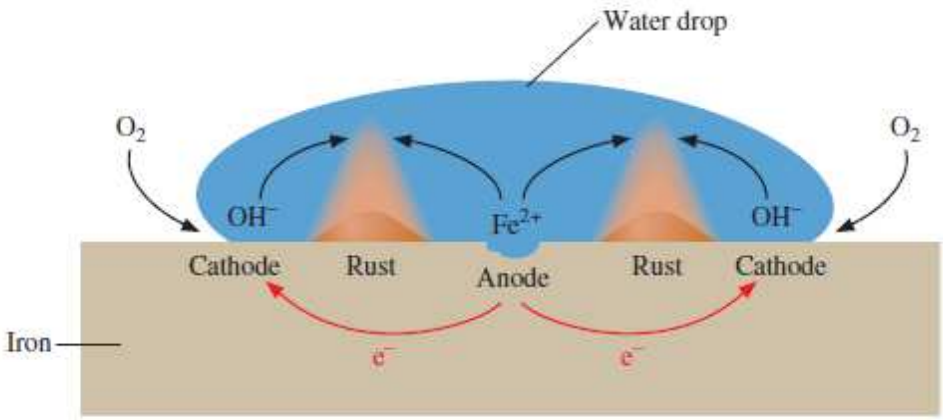

Figure 1-3. The electrochemical process involved in the rusting of iron.

1.6.4 Corrosion protection [42]

Electrochemical and non-electrochemical ways to protect metals against corrosion can be distinguished. The non-electrochemical ways include dense protective films that isolate the metal against effects of the medium and may be paint, polymer, bitumen, enamel, and the like. It is a general shortcoming of these coatings that when they are damaged mechanically, they lose their protective action, and local corrosion activity arises. The polarization characteristic (cathodically, anodically) of a corroding metal can be controlled by various additives to the solution, called corrosion inhibitors, which adsorb on the metal and lower the rates of the cathodic and/or anodic reaction. Inhibitors are used primarily for acidic electrolyte solutions, sometimes also for neutral solutions. Various organic compounds with –OH, –SH, $–NH_2$, –COOH, and so on, as the functional groups are used as inhibitors and act to retard the cathodic and/or anodic electrochemical corrosion processes.

1.6.5 Organic inhibitors

Organic compounds could be used as corrosion inhibitors to reduce the metallic dissolution are an attractive research field. The mineral acids are generally used for pickling in various industrial processes. The organic compounds which contain heteroatoms such as N, O, S, and π electrons are most effective corrosion inhibitors. They are adsorbed on the metal surface by replacing water molecules from that surface. Their adsorption depends upon electron density at the donor atom, functional group, π bond character and electronic structure [43-48].

Some common plants and plant products have been tried as corrosion inhibitors for metals and alloys under different environment. These plants become an important source of a wide range of eco-friendly (green) corrosion inhibitors [49,50]. Chaieb *et al.* [51] investigated the effect of eugenol and its derivative (acetyleugenol) extracted from the nail of giroflier (*Eugenia caryophyllata*) on the corrosion inhibition of steel in 1 M HCl solution.

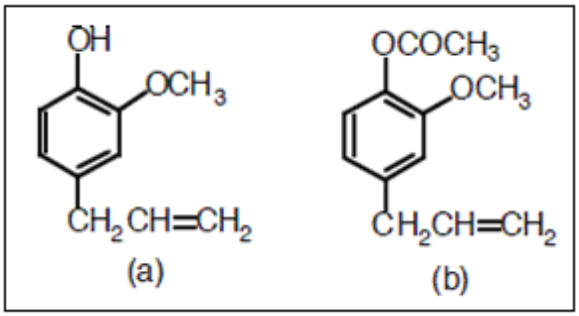

Molecular structures of chemicals extracted from *Eugenia caryophyllata*: (a) Eugenol and (b) Acetyleugenol.

Schiff bases have been investigated for the inhibition of acid corrosion of mild steel [52,53], aluminium [54] and copper[55], and for the neutral halide corrosion of copper [56-58].

The effect of Schiff base compounds, namely, (3Z,3'Z)-3,3'-(ethane-1,2-diylbis(azan-1-yl-1-ylidene))diindolin-2-one (a), (3Z,3'Z)-3,3'-(butane-1,4-diylbis(azan-1-yl-1-ylidene))diindolin-2-one (b) and thiocarbohydrazide bis-isatin (c) were investigated by gravimetric, potentiodynamic polarization as corrosion inhibitor of mild steel in acidic solution [59].

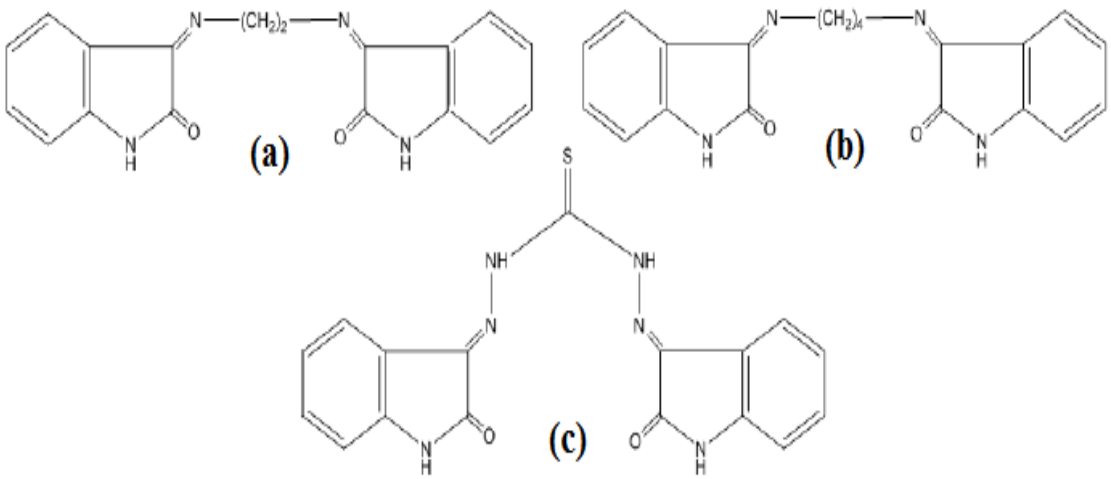

Structure of all the three Schiff's bases:
(a), (b) and (c).

A new class of corrosion inhibitors namely dianiline Schiff bases was synthesized and its inhibiting action on the corrosion of mild steel in 1M sulphuric acid at 30^{o}C was investigated by various corrosion monitoring techniques [60].

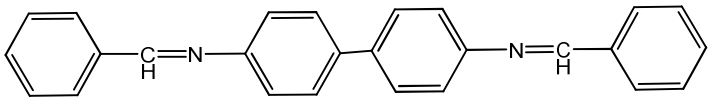

N,*N*'-dibenzylidenebiphenyl-4,4'-diamine

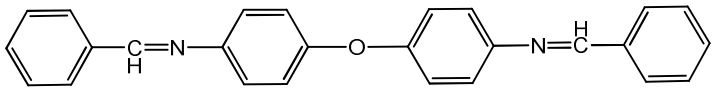

4,4'-oxybis(*N*-benzylideneaniline)

Inhibition effect of 3-pyridinecarboxaldehyde thiosemicarbazone (META) on the mild steel corrosion in 1M hydrochloric acid was investigated using weight loss, potentiodynamic polarization and electrochemical impedance spectroscopy [61].

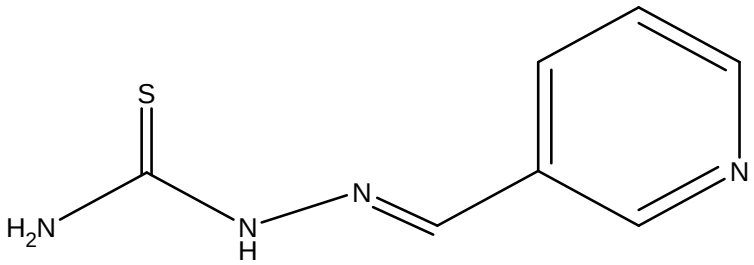

3-pyridinecarboxaldehyde thiosemicarbazone

2-amino-1, 3, 4-thiadiazoles (AT), 2-amino-5-methyl-1, 3, 4-thiadiazoles (AMT), 2-amino-5-ethyl -1, 3, 4-thiadiazoles (AET) and 2-amino-5-propyl -1, 3, 4-thiadiazoles (APT) were synthesized as inhibitors for mild steel in 20% formic acid and 20% acetic acid by weight loss, potentiodynamic polarization and electrochemical impedance techniques [62].

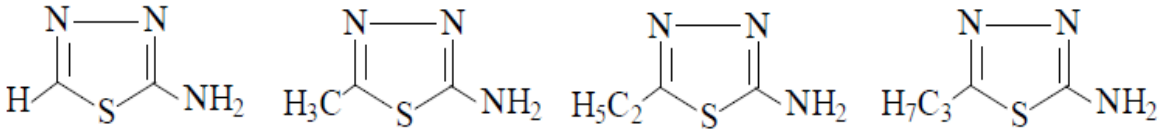

AT AMT AET APT

1.6.6 Adsorption from Solution:

Generally adsorption could be defined as a phenomenon of a material aggregation as ions or molecules or atoms on a surface of another material [63]. Naturally the physical states of the matter which contain limit surfaces are in solid or in liquid state. Hence the adsorption phenomenon would be solid-liquid, solid-gas, liquid-liquid, liquid-gas and solid-solid [64]. The adsorption process in solution, include attach surface between liquid-phase and solid-phase.

The reason for adsorption phenomenon is the existence of some unsaturated forces on the adsorbent due to the incomplete coordination or

insufficient material-surface particles, like the liquid or solid phase adsorption which leads to saturate those forces on surface as well. This may cause a decrement in energy (free energy) of the surface. Hence, the adsorption is spontaneous process, with decreasing the degrees of freedom for the adsorbate.

The adsorption could be divided into, physisorption (characteristic of weak van der Waals forces), and chemisorptions (characteristic of covalent bonding), It may also occur due to electrostatic attraction [(65)]. The major differences between them are in the field of interaction forces between the adsorbate particle the adsorbent surface and in the energy evolved from both processes. The energy evolved in chemisorptions is greater than that in physisorption. In addition, the chemisorptions are a uni-molecular adsorption, it occurs on single layer, while physisorption often occurs on multi-layer adsorption.

An example to show the mechanism of cardanol (green inhibitor) adsorption to involve electrostatic attraction between the positively charged metal surface and negatively charged phenoxide ions as schematically shown in Figure 1-4 [(66)].

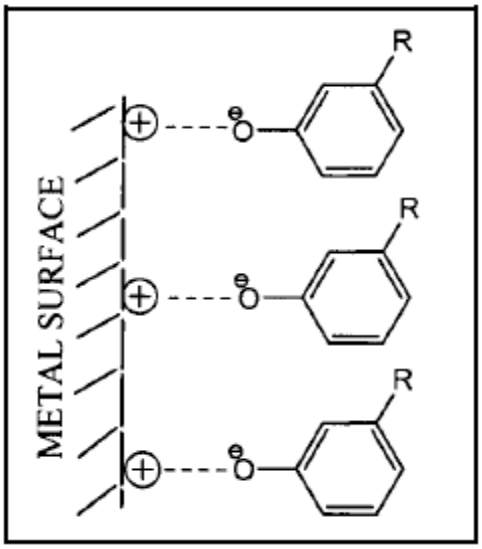

Figure 1-4. The schematic diagram for the cardanol adsorption mechanism on carbon steel Surface.

1.7 Computational chemistry

Computational chemistry is the application of chemical, mathematical and computing skills to the solution of interesting chemical problems. It uses computers to generate information such as properties of molecules or simulated experimental results. Very few aspects of chemistry can be computed exactly, but almost every aspect of chemistry has been described in a qualitative or approximate quantitative computational scheme [67].

Computational chemistry has become a useful way to investigate materials that are too difficult to find or too expensive to purchase. It also helps chemists make predictions before running the actual experiments so that they can be better prepared for making observations. The quantum and classical mechanics as well as statistical physics and thermodynamics are the foundation for most of the computational chemistry theory and computer programs. This is because they model the atoms and molecules

with mathematics. Using computational chemistry software you can in particular perform [67]: Electronic structure determinations, Geometry optimizations, Frequency calculations, Definition of transition structures and reaction paths, Protein calculations, i.e. docking, Electron and charge distributions calculations, Calculations of potential energy surfaces, Calculations of rate constants for chemical reactions (kinetics), Thermodynamic calculations- heat of reactions, energy of activation, Calculation of many other molecular physical and chemical properties. The most important numerical techniques are ab-initio, semi-empirical and molecular mechanics. Definitions of these terms are helpful in understanding the use of computational techniques for chemistry [67]. Semi-empirical methods use parameters derived from experimental values that simplify theoretical calculations. These methods usually do not require long computation times, and lead to qualitative descriptions of molecular systems. In particular, the semi-empirical PM3 method makes uses of an accurate procedure to predict chemical properties, through a simplified Hartree-Fock (HF) Hamiltonian [68].

The correlation between theoretically calculated properties and experimentally determined inhibition efficiencies has been studied successfully for uniform corrosion [69-72].

Aim of work :

The aim of this work is to synthesize organic compounds [1-5] and [12-21] that containing hetero atoms (sulfur and oxygen) to act as corrosion inhibitors on mild steel in acidic media by measuring some parameters by using Mass loss method , and by using the theoretical calculation we make comparison between the results of theoretical study by using semi-empirical molecular quantum calculations within the PM3 method as implemented in Hyper Chem package.

2.1. Instruments

A) Fourier Transform infrared spectrophotometer (FTIR):

The infrared spectra of the prepared compounds were recoded using FTIR 8300 Fourier transform infrared spectrophotometer of SHIMADZU Company as a potassium bromide (KBr) discs in the wave number range of (4000-400) cm^{-1}.

B) Ultraviolet spectra were recorded on SHIMADAZ U.V-visible recording spectrophotometer U.V. 1650 by using DMSO as solvent.

C) ^{1}H-NMR was recorded on nuclear magnetic resonance Bruker, Ultrasheild 300 MHZ in Jordan, using tetramethyl silane as internal standard and DMSO-d6 as solvent.

D) Melting points

Melting points were determined by the open capillary method using hot stage Gallen Kamp melting point apparatus and were uncorrected.

E) Polarizing microscope

Infinity corrected optical system, MT 9900 series, incident and transmitted light models, Camera Infinity I, MEIJI TECHNO.

F) Spectro max – Germany , 2009 .

G) Balance

Sartorius AGGOTTINGEN, Germany, BL210S .

2.2. Chemicals

All the chemicals used in this work were of highest purity available and they supplied without further purification. The following Table (2-1) shows the chemicals and the companies which supply themes.

Table (2-1): Chemicals and their Manufacturers.

Chemicals	Company
Thiosemicarbazide	Fluka
Hydrochloric acid	Thomas
Carbon disulfide	Scharlau
Glacial Acetic acid	Hopkin&Wiliams
Ethanol (absolute)	Scharlau
Acetone	Fluka
anhy. Sodium Carbonate	BDH
Benzaldehyde	RIEDL-DEHAEN AG SEELZE-HANNOVER
p-nitro Benzaldehyde	Merck
m-nitro Benzaldehyde	Merck
p-N,N-dimethyl amino benzaldehyde	BDH
Benzyl Chloride	BDH
1,2-dichloro ethane	Fluka
Potassium hydroxide	Fluka
Acetophenone	BDH
Sulfuric acid	HIMEDIA
DMSO	Merck

2.3. Preparation methods

1) Preparation of 2-[substituted-hydrazine]Carbothioamide[73] [1-5] :

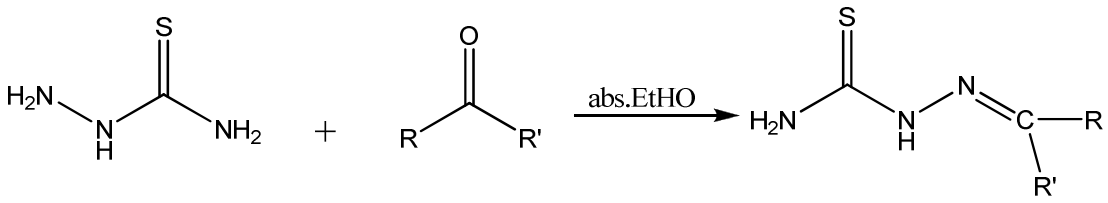

[1] R=C_6H_5, R'=H; **[2]** R=***p***-NO_2-C_6H_4, R'=H; **[3]** R=***p***-$(CH_3)_2N$-C_6H_4, R'=H; **[4]** R=***m***-NO_2-C_6H_4, R'=H; **[5]** R=C_6H_5, R'=CH_3

A mixture of Thiosemicarbazide (0.01mol, 0.91g), absolute ethanol (20mL) and appropriate aromatic aldehydes or ketone (0.01mol) and few drops from glacial acetic acid were refluxed for (4-5) hours. After cooling to room temperature the precipitate was filtered and dried. The products were recrystallized from ethanol. The physical properties of the synthesized compounds are given in Table (2-2).

Table (2-2): Physical properties for prepared compounds [**1-5**].

Comp. No.	Molecular Formula	Colour	Molecular Weight	M.P.˚C	% Yield
[1]	$C_8H_9N_3S_1$	Brown	179.16	221-222	64
[2]	$C_8H_8N_4O_2S_1$	Deep yellow	224.16	224-226	71
[3]	$C_{10}H_{14}N_4S_1$	Yellowish-green	222.16	190-193	55
[4]	$C_9H_6N_4O_2S_2$	White	224.16	210-213	65
[5]	$C_9H_{11}N_3S_1$	Pale yellow	193.16	94-97	56

2) Preparation of 2-amino-5-mercapto-1,3,4-thiadiazole[73] [6] :

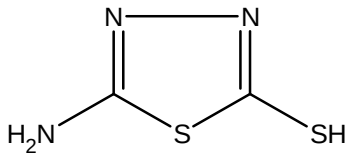

[6]

Molecular formula $C_2H_3N_3S_2$

M. W. 133.21

Thiosemicarbazide (0.25mol,45.5g) was suspended in absolute ethanol and anhydrous sodium carbonate (24g) and carbon disulphide (0.25mol ,46g) was added slowly. The mixture was stirred under refluxing for 5hrs. After that, solvent was removed and the residue was dissolved in water (200 mL), acidified with conc. HCl to give the product as hydrochloride salt, yield 84% (54g). Some data of product **[6]** .

3) Preparation of 2-[substituted-benzylidine]amino-5-mercapto-1,3,4-thiadiazole[73] [7-11] :

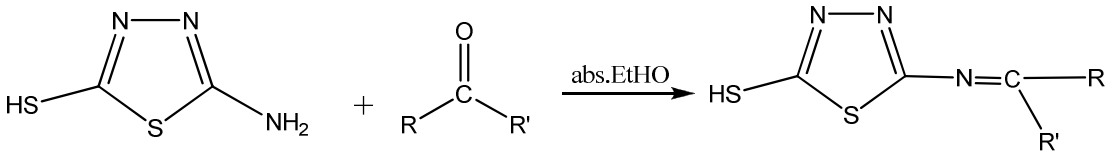

[7] R=C_6H_5, R'=H; **[8]** R=***p***-NO_2-C_6H_4, R'=H; **[9]** R=***p***-$(CH_3)_2N$-C_6H_4, R'=H; **[10]** R= ***m***-NO_2-C_6H_4, R'=H; **[11]** R=C_6H_5, R'=CH_3

A mixture of 2-amino-5-mercapto-1,3,4-thiadiazole (1.33g,0.01mol), abs. ethanol (20ml) and appropriate aromatic aldehydes or ketone (0.01mol) and few drops glacial acetic acid was refluxed for (4-5) hours. After cooling to room temperature the precipitate was filtered and dried. The products were recrystallized from ethanol.

By modification of the procedure in the reference [73] , a mixture of 2-amino-5-mercapto-1,3,4-thiadiazole(1.995g,0.015mol), (1.8g,0.015mol) of acetophenone and (1.753mL) glacial acetic acid was heated for (7-8) hours at 100 ºC by using heating mental with continuous shaking. After cooling to room temperature the solution evaporated and precipitate was filtered and washed by Ether. The physical properties of the synthesized compounds are given in Table (2-3).

Table (2-3): Physical properties for the prepared compounds [**7-11**]**.**

Comp. No.	Molecular Formula	Colour	Molecular Weight	M.P.˚C	Yield %
[**7**]	$C_9H_7N_3S_2$	Yellow	221.30	220-222	54
[**8**]	$C_9H_6N_4O_2S_2$	Deep yellow	266.30	187-190	72
[**9**]	$C_{11}H_{12}N_4S_2$	Orange	264.37	217-220	51
[**10**]	$C_9H_6N_4O_2S_2$	Yellow	266.30	197-200	70
[**11**]	$C_{10}H_9N_3S_2$	Brown	235.33	223-225	55

4) Preparation of (E)-N-substituted benzylidene -5-(benzylthio)-1,3,4-thiadiazol-2-amine[74] **[12-16]:**

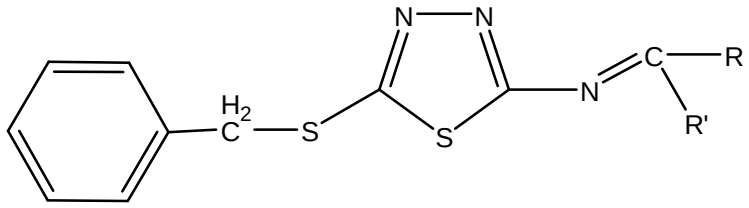

[12] R**=** C_6H_5, R'=H; **[13]** R=***p***-NO_2-C_6H_4, R'=H; **[14]** R=***p***-$(CH_3)_2N$-C_6H_4, R'=H; **[15]** R=***m***-NO_2-C_6H_4, R'=H; **[16]** R=C_6H_5, R'=CH_3

A mixture of appropriate Schiff base (0.0025 mol) and (0.0025 mol) of benzyl chloride in ethanolic alkali solution (0.04 g KOH in 10 mL EtOH) was refluxed for 2 hours. After cooling, the reaction mixture was poured into crushed ice, and the precipitate was obtained, which was filtered and then recrystallized from acetone. The physical properties for the prepared compounds are given in Table (2-4).

Table (2-4): Physical properties for prepared compounds **[12-16]**.

Comp. No.	Molecular Formula	Colour	Molecular Weight	M.P.˚C	% Yield
[**12**]	$C_{16}H_{13}N_3S_2$	Yellow	311.42	197-199	50
[**13**]	$C_{16}H_{12}N_4O_2S_2$	Yellow	356.42	145-148	66
[**14**]	$C_{18}H_{18}N_4S_2$	Pale orange	354.49	123-126	59
[**15**]	$C_{16}H_{12}N_4O_2S_2$	Yellow	356.42	174-176	65
[**16**]	$C_{17}H_{15}N_3S_2$	White	325.45	127-130	53

5) Preparation of (E)-N-substituted benzylidene -5-(2-chloroethylthio)-1,3,4-thiadiazol-2-amine[74] **[17-21]:**

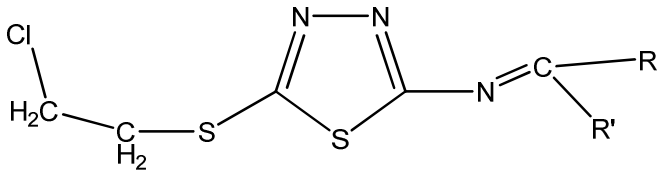

[17] R=C_6H_5, R'=H; **[18]** R=***p***-NO_2-C_6H_4, R'=H; **[19]** R=***p***-$(CH_3)_2$N-C_6H_4, R'=H; **[20]** R=***m***-NO_2-C_6H_4, R'=H; **[21]** R=C_6H_5, R'=CH_3

A mixture of appropriate Schiff base (0.0025 mol) and (0.0025 mol) of 1,2-dichloroethane in ethanolic alkali solution (0.04 g KOH in 10 mL EtOH) was refluxed for (2) hours. After cooling, the reaction mixture was poured into crushed ice, and the precipitate was obtained, which was filtered and then recrystallized from acetone. The physical properties for the prepared compounds are given in Table (2-6).

Table (2-5): Physical properties for prepared compounds **[17-21].**

Comp. No.	Molecular Formula	Color	Molecular Weight	M.P. ˚C	% Yield
[**17**]	$C_{16}H_{13}N_3S_2$	Yellow	283.80	220-224	52
[**18**]	$C_{16}H_{12}N_4O_2S_2$	Yellow	328.80	180-183	67
[**19**]	$C_{18}H_{18}N_4S_2$	Deep orange	326.87	164-165	50
[**20**]	$C_{16}H_{12}N_4O_2S_2$	Yellow	328.80	200-204	70
[**21**]	$C_{17}H_{15}N_3S_2$	Yellow	297.83	198-203	50

6) Preparation of (*z*)-*N*-substituted benzylidene-5-(2-(5-((*E*)-substituted benzylidene amino)-1,3,4-thiadiazol-2-amine [22-26]:

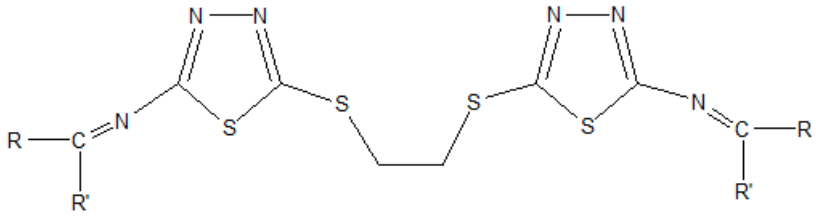

[22] R=C_6H_5, R'=H; **[23]** R=***p*-**NO_2-C_6H_4, R'=H; **[24]** R=***p*-**$(CH_3)_2N$-C_6H_4, R'=H; **[25]** R=***m*-**NO_2-C_6H_4, R'=H; **[26]** R=C_6H_5, R'=CH_3

A mixture of appropriate Schiff base (0.0025 mol) and (0.0025 mol) of 1,2-dichloroethane in ethanolic alkali solution (0.04 g KOH in 10 mL EtOH) was refluxed for (2) hours. After cooling, the reaction mixture was poured into crushed ice, and the precipitate was obtained, which was filtered and then recrystallized by using acetone**.**

2.4. Weight loss measurement:

The sheet of mild steel used has the composition percentages (0.002% P, 0.288% Mn, 0.03% C, 0.0154% S, 0.0199% Cr,0.002% Mo, 0.065% Cu, 0.0005%V and the remainder iron)which obtained by using spectro max. The mild steel sheet was mechanically press-cut into disc shape with diameter (2.5 cm). These disc shapes were polished with emery papers ranging from 110 to 410 grades to get very smooth surface. However, surface treatments of the mild steel involve degreasing in absolute ethanol and drying in acetone. The treated specimens were then stored in a moisture-free desiccator before their use in corrosion studies. Mild steel specimens were initially weighed in an electronic balance. After that the specimens were suspended and completely immersed in 250 ml beaker containing 1M sulphuric acid in the presence and absence of inhibitors. The specimens were removed after 8 hours exposure period at 30ºC, washed with water to remove any corrosion products and finally washed with acetone. Then they were dried and reweighed. Mass loss measurements were performed as ASTM method described previously [75,76]. The tests were performed in duplicate to guarantee the reliability of the results and the mean value of the weight loss is reported. Weight loss allowed calculation of the mean corrosion rate in (mg cm^{-2} h^{-1}) [76] . The corrosion rate of mild steel was determined using the relation:

$$W = \frac{\Delta m}{St} \qquad (2\text{-}1)$$

Where (Δm) is the mass loss, (S) the area and (t) is the immersion time.

The percentage inhibition efficiency (E%) was calculated using the relationship[76]:

$$E\% = \left(\frac{W_{corr} - W_{corr(inh)}}{W_{corr}}\right) x\ 100 \qquad (2\text{-}2)$$

Where W_{corr} and $W_{corr(inh)}$ are the corrosion rates of mild steel in absence and presence of inhibitor, respectively.

Basic information can be provided from the adsorption isotherms to explain the interaction between the organic compounds and metal surfaces. So that, the degree of surface coverage values (θ) at different inhibitor concentrations in 1M H_2SO_4 was achieved from weight loss measurements **[θ = E (%) /100]** at 30°C and tested with Langmuir isotherm relationship [77].

$$\frac{C}{\theta} = \frac{1}{K_{ads}} + C \qquad (2\text{-}3)$$

Where K_{ads} is the equilibrium constant of the adsorption/desorption process, C (M) is the inhibitor concentration in the test solution.

According to the Langmuir isotherm, K_{ads} values can be calculated from the intercepts of the straight line of plotting (C/θ versus C). K_{ads} is related to the standard free energy of adsorption, ΔG^{o}_{ads}, with the following equation: (The value 55.5 is the molar concentration of water in the solution)

$$K_{ads} = \frac{1}{55.5}\exp(-\Delta G^{o}_{ads}/RT) \qquad (2\text{-}4)$$

2.5. Theoretical calculations:

Theoretical calculations were carried out using the semi-empirical calculations with PM3 method [78]. For this purpose the Hyperchem Program [79] with complete geometry optimization was used.

The purpose of these calculations is to provide information about the electron configuration of several organic inhibitors by quantum chemical calculations and to investigate the relationship between molecular structure and inhibition efficiency. Some electronic properties such as energy of the highest occupied molecular orbital (E_{HOMO}), energy of the lowest unoccupied molecular orbital (E_{LUMO}), energy gap (ΔE) between LUMO and HOMO and Mulliken charges on the backbone atoms for prepared molecules [**1**-**21**] were planned to determine.

3.1. Characterization of 2-[substituted-hydrazine] carbothioamide [**1-5**]:

These compounds were prepared by condensation reaction of thiosemicarbazide with aldehyde or ketone in abs. ethanol. The reaction occures according to the steps mechanism [80] which shown below:

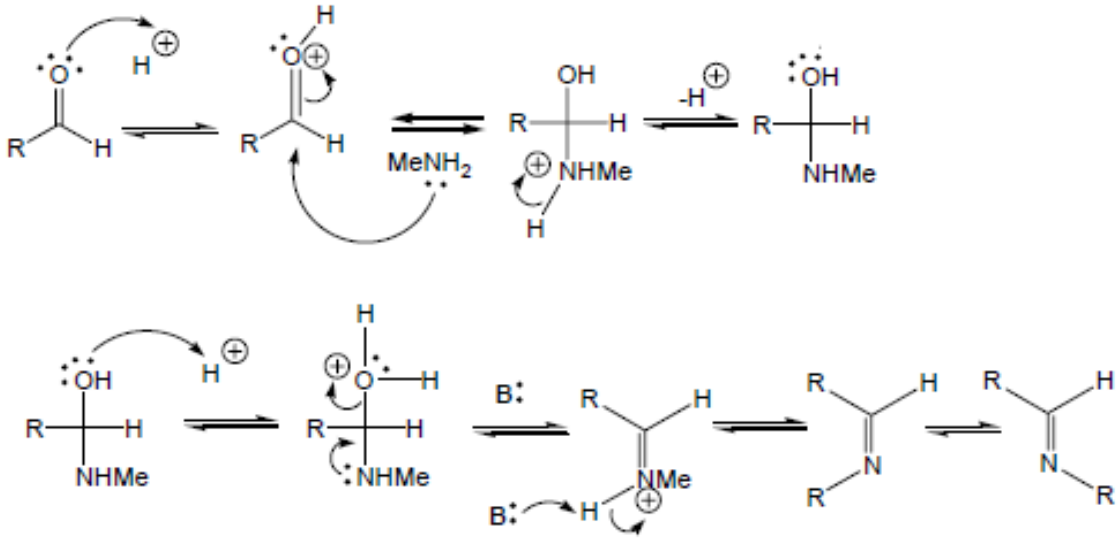

The FTIR spectra of prepared compounds [**1-5**] (figures (3-1)- (3-5)) which are shown that there is a tautomerism could be occurred in prepared compounds [**3, 4**] as below:

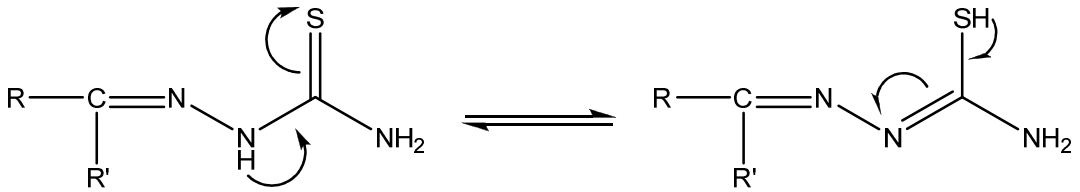

The appearance of weak absorption band of (S-H, 2550-2600 cm^{-1}) indicated the tautomerism behavior (Table 3-1).

The disappearance of bands at (1660-1700 cm^{-1}) and (2700-2850 cm^{-1}) which belong to (C=O) and (C-H aldehyde hydrogen), respectively. And

also, appearance of absorption band at (1690cm^{-1}) for the imine (C=N) as evidence for formation of the above compounds [81]. The most important absorption bands were shown in Table (3-1).

Table (3-1): The most important absorption bands.

Comp. No.	ν(C-H) arom. cm^{-1}	ν(C-H) aliph. cm^{-1}	ν(C=N) cm^{-1}	ν(S-H) cm^{-1}	ν (C=S) cm^{-1}	ν(C-S) cm^{-1}
[**1**]	3050	-	1595	-	1280	727
[**2**]	3100	-	1564	-	1263	667
[**3**]	3040	2902	1598	2561	1280	727
[**4**]	3040	-	1602	2599	1296	732
[**5**]	3060	2860	1587	-	1286	759

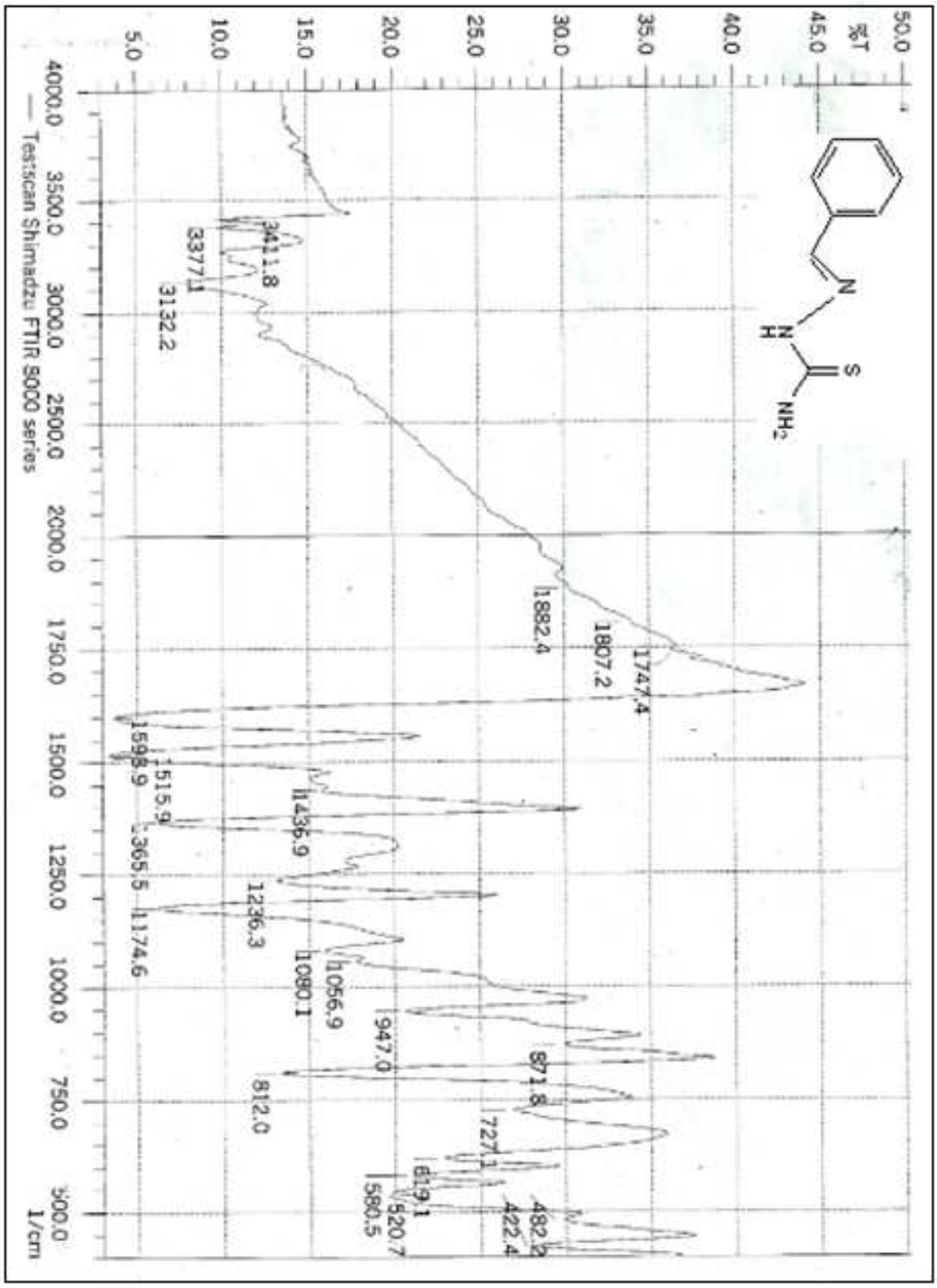

Figure (3-1). FTIR spectrum of compound [**1**].

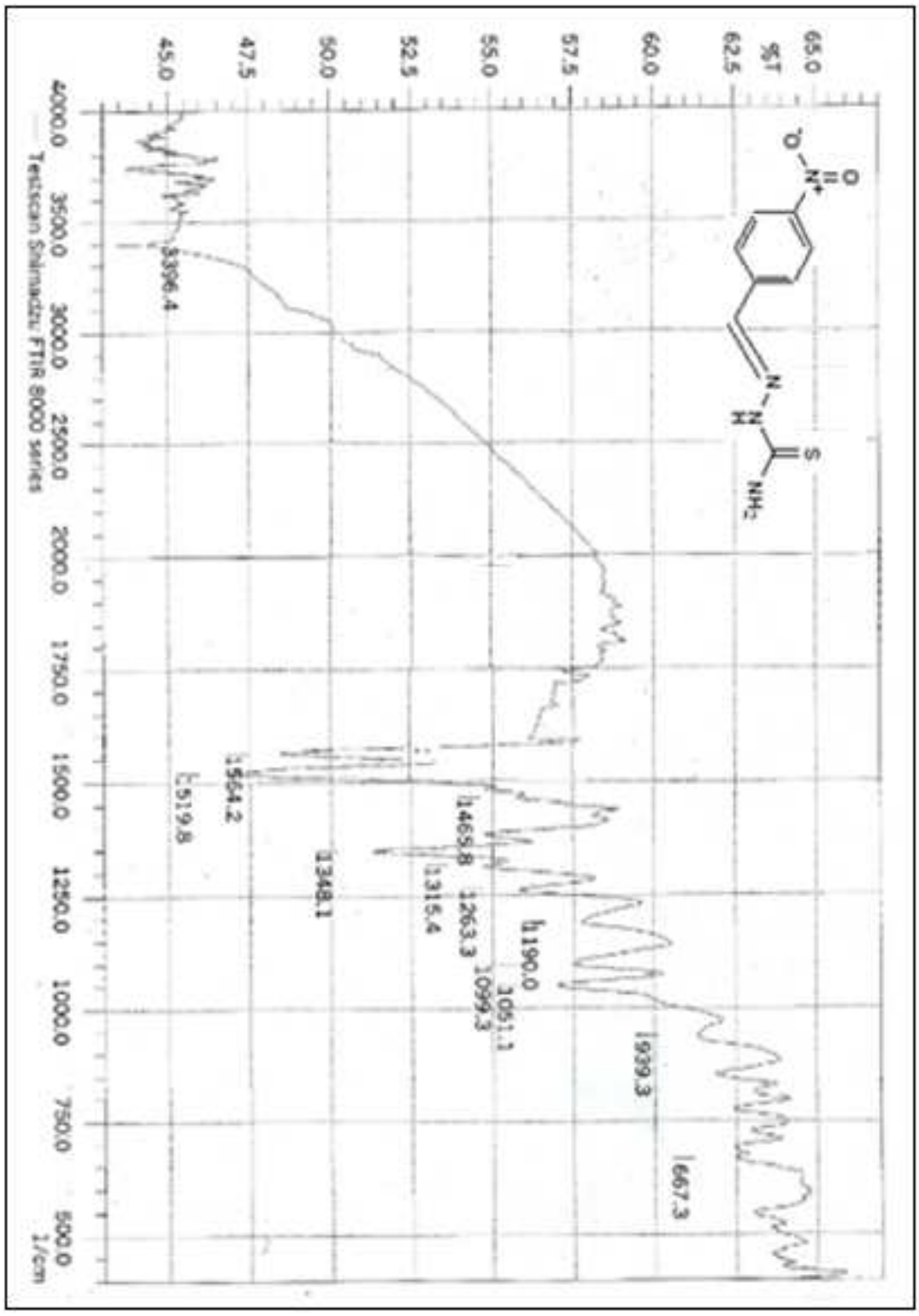

Figure (3-2). FTIR spectrum of compound [**2**]

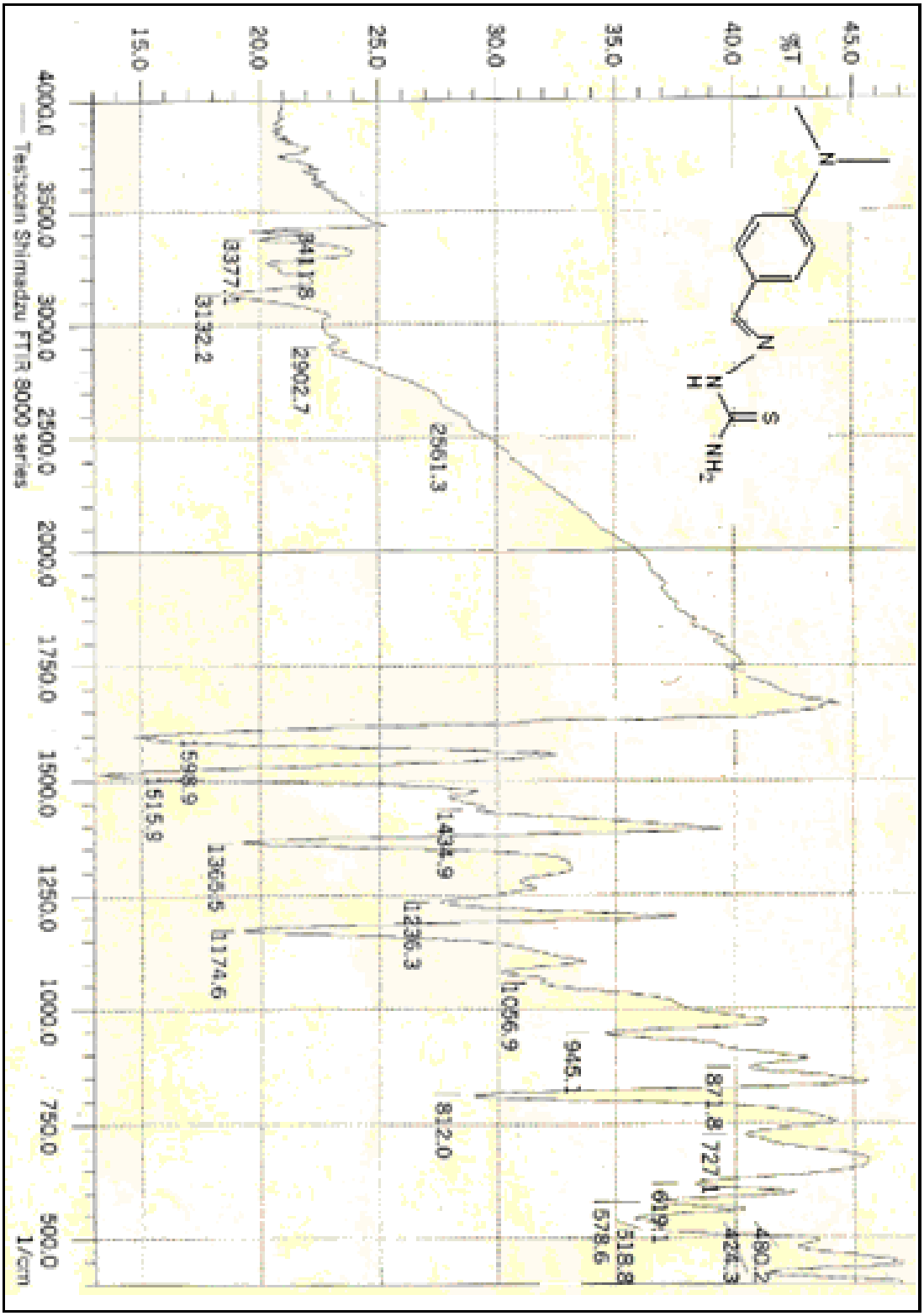

Figure (3-3). FTIR spectrum of compound [**3**].

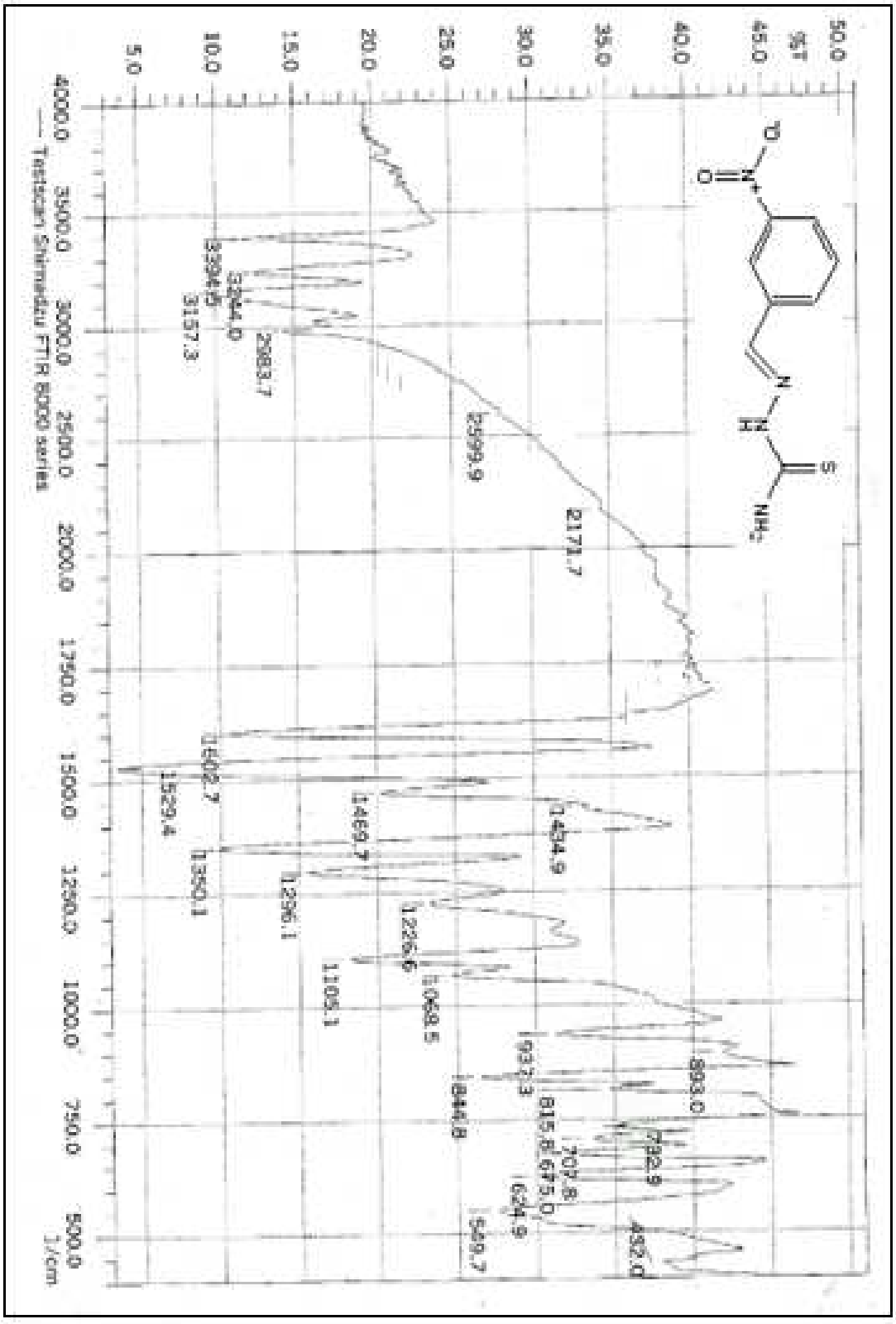

Figure (3-4). FTIR spectrum of compound [**4**].

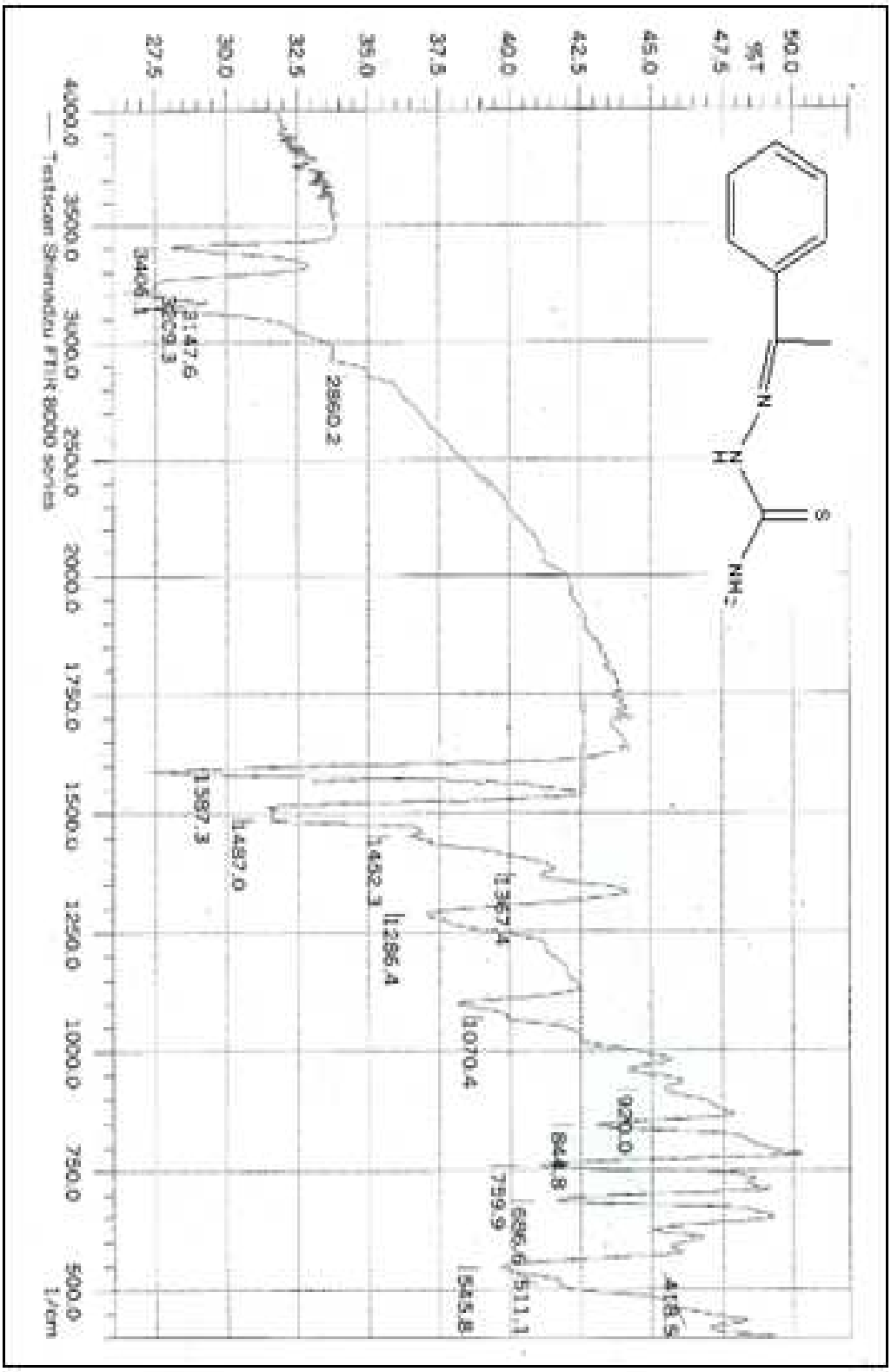

Figure (3-5). FTIR spectrum of compound [**5**].

The UV-visible spectra of 2-[substituted-hydrazine] carbothioamide compounds **[1]-[5**] in DMSO as a solvent and at room temperature, main bands (λ_{max}) [81-84] are to be expected, namely the first (230–260 nm) low intensity bands are attributed to the $\pi \rightarrow \pi^*$ transitions of aromatic rings. The second band at 300–340 nm (or >300 nm, it depends on environment) is assigned to the $\pi \rightarrow \pi^*$ transitions (high intensity) of C=N group. The third band at < 400 nm due to $n \rightarrow \pi^*$ transitions (low intensity) of C=N group. Fourth band at >300 nm involves $n \rightarrow \pi^*$ transitions (low intensity) of C=S group. In addition, auxochromes (like, $-NO_2$, $-N(R)_2$) give blue shift to $n \rightarrow \pi^*$ transitions, and red shift to $\pi \rightarrow \pi^*$[84]. For compound **[1]**, the $n\rightarrow \pi^*$ bands of C=S group and C=N group seem to get completely masked by high intensity of $\pi \rightarrow \pi^*$ of C=N and take place at 357 nm and 373 nm (fig. 3-6). For compound **[2]**, the $n \rightarrow \pi^*$ of C=N group and C=S group seem to get completely masked by high intensity of $\pi \rightarrow \pi^*$ of C=N group and take place at λ_{max} 376 nm, and red shift of $\pi \rightarrow \pi^*$ bands could be occurred and that caused by resonance effects of $–NO_2$ group (fig. 3-7). For compound **[3]**, the $n \rightarrow \pi^*$ peak of C=N group and C=S group seem to get completely masked by high intensity of $\pi \rightarrow \pi^*$ of C=N group and take place at λ_{max} 360 nm, and red shift of $\pi \rightarrow \pi^*$ bands could be occurred and that caused by resonance effects of $–N(CH_3)_2$ group (fig. 3-8). For compound **[4]**, the $n \rightarrow \pi^*$ bands of C=N group and C=S group seem to get completely masked by high intensity of $\pi \rightarrow \pi^*$ of C=N group and take place at λ_{max} 326 nm, and the presence of nitro group in meta position gives rise to a less pronounced bathochromic effect as only inductive effect of nitro group is in operation [85] (fig. 3-9).

For compound **[5]**, the n → π* bands of C=N group and C=S group seem to get completely masked by high intensity of π → π* of C=N group and take place at λ_{max} 312 nm, steric hindrance to conjugated system (C=N with the ring) could be happened by methyl group of imine bond and lead to blue shift [86] (fig. 3-10).

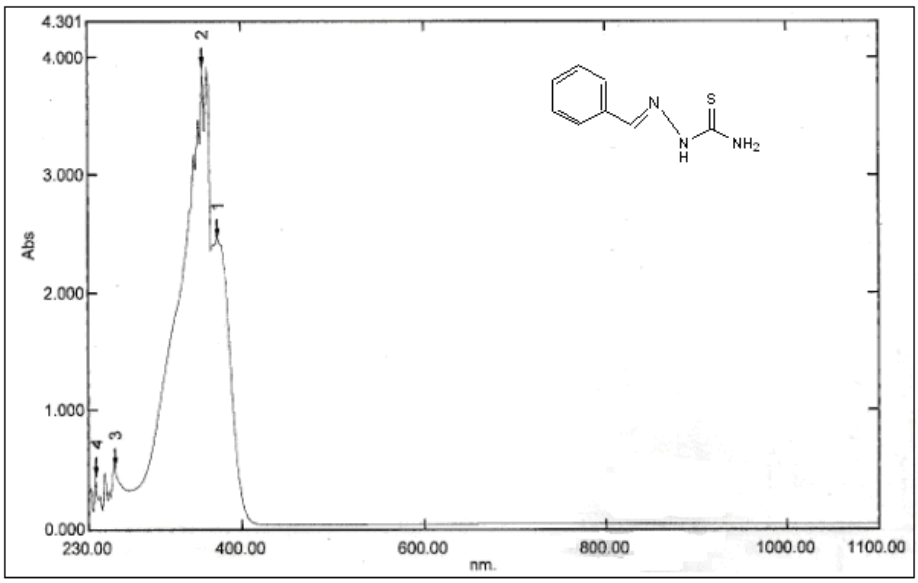

Figure (3-6). U.V. spectrum of compound [**1**].

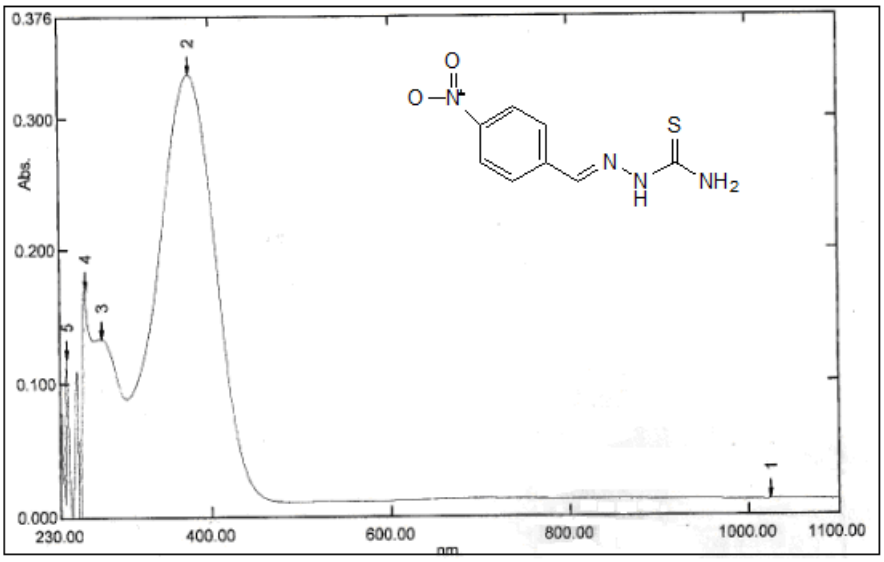

Figure (3-7). U.V. spectrum of compound [**2**].

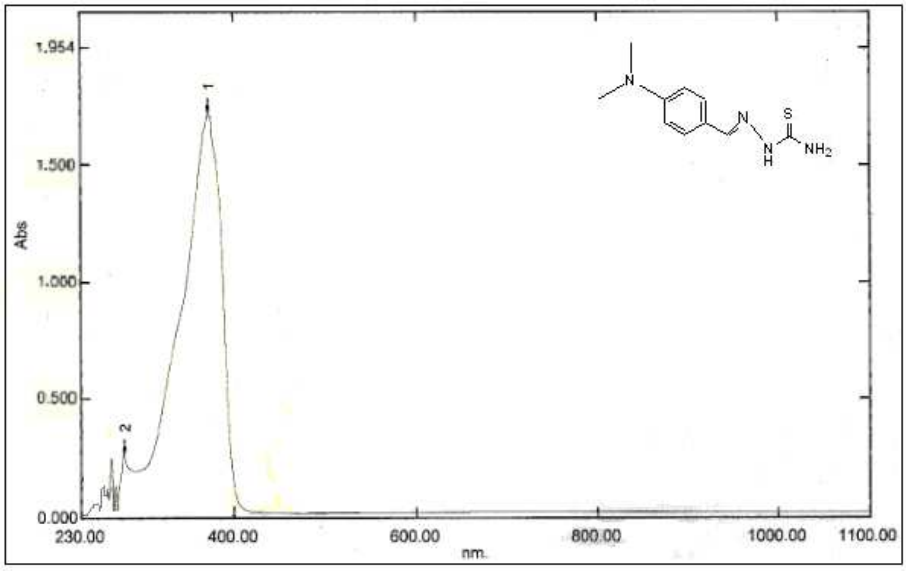

Figure (3-8). U.V. spectrum of compound [**3**].

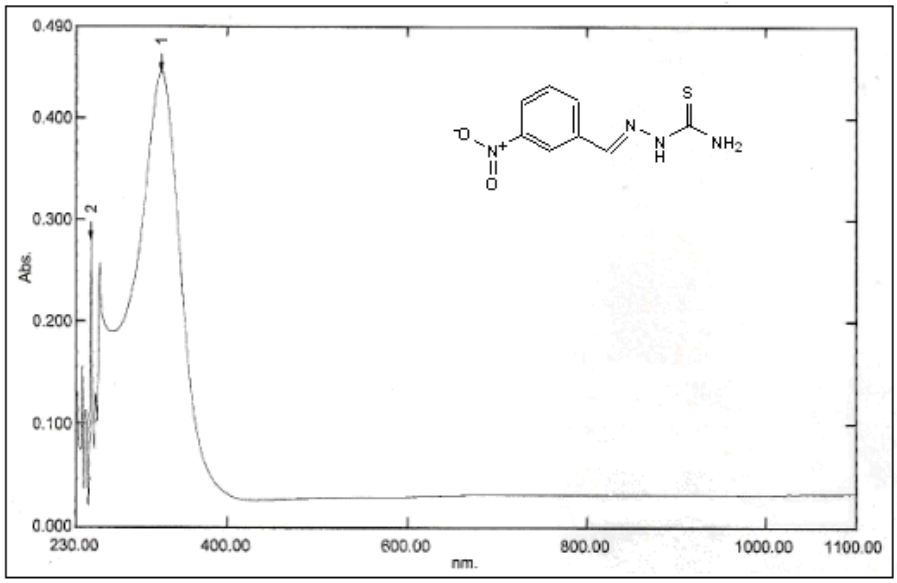

Figure (3-9). U.V. spectrum of compound [**4**].

Figure (3-10). U.V. spectrum of compound [**5**].

3.2. Characterization of 2-amino-5- mercapto-1,3,4-thiadiazole [**6**]:

Compound [**6**] was prepared through the reaction of thiosemicarbazide with CS_2 in the presence of anhydrous sodium carbonate in abs. ethanol. The mechanism of the reactions may be as follow:

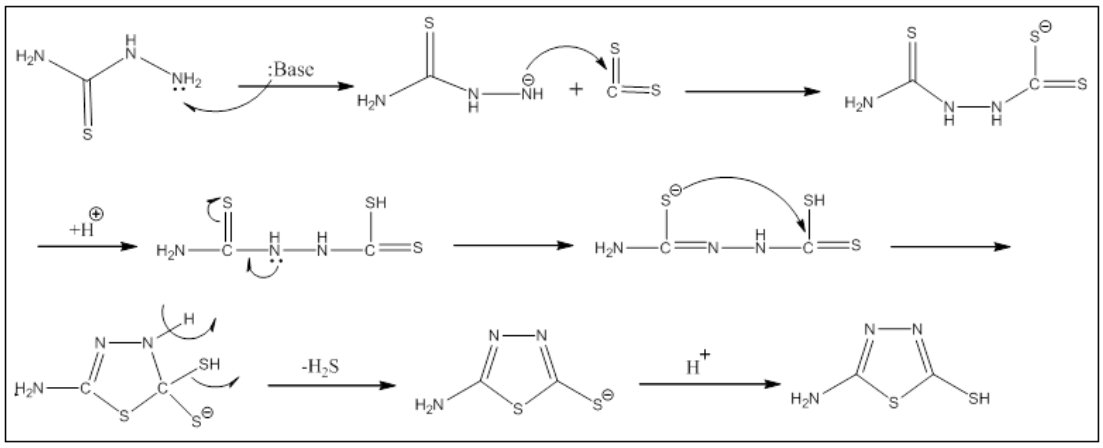

First, carbon disulfide reacts as an electrophile with amines in the presence of anhydrous sodium carbonate to give dithiocarbamates; the reaction involves nucleophilic addition of the amine to the electrophilic thiocarbonyl bond [87]. Second, the Cyclization involves attack at thiocarbonyl carbon and the ring-closing step [88]. The FTIR spectrum of [**6**] (fig. 3-11) shows the following characteristic bands: the two bands in the 3336 cm^{-1} and 3247 cm^{-1} were due to asymmetric and symmetric stretching vibrations of $–NH_2$ group, respectively, an absorption band at 3122cm^{-1} was due to the –NH stretching (tautomeric form). The bands at 2922cm^{-1} and 2771cm^{-1} were attributable to the intra molecularly hydrogen bonding of –NH group[89]. The SH stretching band found as very weak shoulder at 2648.1cm^{-1}. The bands at 1548cm^{-1} and 1606 cm^{-1} are due to (C=N) stretching of the thiadiazole ring moiety. The band at 1473 cm^{-1} is due to (C-N) stretching vibration. Also, the absorption band at 1326.9cm^{-1} for the (C=S) group which evidence that compound [**6**] can exist in two tautomeric forms, thiol [I] and thione form [II][90].

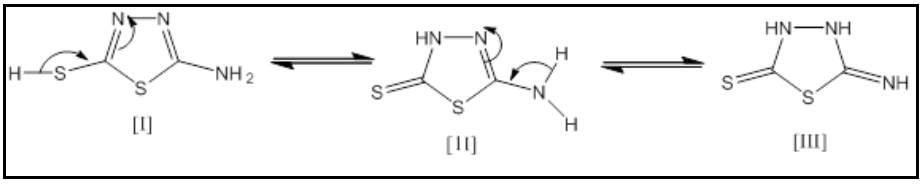

Beside this, the band at 682 cm^{-1} due to (C-S) bond is good evidence for the structure given to the product, as shown in Figure (3-11).

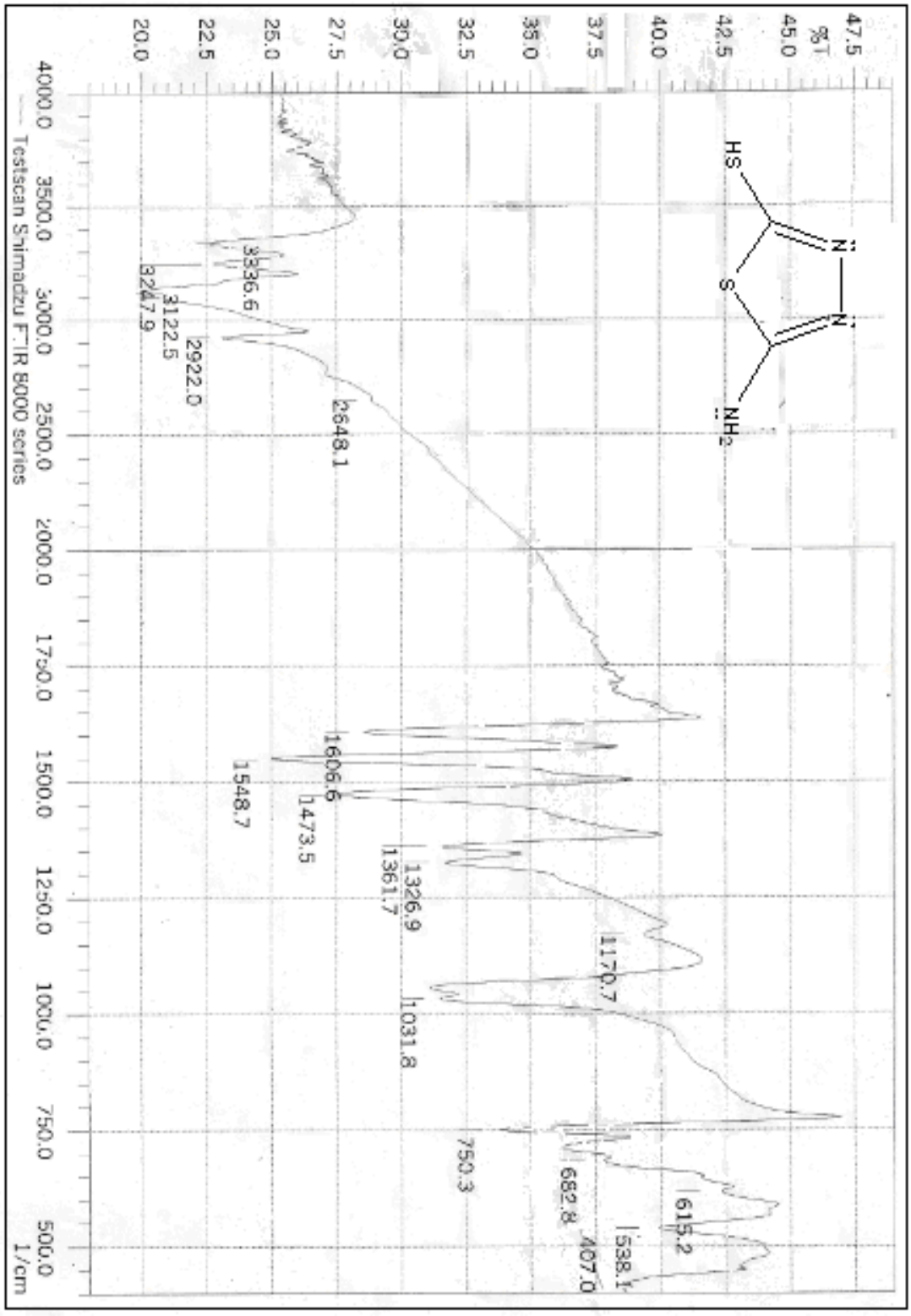

Figure (3-11). FTIR spectrum of compound [**6**].

As showing below, the structure (b) is more stable than others in solid state of 2-amino-5- mercapto-1,3,4-thiadiazole. This is in accordance with the fact that these compounds exist as a tautomeric mixture of the thione and thiol forms with the predominance of the thione form [٩١,٩٢].

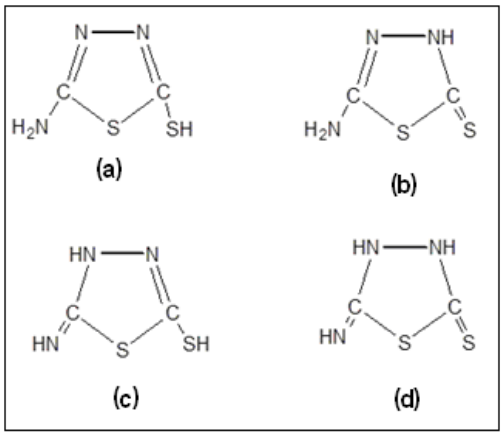

3.3. Characterization of 2-[substitutedbenzylidine]amino-5-mercapto-1,3,4- thiadiazole [**7-11**]:

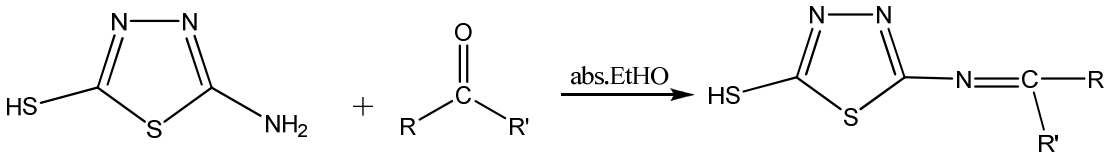

[7] R=C_6H_5, R'=H; **[8]** R=p-NO_2-C_6H_4, R'=H; **[9]** R=p-$(CH_3)_2N$-C_6H_4, R'=H; **[10] R=**m-NO_2-C_6H_4, R'=H; **[11]** R=C_6H_5, R'=CH_3

These compounds were prepared from the reaction of compound [**6**] with the aldehydes or ketone, in abs. ethanol by following the same condensation mechanism that mentioned in the preparation of the compounds [**1-5**].

The FTIR spectra of compounds (7-11), figures (3-12 to 3-16) show absorption bands of different bonds which are also listed in Table (3-2).

Moreover, all compounds exhibit a disappearance of bands at (1680-1715) cm^{-1}, (2830-2695) cm^{-1} and (3400-3500) cm^{-1} which due to (C=O), (C-H aldehydic) and (-NH_2 group), respectively, but in compounds [7] and [9] the appearance of bands at 3446 and 3409 cm^{-1} respectively may be caused by the remaining of reactants. That regarded as confirmation on the formation of the above compounds. Other informative bands are listed in Table (3-2).

Table (3-2): FTIR spectral data of compounds [**7**-**11**] (in cm^{-1}).

Comp No.	Fig. No.	ν S-H	ν C-H aromatic	ν C-H aliphatic	ν C=S	ν C=N	ν C-S	Other bands
[7]	(3-12)	2600	3040	-	1261	1562	682	-
[8]	(3-13)	2600	3060	-	1263	1566	682	[93]ν p-NO_2 1590, 1348
[9]	(3-14)	2600	3087.8	2930	1257	1587	669	ν p-N-CH_3 819
[10]	(3-15)	2700	3078	-	1265	1570	682	[93]ν m-NO_2 1510,1390
[11]	(3-16)	2796	3050	2920	1271	1554	690	-

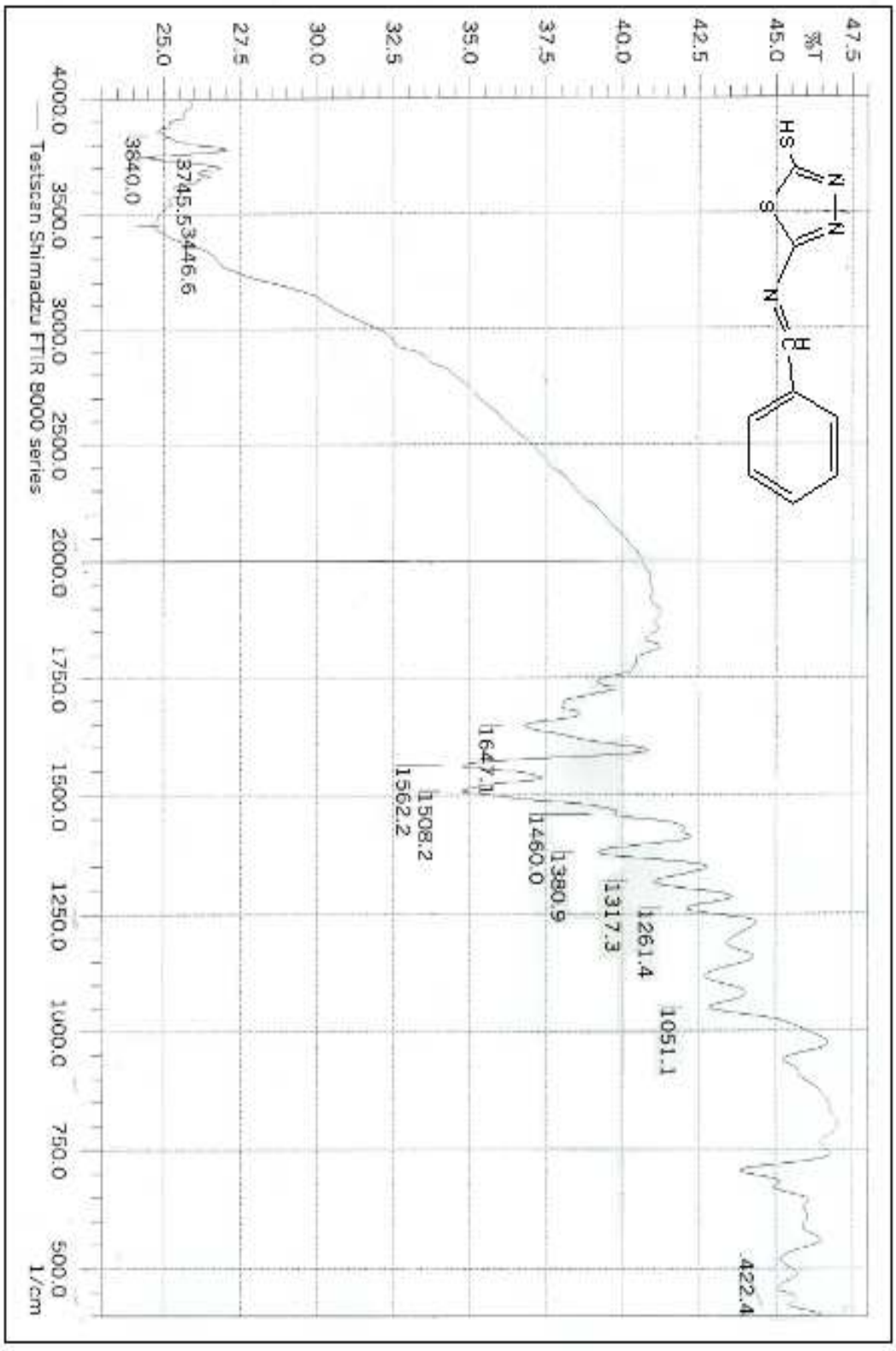

Figure (3-12). FTIR spectrum of compound [**7**].

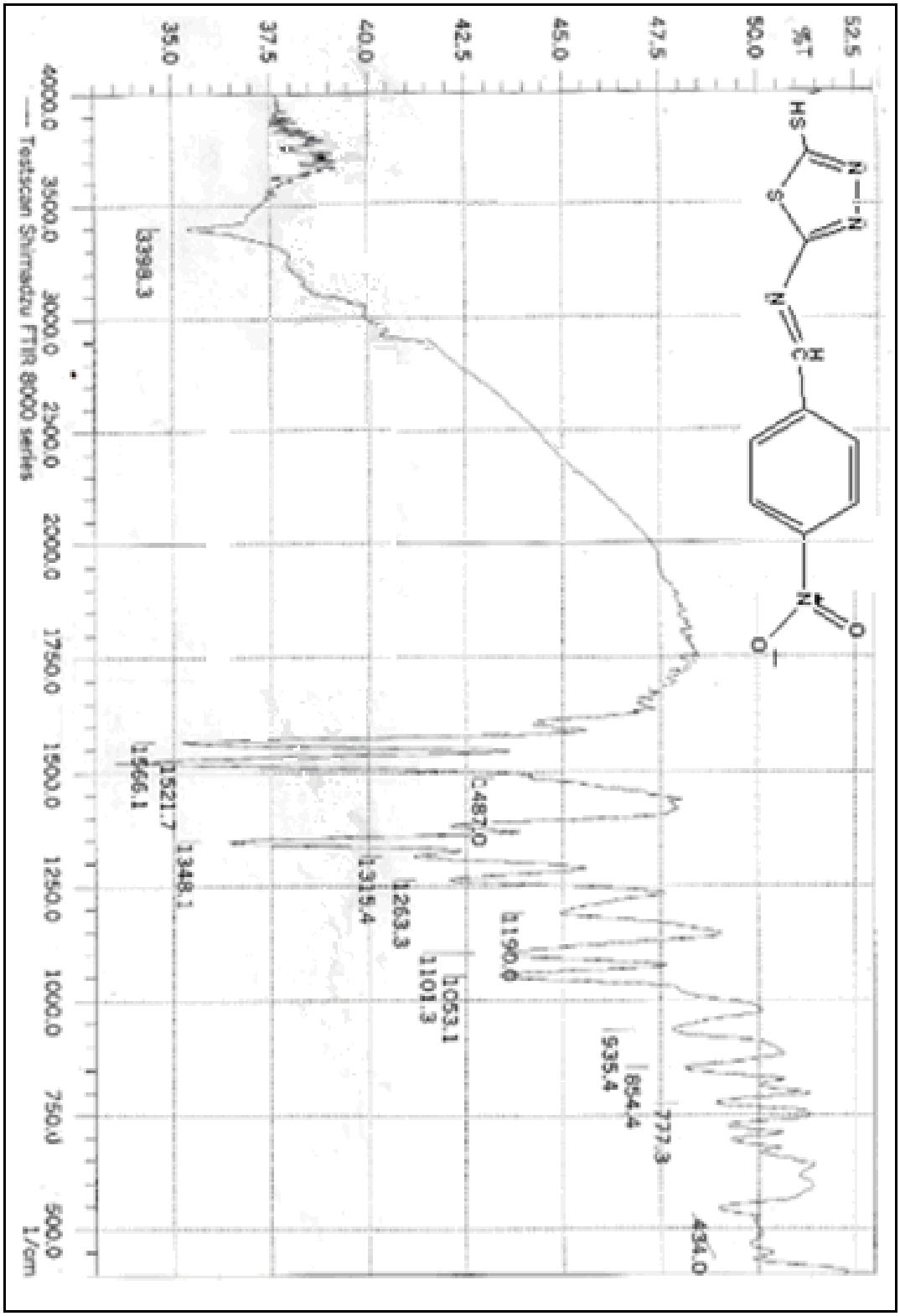

Figure (3-13). FTIR spectrum of compound [**8**].

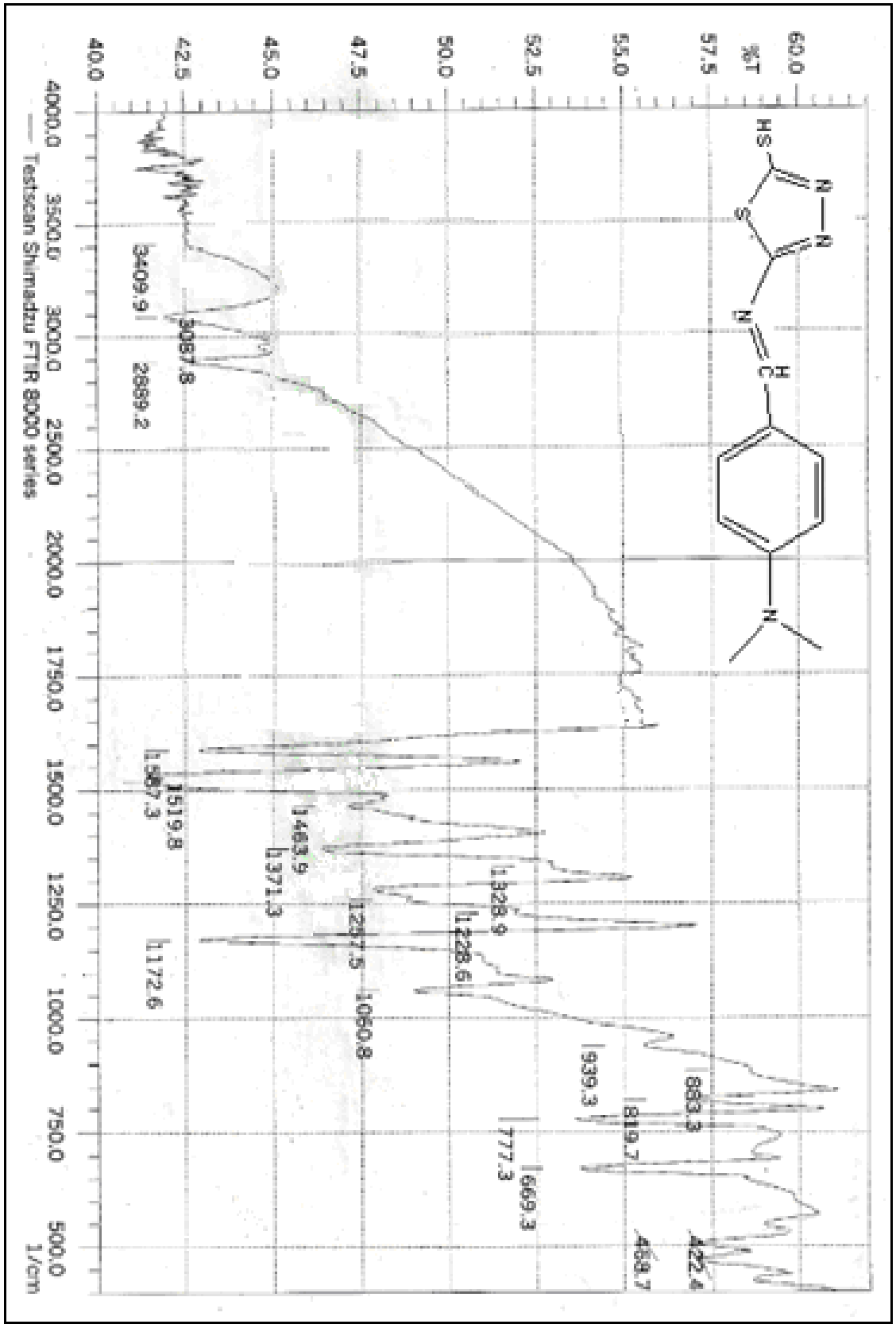

Figure (3-14). FTIR spectrum of compound [**9**].

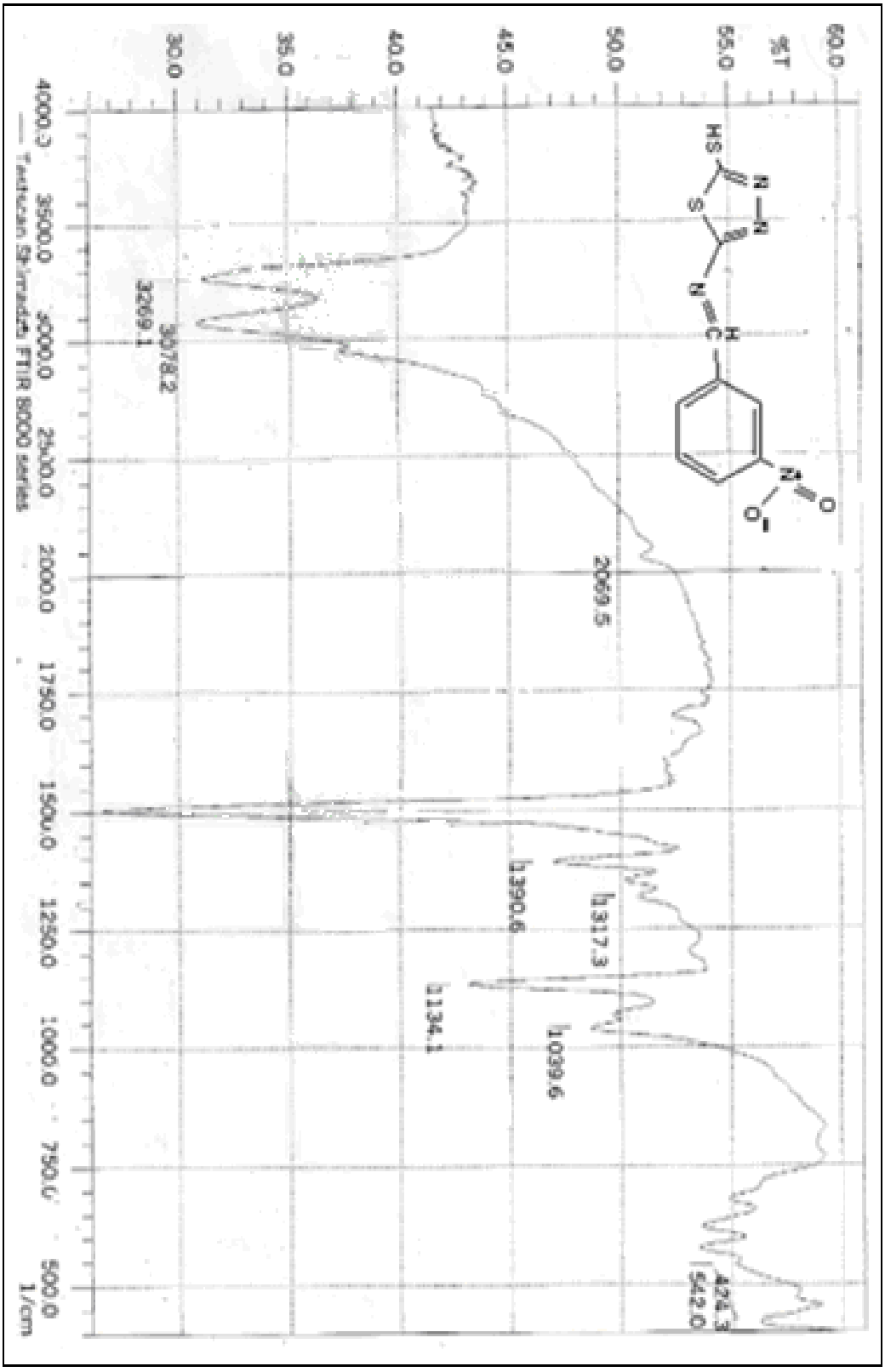

Figure (3-15). FTIR spectrum of compound [**10**].

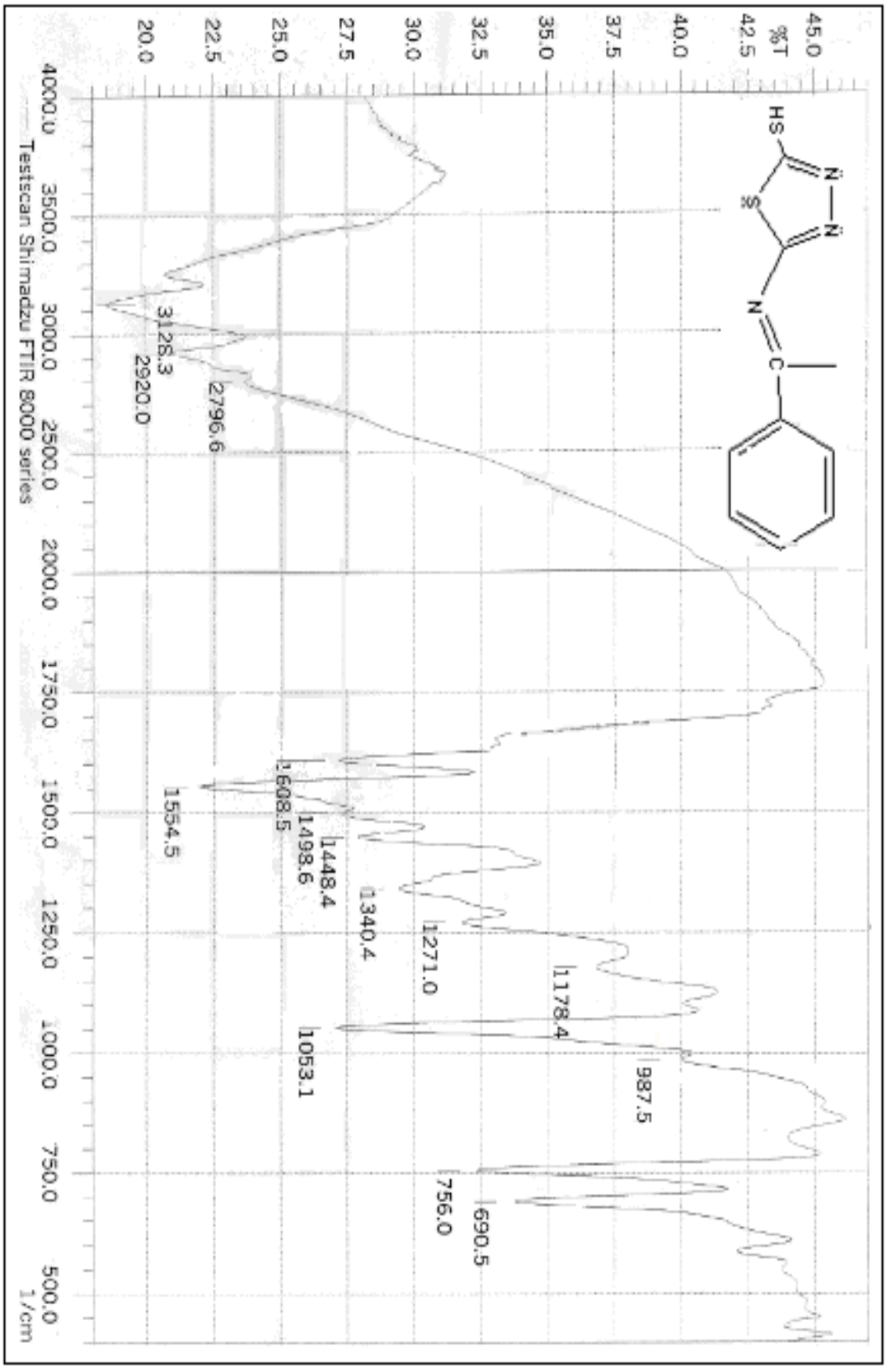

Figure (3-16). FTIR spectrum of compound [**11**].

3.4. Characterization of (E)-N-substituted benzylidene -5-(benzylthio)-1,3,4-thiadiazol-2-amine [**12-16**]:

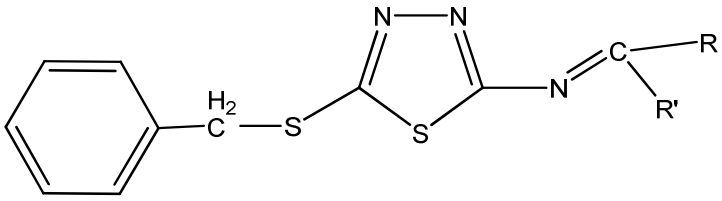

[12] R=C_6H_5, R'=H; **[13]** R=***p***-NO_2-C_6H_4, R'=H; **[14]** R=***p***-$(CH_3)_2N$-C_6H_4, R'=H; **[15]** R=***m***-NO_2-C_6H_4, R'=H; **[16]** R=C_6H_5, R'=CH_3

Compounds [**12, 13, 14, 15** and **16**] were prepared via SN_2 reaction of each compound [**7, 8, 9, 10** or **11**] with benzyl chloride in alcoholic potassium hydroxide. Mechanism of this reaction involved abstraction of proton from thiol group to form nucleophile which can be attacked carbon of benzyl chloride within SN_2 reaction to give (E)-N-substituted benzylidene-5-(benzylthio)-1,3,4-thiadiazol-2-amine [**12-16**], mechanism of SN_2 reaction is shown below:

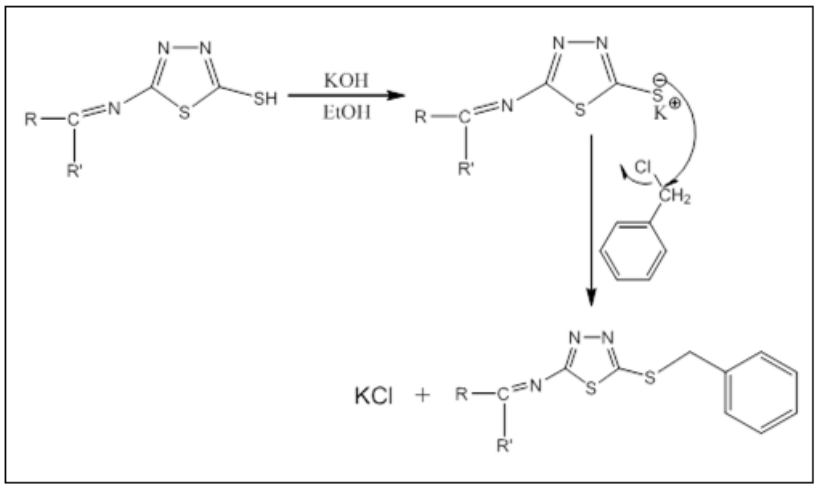

The FTIR spectra of compounds (12-16), figures (3-17 to 3-21) show absorption stretching bands of different groups which are also listed in Table (3-3).

Table (3-3): FT-IR data of compounds [**12-16**] (in cm^{-1}).

Comp. No.	Fig. No.	ν C-H aromatic	ν C-H aliphatic	ν C=N	ν C-S	Other Bands
[12]	(3-17)	3101	2929	1566	705	-
[13]	(3-18)	3112	2937	1566	700	[93] ν p-NO_2 1465 1348
[14]	(3-19)	3105	2929	1591	694	ν p-N-CH_3 823
[15]	(3-20)	3070	2929	1560	730	[93] ν m-NO_2 1485 1350
[16]	(3-21)	3107	2966	1550	705	-

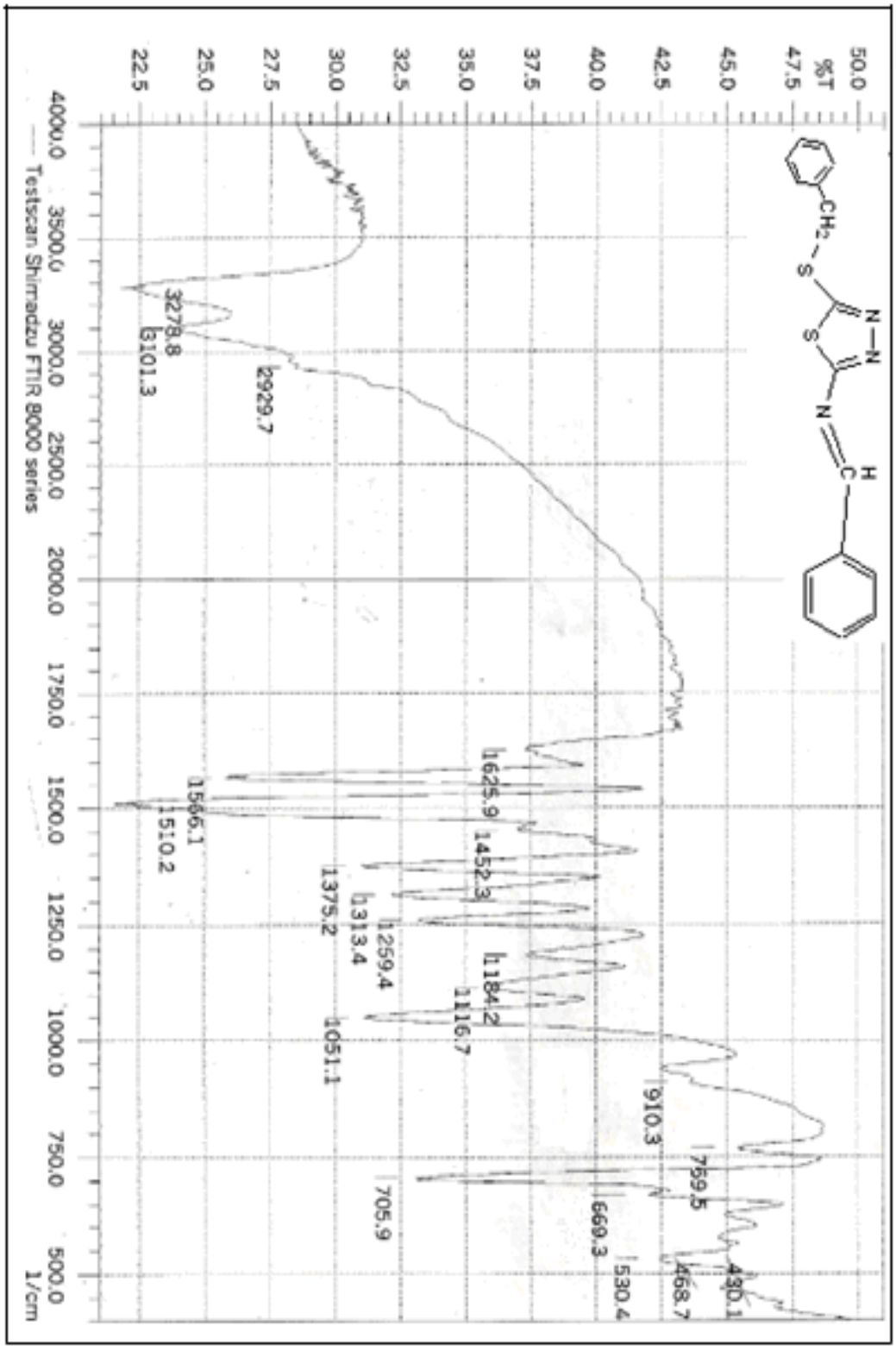

Figure (3-17). F.T.I.R spectrum of compound [**12**].

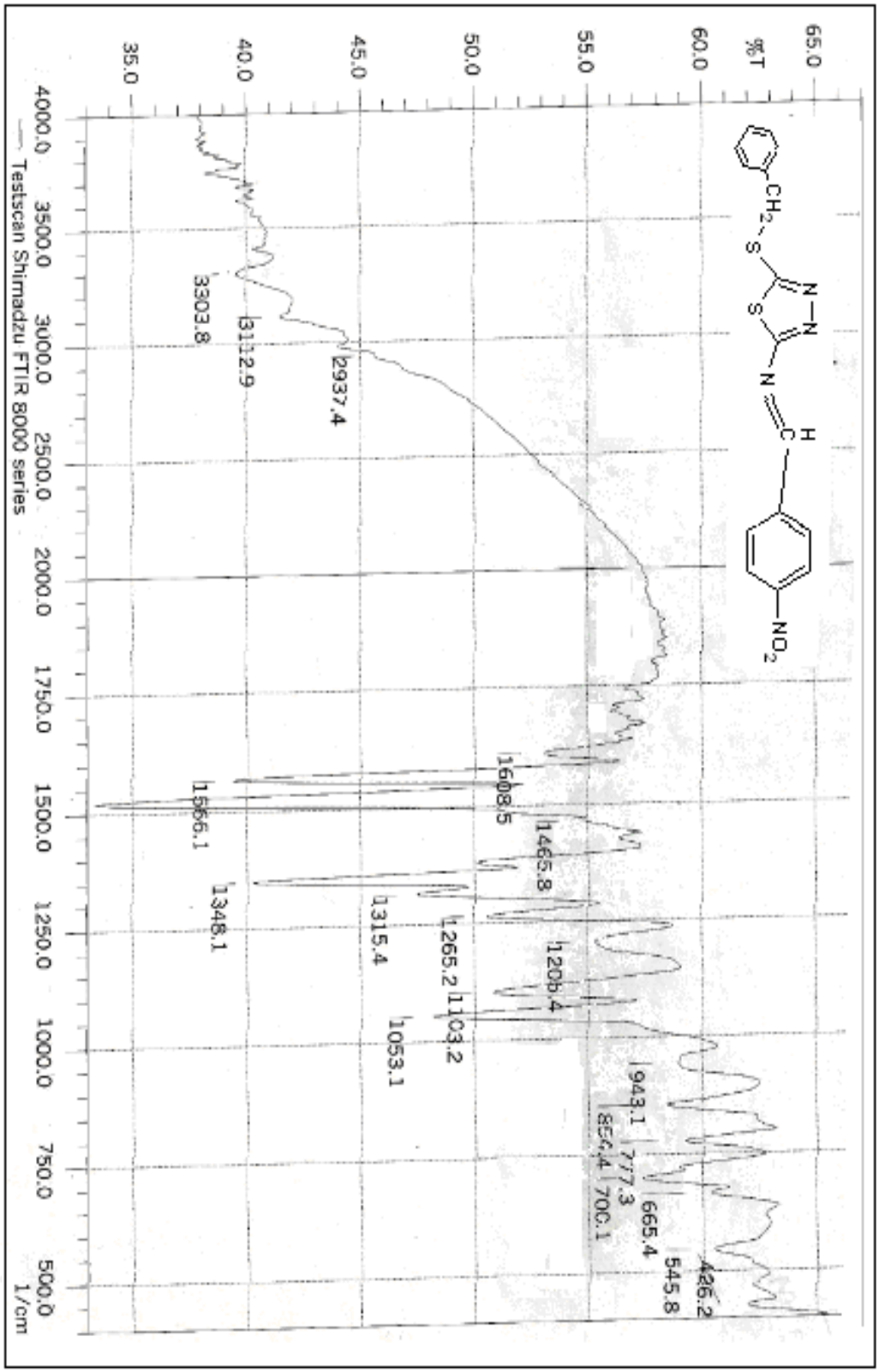

Figure (3-18). F.T.I.R spectrum of compound [**13**]

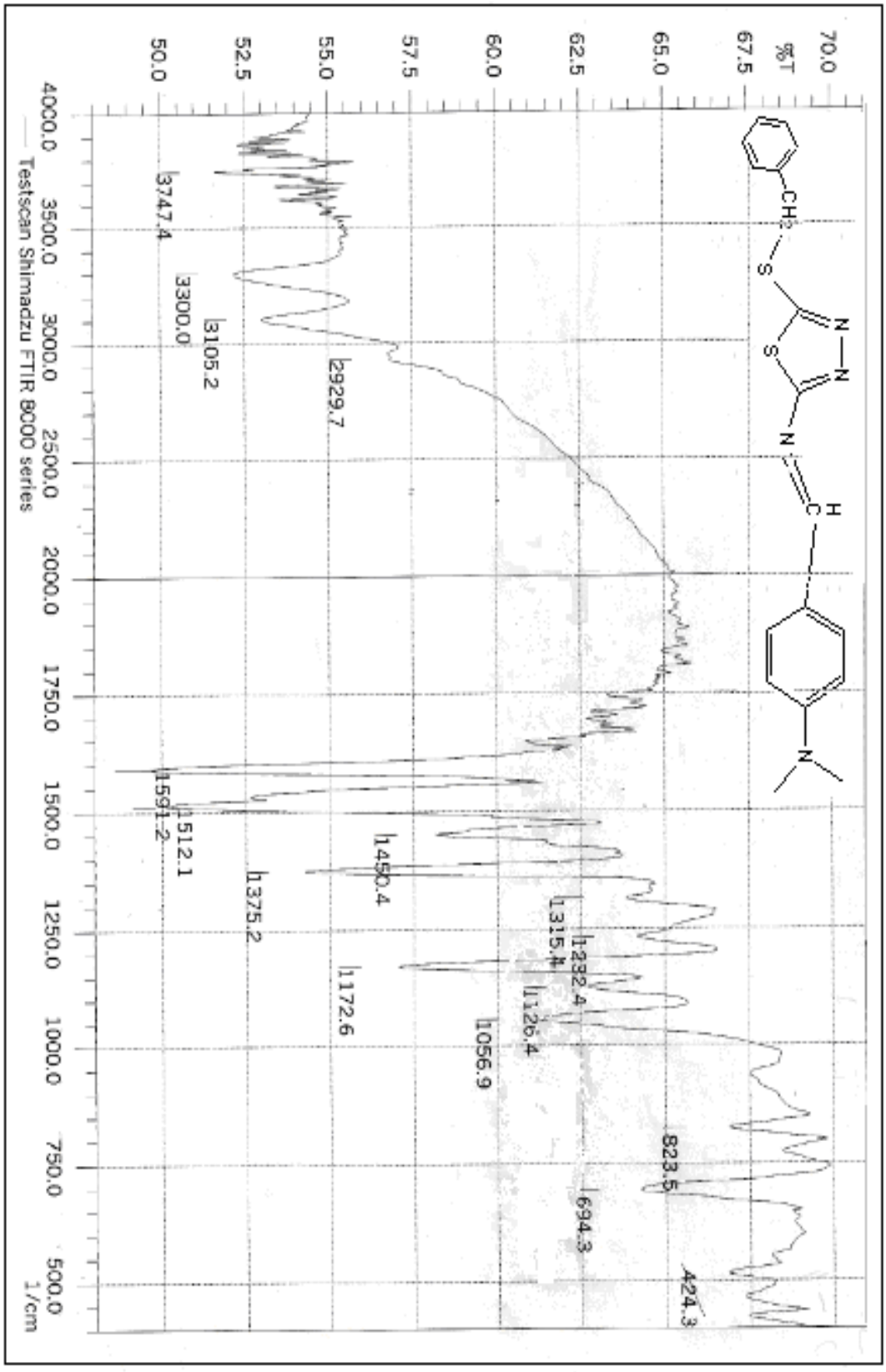

Figure (3-19). F.T.I.R spectrum of compound [**14**].

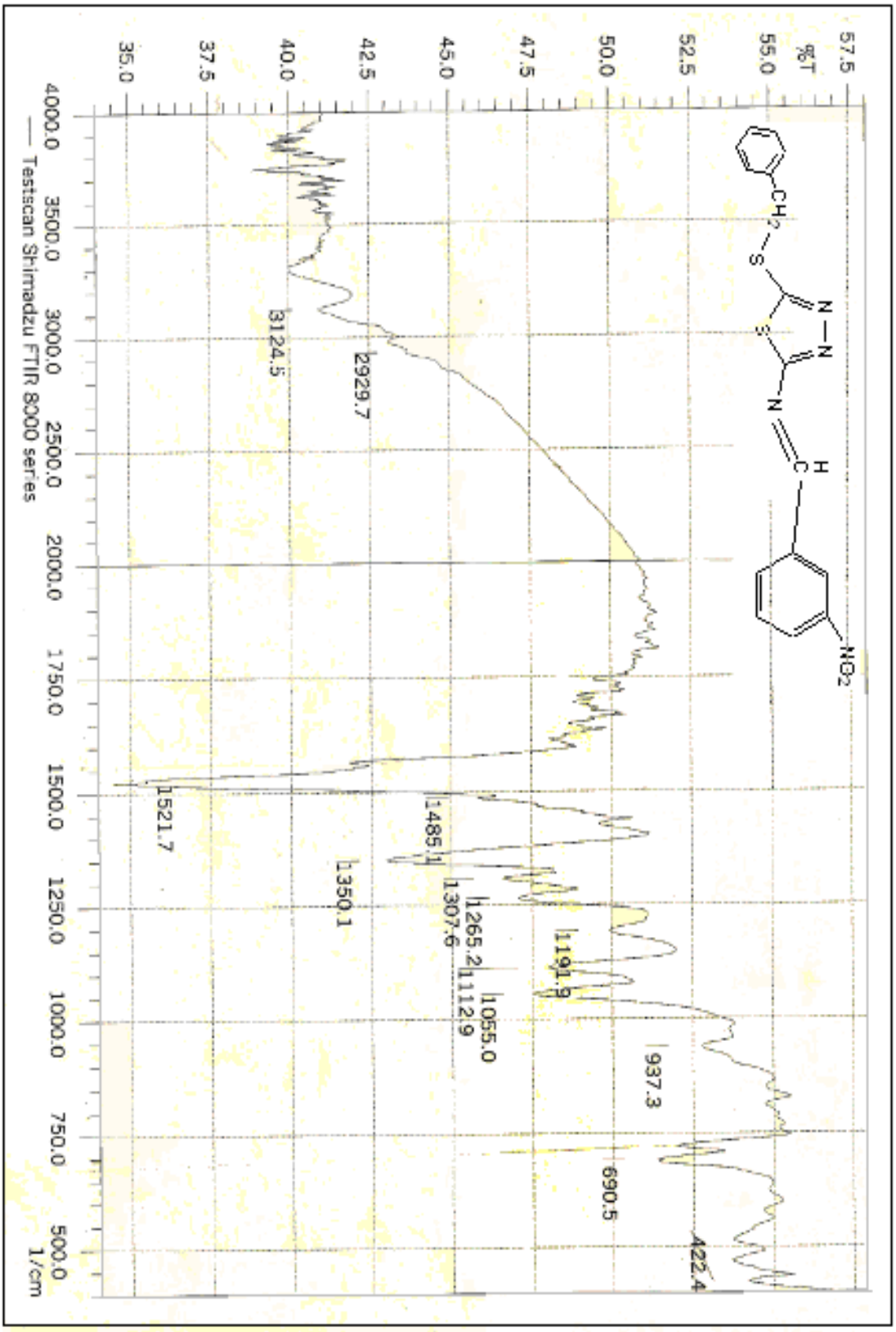

Figure (3-20). F.T.I.R spectrum of compound [**15**].

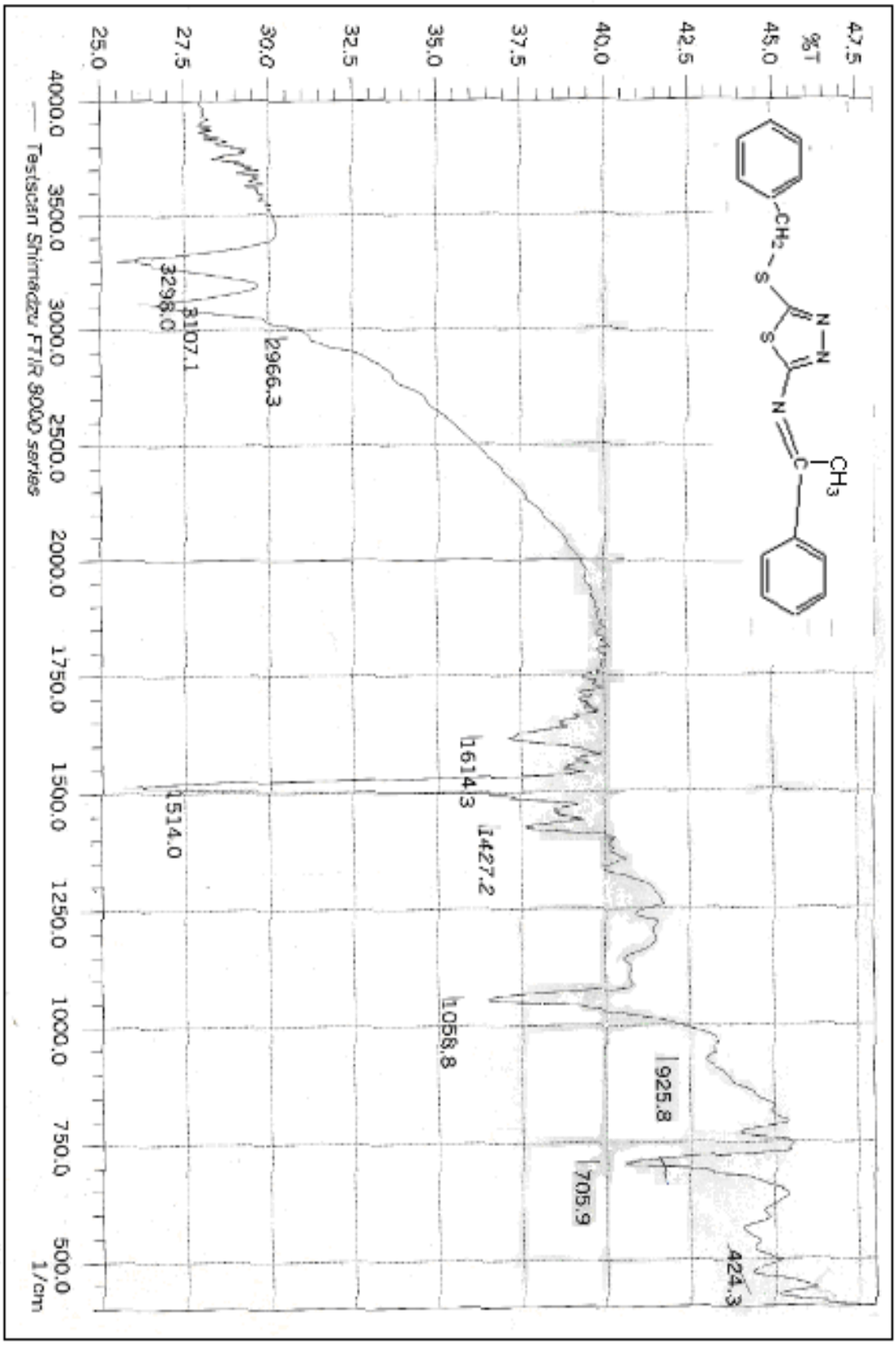

Figure (3-21). F.T.I.R spectrum of compound [**16**].

^{1}H-NMR spectra was also used for confirming of final compounds formation. ^{1}H-NMR spectrum of compound [**12**], (fig. 3-22), shows the following characteristic chemical shifts (DMSO-d_6, ppm). The signal at δ=2.503 ppm was due to DMSO and showed signals at δ=3.320 ppm belong to 2H of (–CH_2). The peaks δ=7.436 -7.747 ppm and δ=8.970 ppm, belong to 10H for the aromatic rings, and 1H for (CH=N) group, respectively.

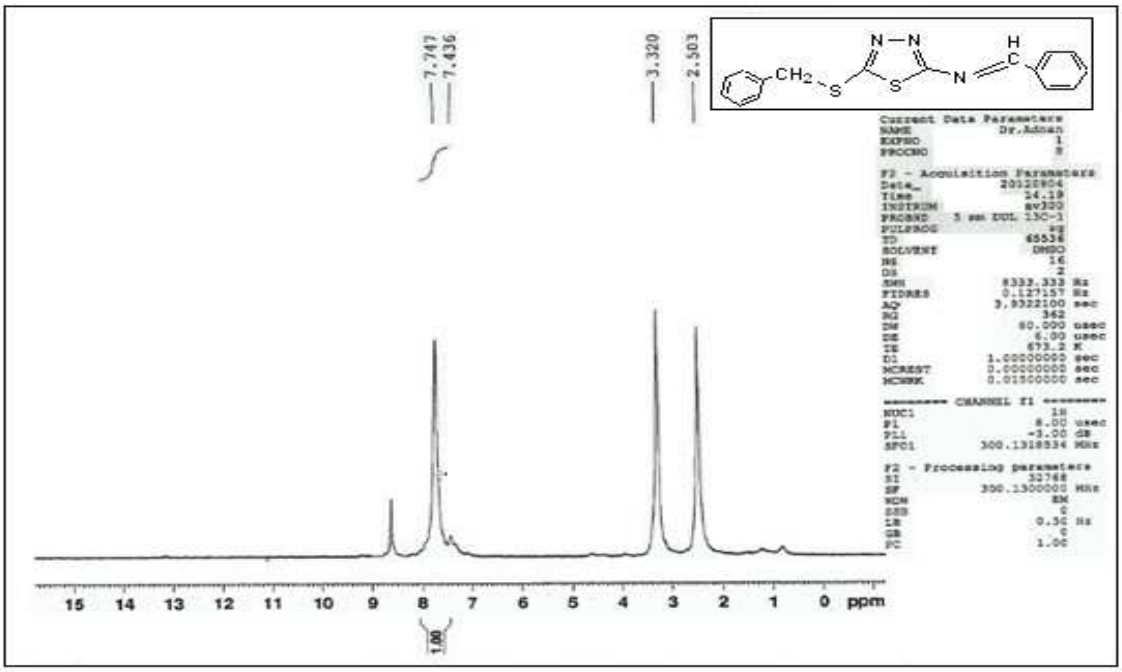

Figure (3-22). ^{1}H-NMR spectrum of compound [**12**].

^{1}H-NMR spectrum of compound [**13**], (fig. 3-23) [characteristic chemical shift at δ=2.503 was due to DMSO-d_6], shows peaks at δ=3.430 ppm, δ=7.556-8.913ppm, δ=8.990 ppm belong to 2H of –CH_2–, 9H for the aromatic rings, and 1H for (CH=N-) group, respectively.

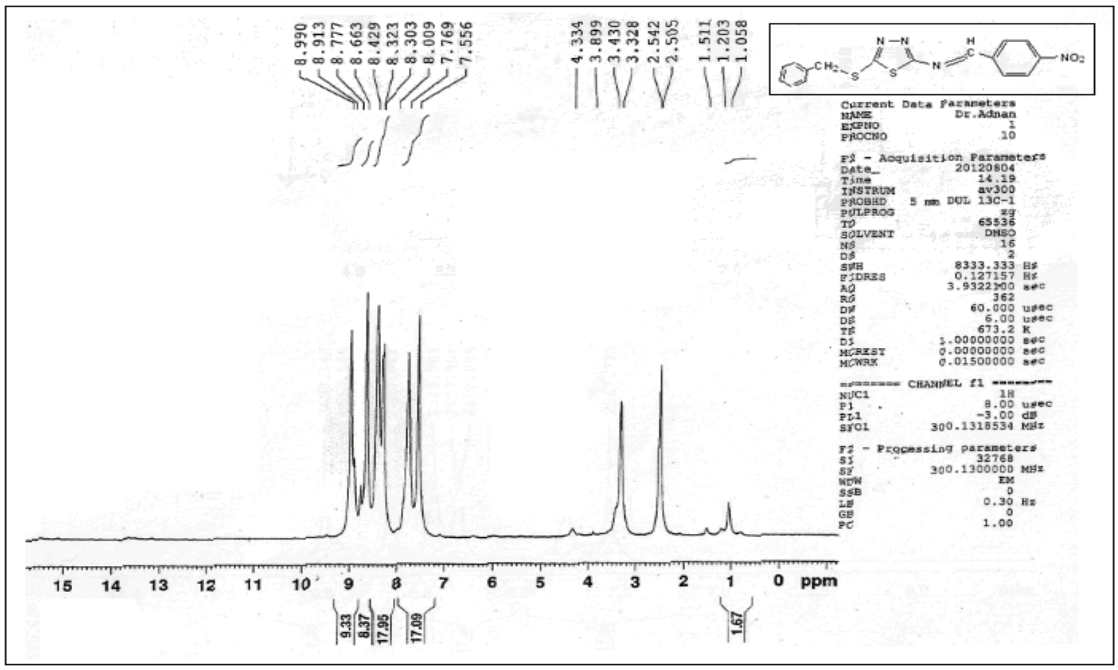

Figure (3-23). ^{1}H-NMR spectrum of compound [**13**].

^{1}H-NMR spectrum of compound [**14**], (fig. 3-24), shows peaks at δ=3.068 ppm, δ=4.549 ppm, and δ=6.798-7.832 ppm, δ=8.594 ppm belong to 6H for N-$(CH_3)_2$, 2H of -CH_2-, 9H for the aromatic rings , and 1H for (CH=N-) group, respectively.

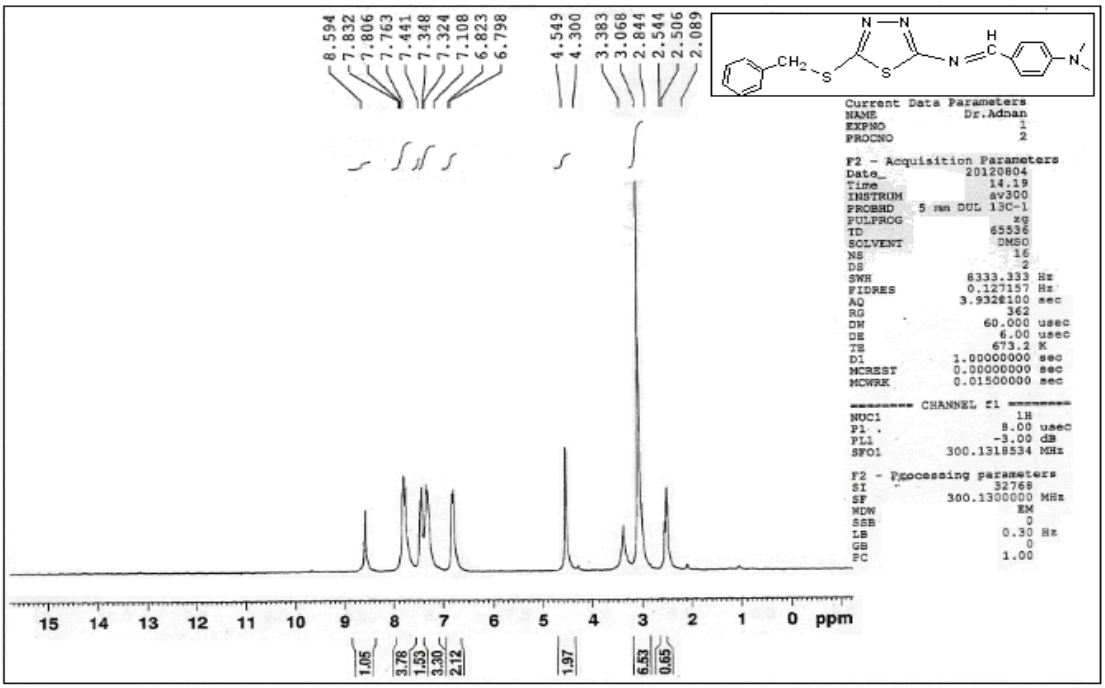

Figure (3-24). ^{1}H-NMR spectrum of compound [**14**].

^{1}H-NMR spectrum of compound [**15**], (fig. 3-25), shows the peaks at δ=3.562 ppm, δ=7.337-8.664 ppm, and δ=8.994 ppm belong to 2H of -CH_2-, 9H for the aromatic rings, and 1H for (CH=N-) group, respectively.

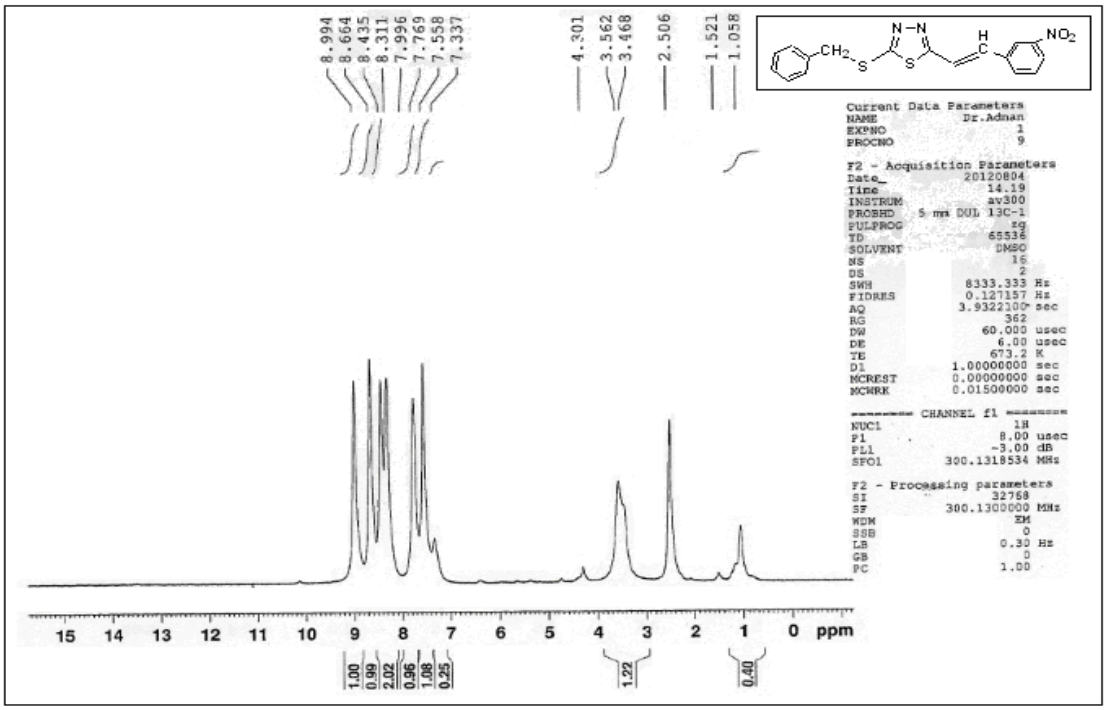

Figure (3-25). ^{1}H-NMR spectrum of compound [**15**].

^{1}H-NMR spectrum of compound [**16**], (fig. 3-26), shows peak at δ=2.511 ppm due to 3H of -CH_3 and peaks at δ=3.344 ppm, δ=7.331-8.214 ppm, belong to 2H of -CH_2-, 9H for the aromatic rings, respectively.

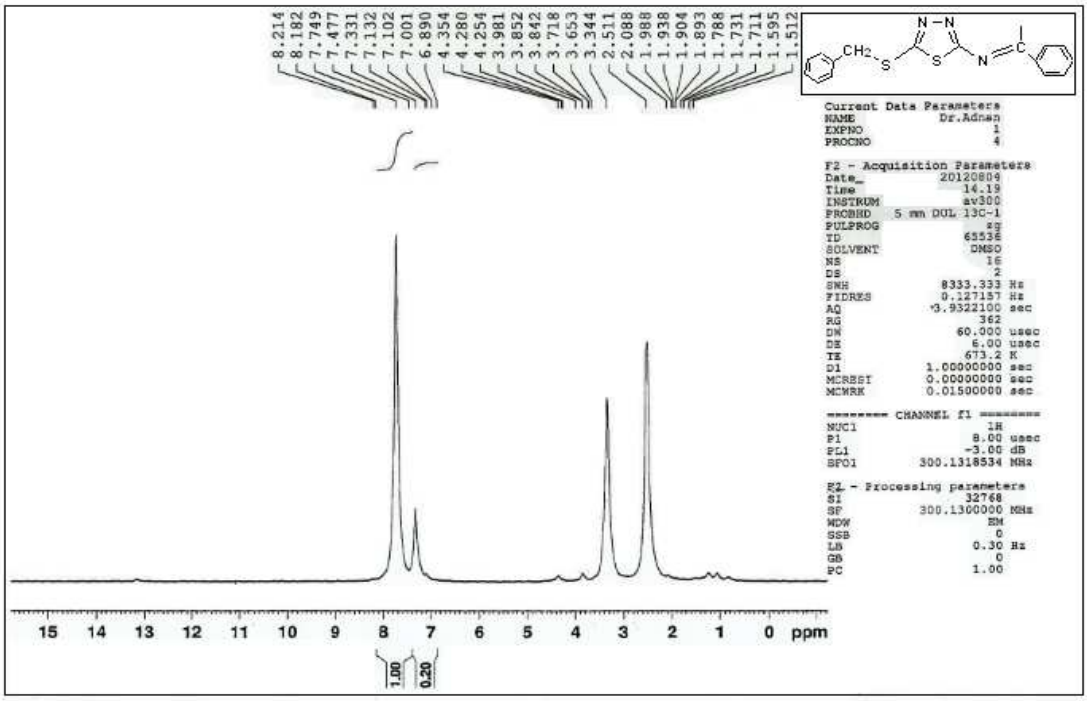

Figure (3-26). ^{1}H-NMR spectrum for compound [**16**].

UV-visible spectra of (E)-N-substituted benzylidene -5-(benzylthio)-1,3,4-thiadiazol-2-amines [**12-16**] in DMSO as a solvent at room temperature, main bands (λ_{max}) [81-84] (230–260 nm) low intensity bands are attributed to the $\pi \rightarrow \pi^*$ transitions of aromatic rings. The second band at 300–340 nm (or >300 nm, it depends on environment) is assigned to the $\pi \rightarrow \pi^*$ transitions (high intensity) of C=N group. The third band at < 400 nm involves $n \rightarrow \pi^*$ transitions (low intensity) of C=N group [84].

For compound **[12]**, the $n \rightarrow \pi^*$ transitions of C=N group seems to get completely masked by high intensity of $\pi \rightarrow \pi^*$ of C=N group and take place at λ_{max} 286 nm (fig. 3-27).

For compound **[13]**, high intensity of $\pi \rightarrow \pi^*$ of C=N group and take place at λ_{max} 294 nm, and red shift of $\pi \rightarrow \pi^*$ bands could be occurred and that caused by resonance effects of $-NO_2$ group (fig. 3-28). Low

intensity of n→ π* C=N group at λ_{max} 402 nm is coming from conjugation effects of presence of -NO_2 group and low intensity n→ π* C=N group at λ_{max} 515 nm could be caused by solute-solvent interactions [95]. For compound **[14]**, the n → π* transitions of C=N group seems to get completely masked by high intensity of π → π* of C=N group and takes place at 424 nm, and red shift of π → π* transitions could be occurred and that caused by resonance effects of –$N(CH_3)_2$ group (fig. 3-29).

For compound **[15]**, high intensity of π → π* of C=N group takes place at λ_{max} 276 nm, and the presence of nitro group at meta position caused low intensity of n→ π* C=N group at λ_{max} 475 nm [85] (fig. 3-30).

For compound **[16]**, the n → π* transitions of C=N group are completely masked by high intensity of π → π* of C=N group and take place at λ_{max} 288 nm [86] (fig. 3-31).

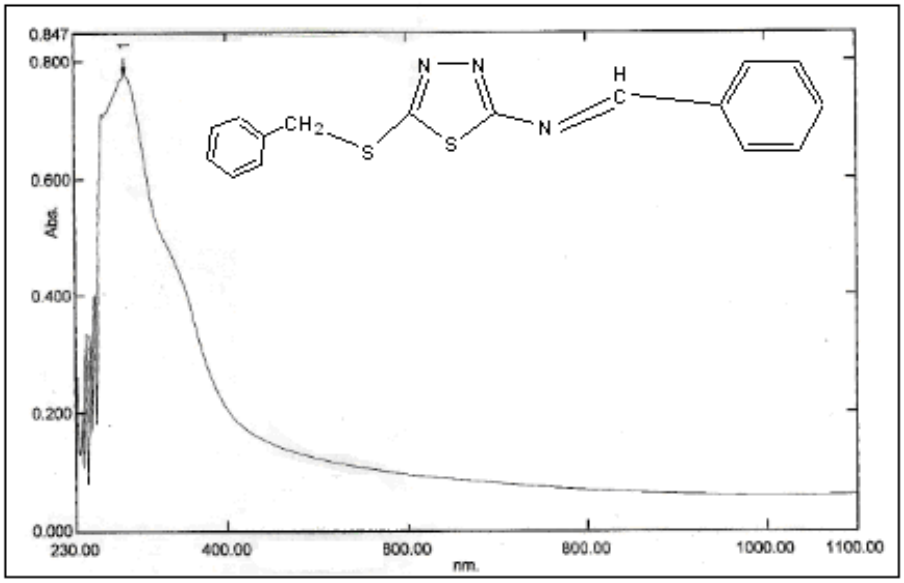

Figure (3-27). U.V. spectrum of compound [**12**].

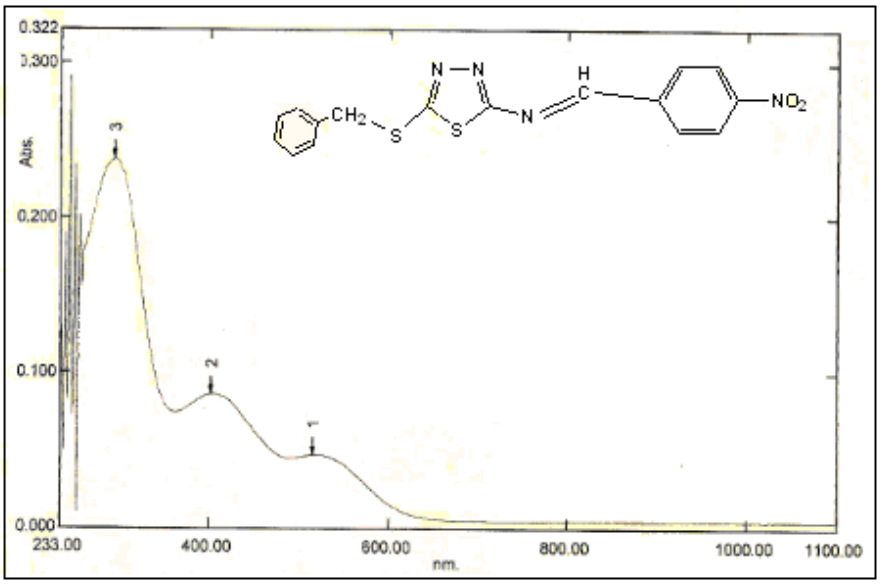

Figure (3-28). U.V. spectrum of compound [**13**].

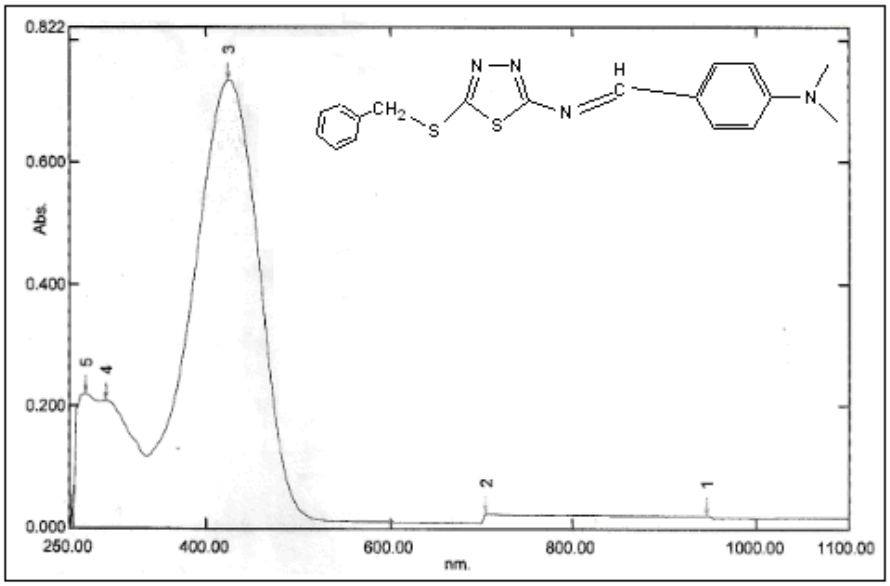

Figure (3-29). U.V. spectrum of compound [**14**].

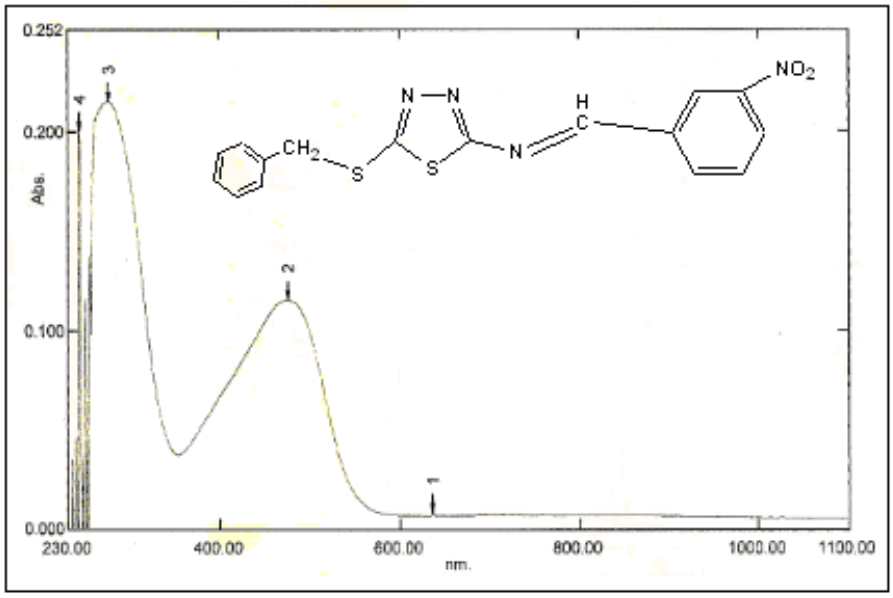

Figure (3-30). U.V. spectrum of compound [**15**].

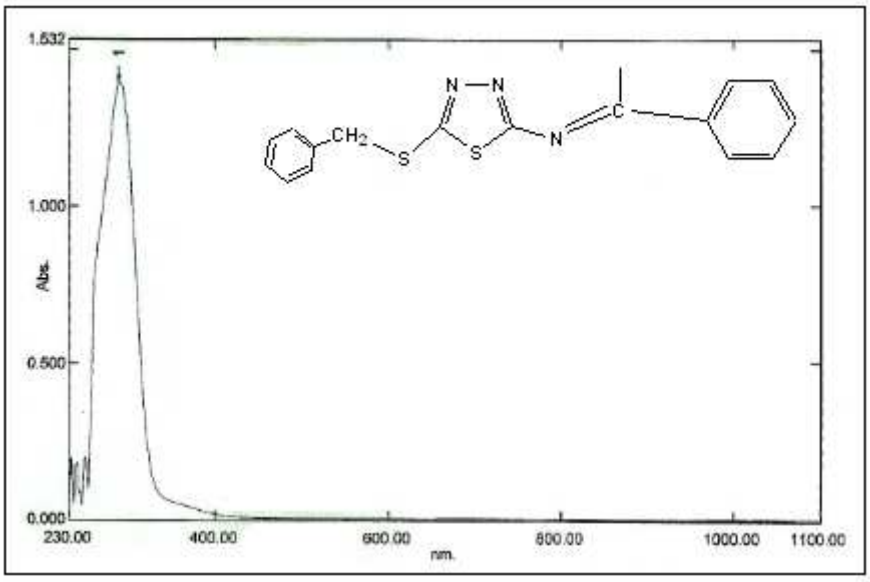

Figure (3-31). U.V. spectrum of compound [**16**].

3.5. Characterization of (E)-N-substituted benzylidene -5-(2-Chloro ethylthio)-1,3,4-thiadiazol-2-amine (**17-21**):

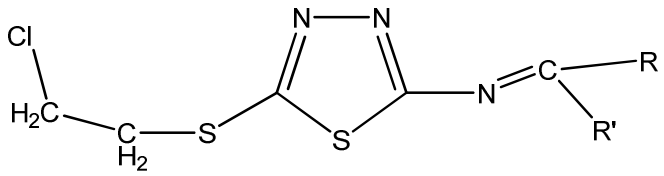

[17] R=C_6H_5, R'=H; **[18]** R=***p*-**NO_2-C_6H_4, R'=H; **[19]** R=***p*-**$(CH_3)_2N$-C_6H_4, R'=H; **[20]** R=***m*-**NO_2-C_6H_4, R'=H; **[21]** R=C_6H_5, R'=CH_3

These compounds [**17, 18, 19, 20, 21**] were prepared via reaction of equimolar of [7, 8, 9, 10 and 11] compounds with 1,2-dichloro ethane in alcoholic potassium hydroxide. Mechanism of this reaction followed SN_2 reaction, as shown below:

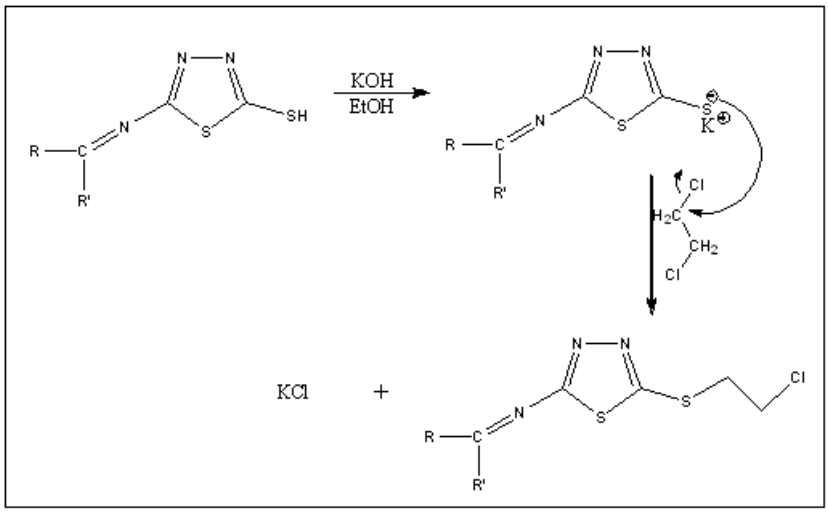

The FT-IR spectra of prepared compounds [**17, 18, 19, 20, 21**] shown in figures (3-32) to (3-36). On the other hand, the FT-IR data of prepared compounds above are listed in Table (3-4):

Table (3-4): FT-IR data of compounds [**17-21**] in cm^{-1}.

Comp No.	Fig. No.	ν C-H Aromatic	ν C-H aliphatic	ν C=N	ν C-S	ν c-cl	Other Bands
[**17**]	(3-32)	3100	2929	1566	705	٦٥٠	-
[**18**]	(3-33)	3090	2937	1566	725	-	ν p-NO_2 1348
[**19**]	(3-34)	3085	2920	1587	671	-	ν p-N-CH_3 817
[**20**]	(3-35)	3080	2927	1570	680	-	ν m-NO_2 1485 1350
[**21**]	(3-36)	3087	2931	1613	700	٦٣٠	-

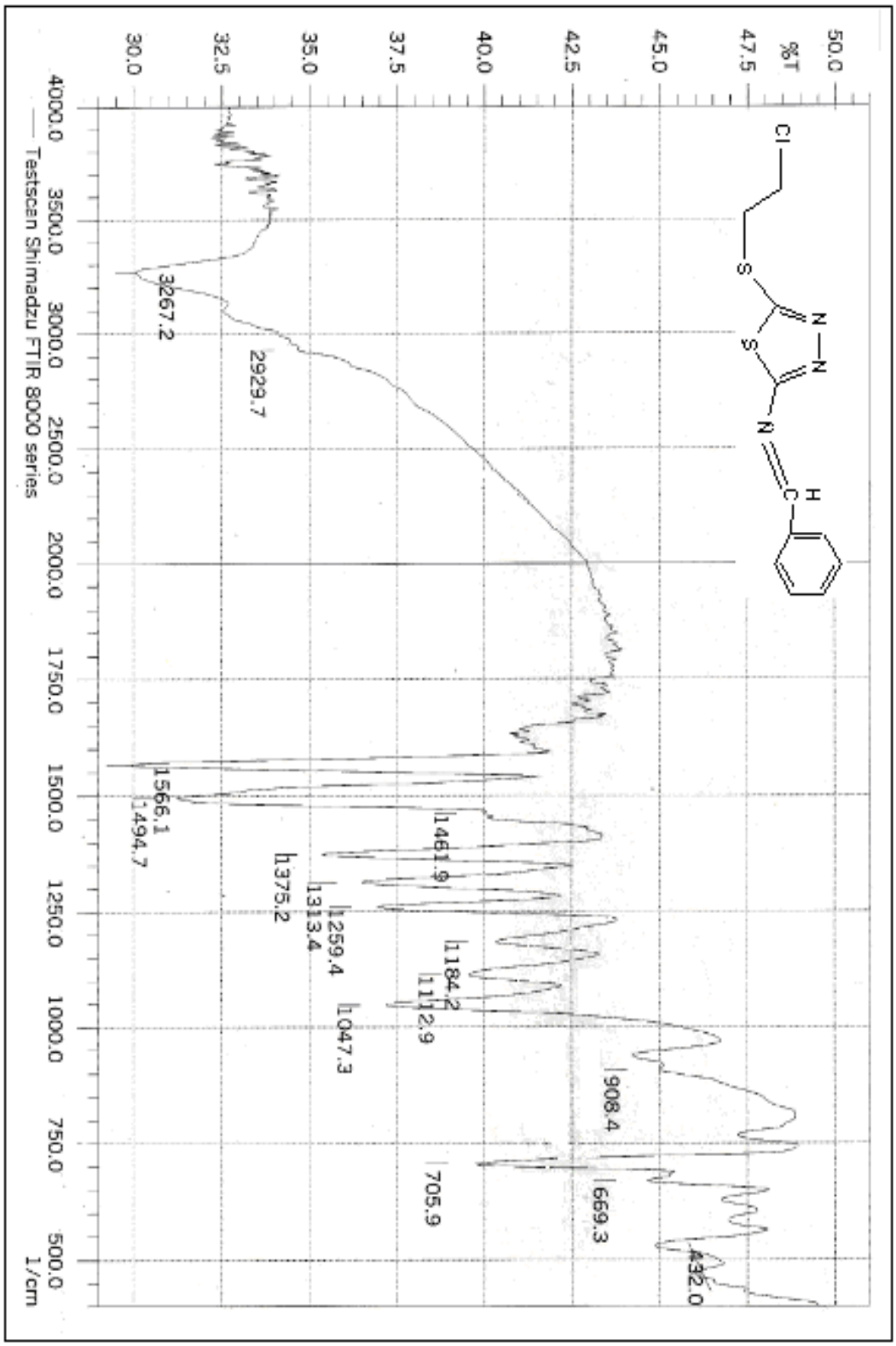

Figure (3-32). F.T.I.R spectrum of compound [**17**].

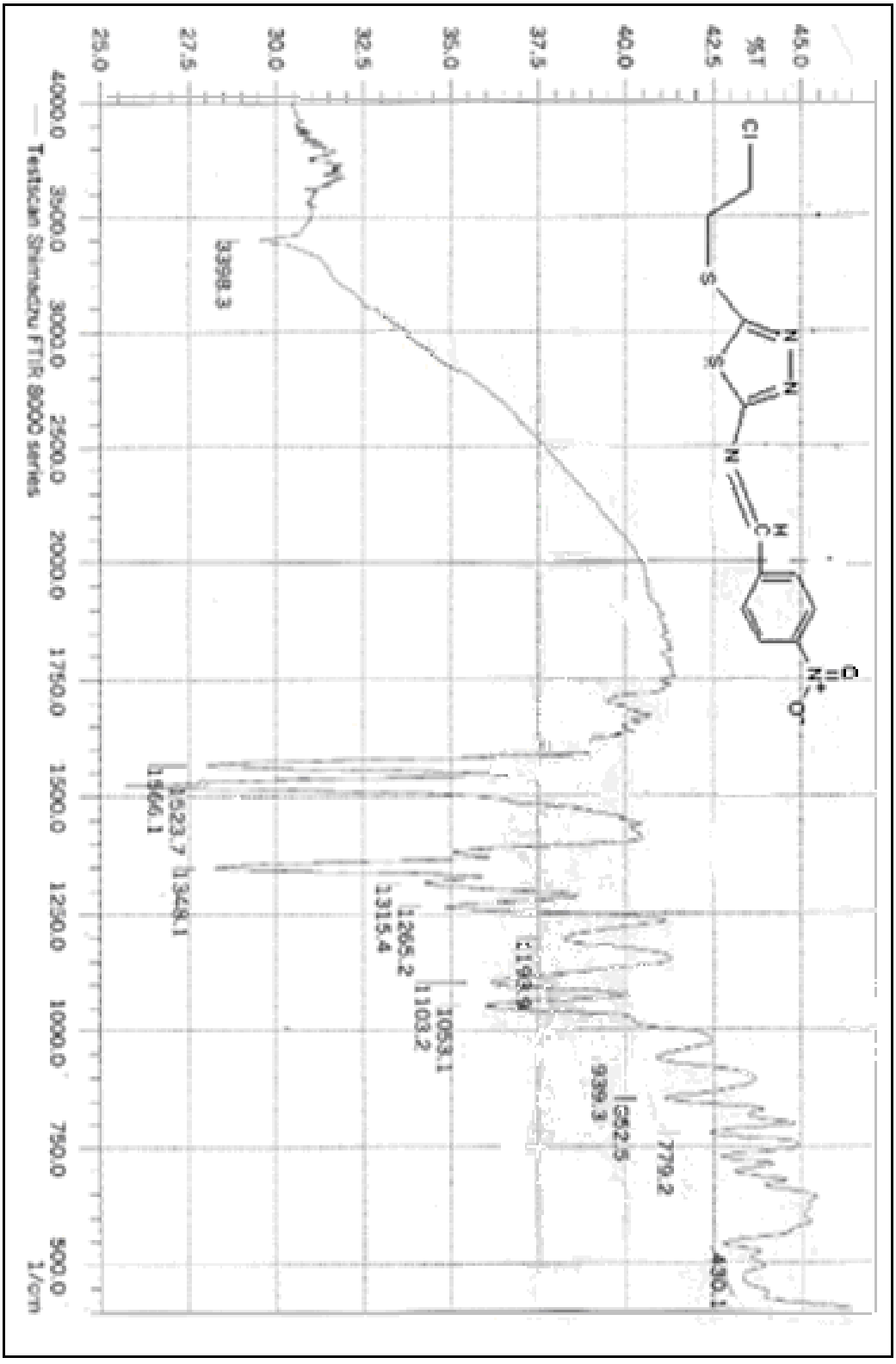

Figure (3-33). F.T.I.R spectrum of compound [**18**].

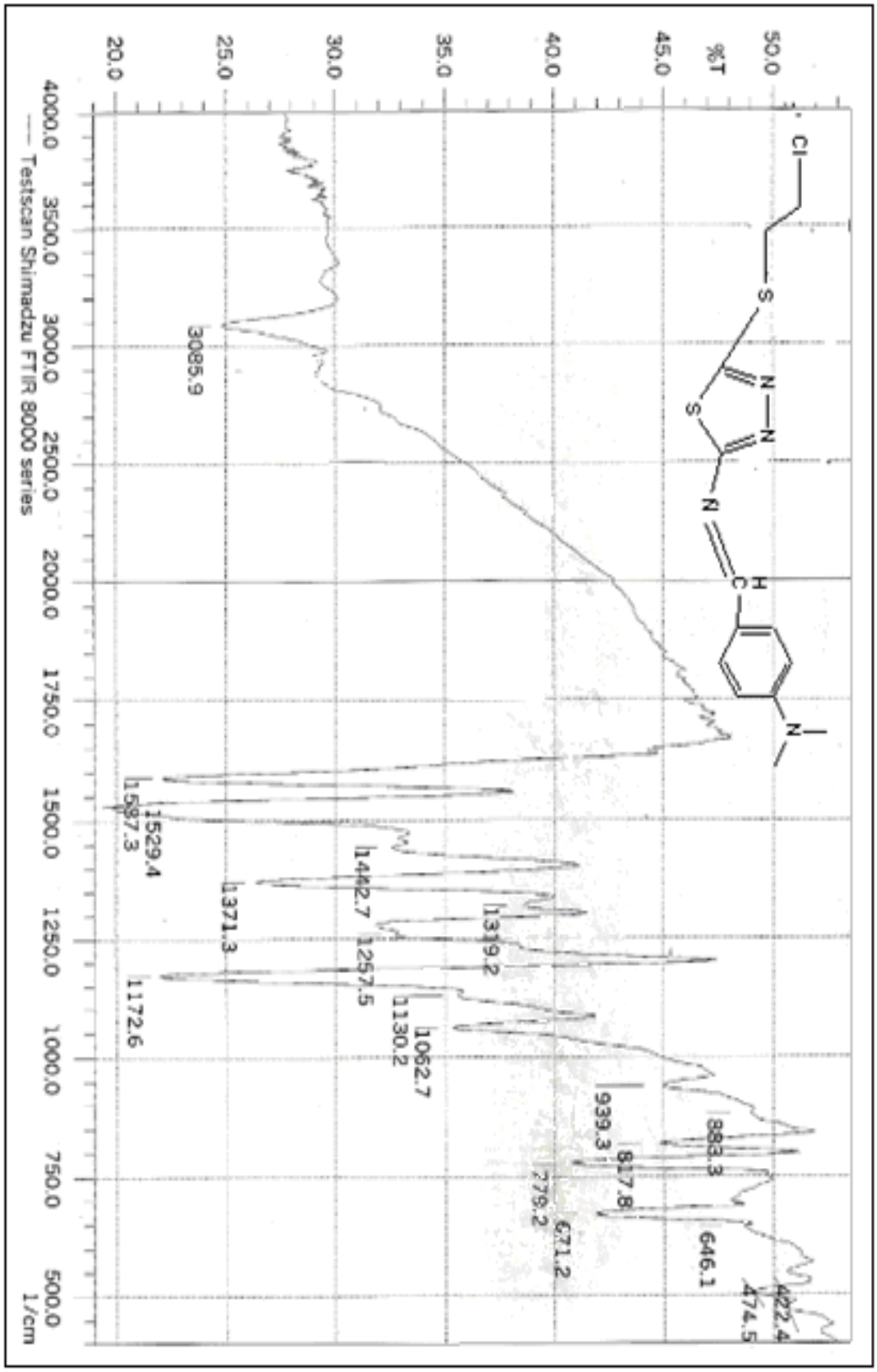

Figure (3-34). F.T.I.R spectrum of compound [**19**].

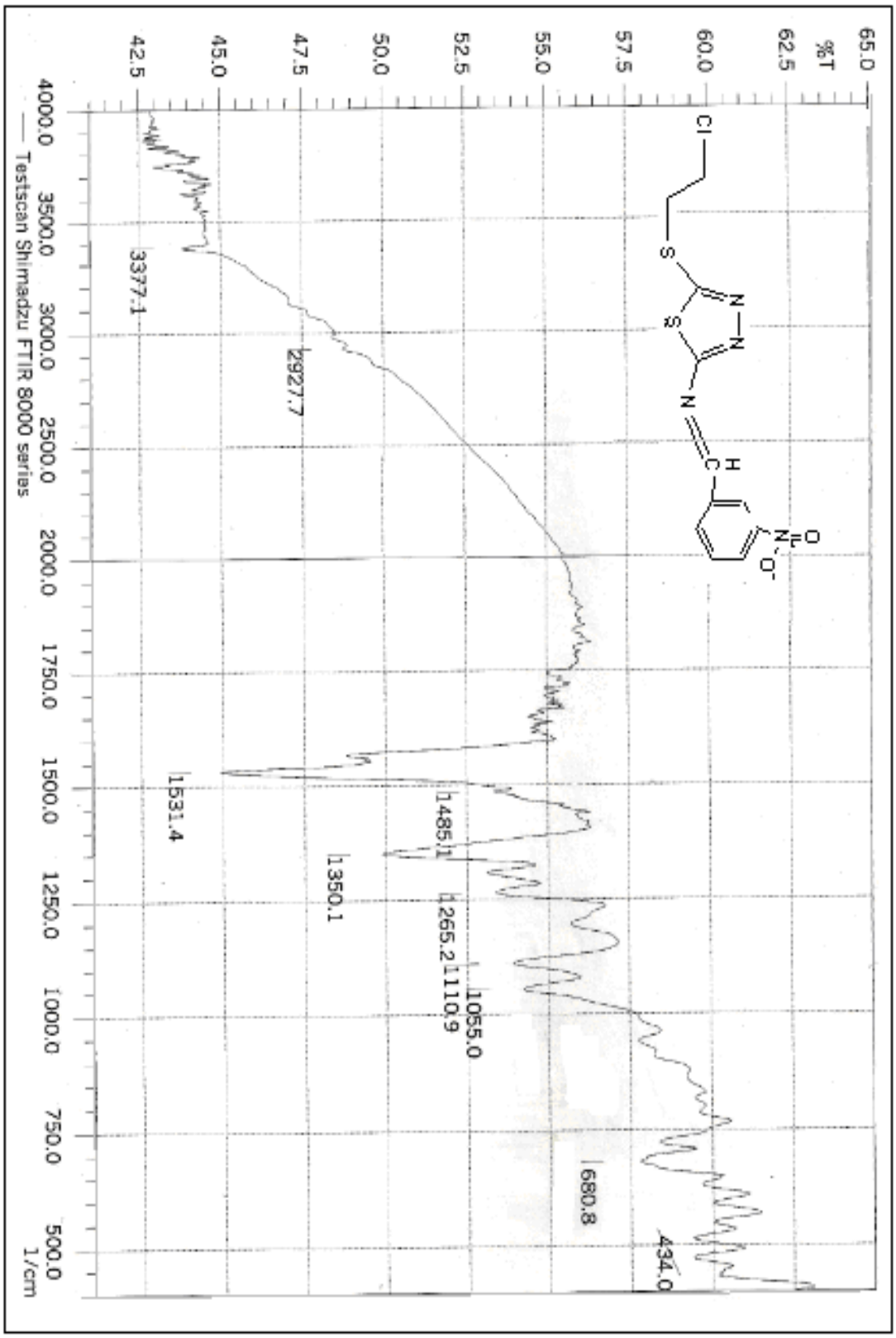

Figure (3-35). F.T.I.R spectrum of compound [**20**].

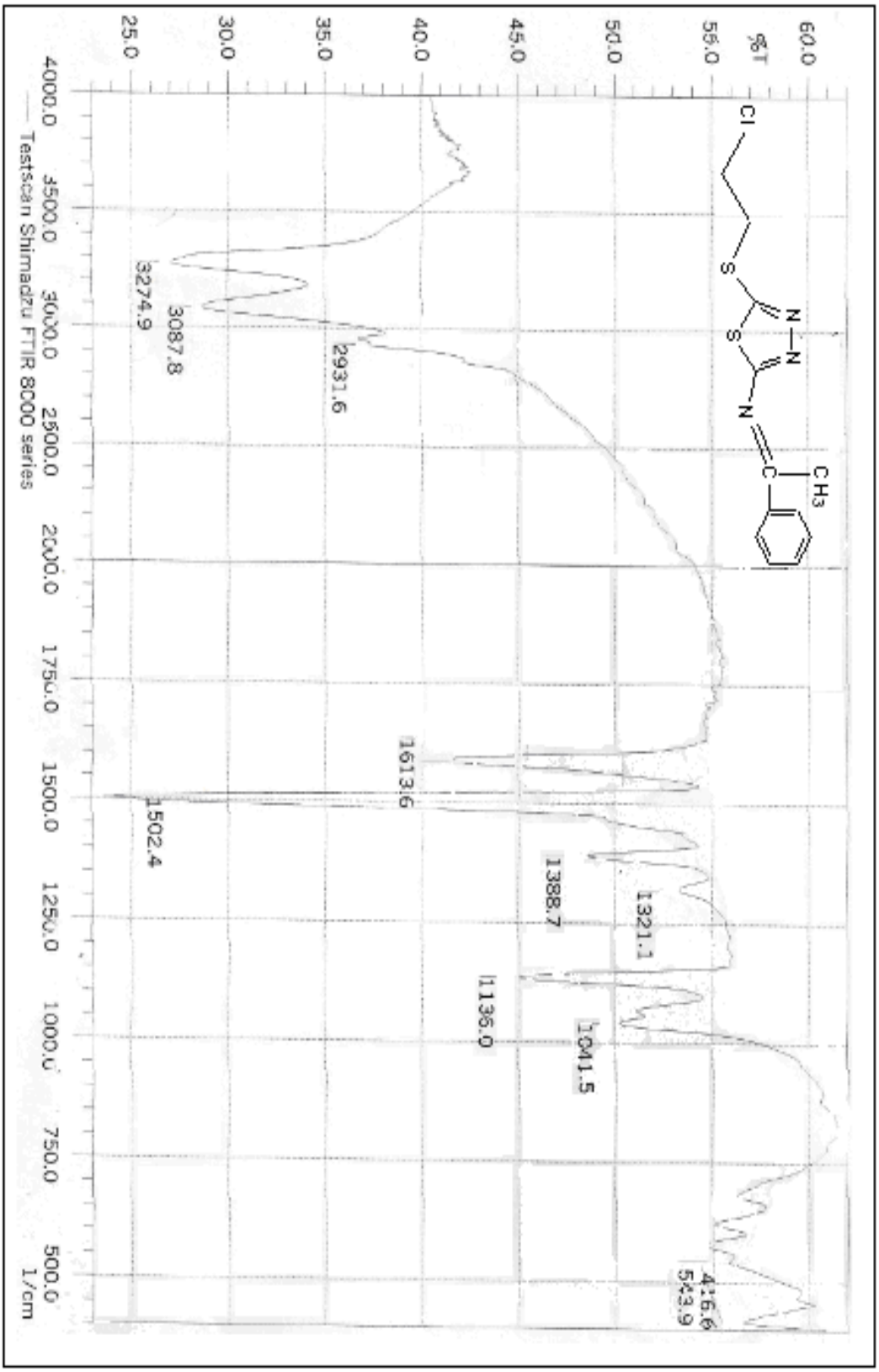

Figure (3-36). F.T.I.R spectrum of compound [**21**].

^{1}H-NMR spectrum of compound [**17**], (fig. 3-37) [characteristic chemical shift at δ=2.503 ppm was due to DMSO-d_6], shows peak at δ=3.366 ppm belong to 4H of (-CH_2-CH_2-), it could be overlap. The peaks δ=7.329-7.750 ppm, δ=8.970 ppm (overlapping), 5H for the aromatic ring, and 1H for imine group, respectively.

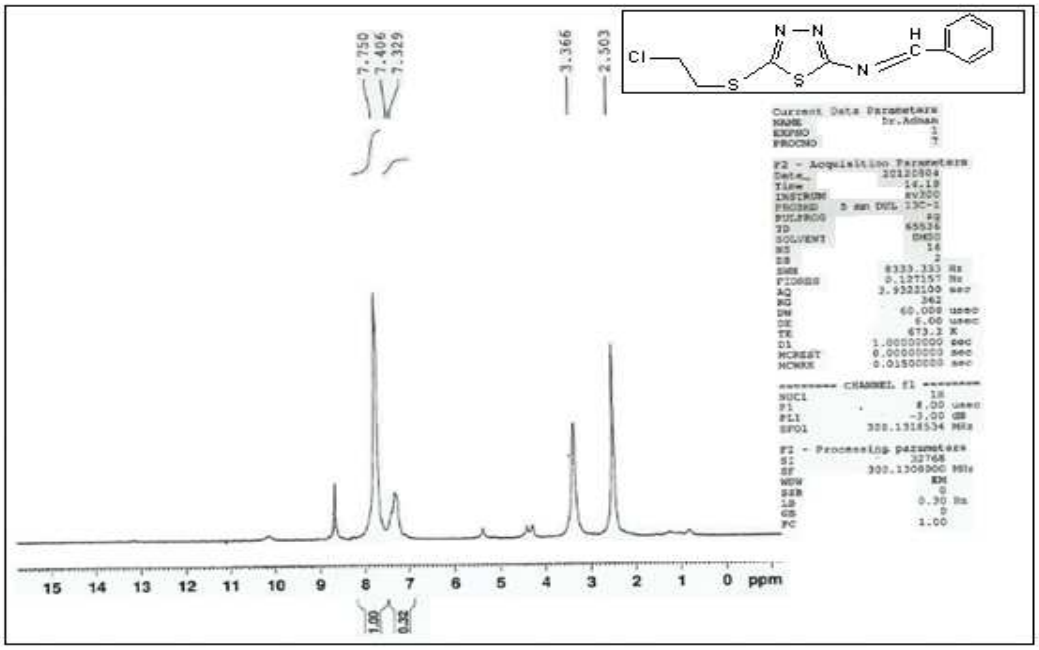

Figure (3-37). ^{1}H-NMR spectrum of compound [**17**].

^{1}H-NMR spectrum of compound [**18**], (fig. 3-38), shows the peaks at δ=3.328 ppm belong to 4H of (-CH_2-CH_2-), it could be overlap. The peaks at δ=7.522-8.251 ppm and δ=8.972 ppm, belong to 4H for the aromatic ring, and 1H for imine group, respectively.

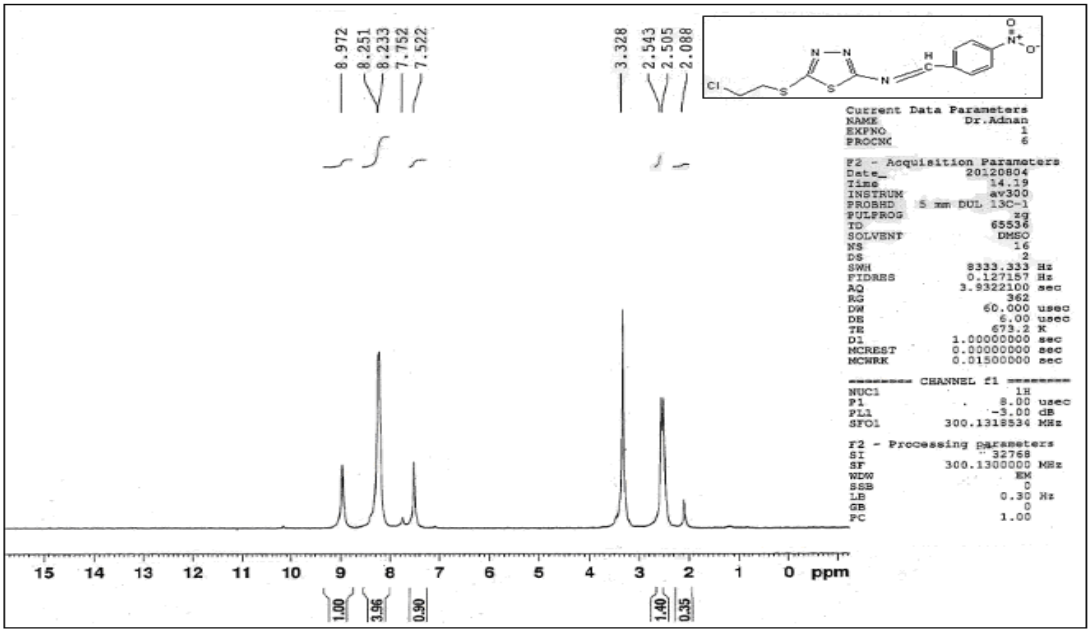

Figure (3-38). ^{1}H-NMR spectrum of compound [**18**].

^{1}H-NMR spectrum of compound [**19**], (fig.3-39), shows the peaks at δ=3.073-3.333 ppm for (-N(CH_3)$_2$) and 4H of (-CH_2-CH_2-). The peaks at δ=6.797-7.82 ppm and δ=8.466 ppm belongs to 4H for the aromatic ring, and 1H for imine group, respectively.

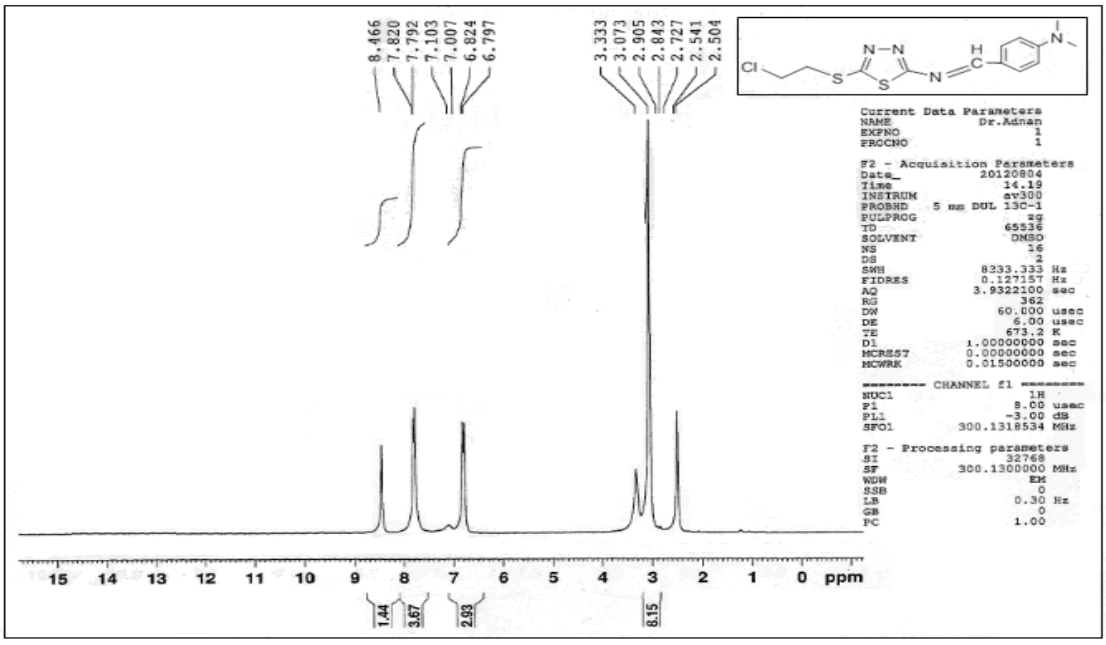

Figure (3-39). ^{1}H-NMR spectrum of compound [**19**].

^{1}H-NMR spectrum of compound [**20**], (fig. 3-40), shows the peak at δ=3.344 ppm for 4H of (-CH_2-CH_2-), it could be overlap. The peaks δ=7.289-8.254 ppm and δ=8.973 ppm belongs to 4H for the aromatic ring, and 1H for imine group, respectively.

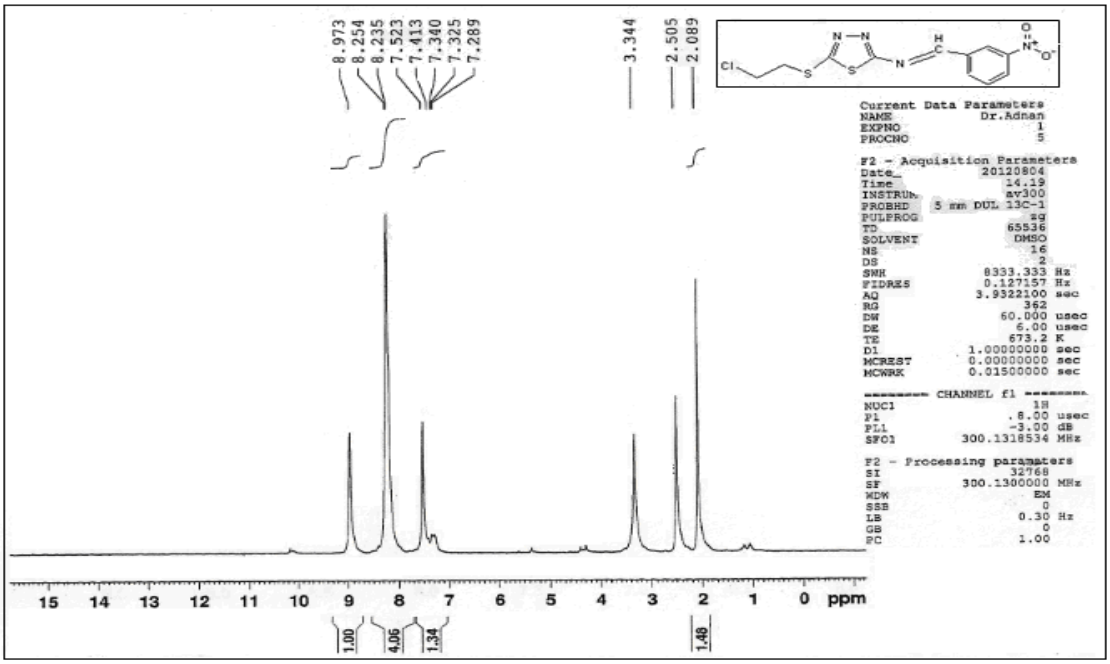

Figure (3-40).^{1}H-NMR spectrum of compound [**20**].

UV-visible spectra of (E)-N-substituted benzylidene -5-(2-Chloroethylthio)-1,3,4-thiadiazol-2-amine compounds [**17**]-[**21**] in DMSO as a solvent and at room temperature.

For compound [**17**], n→ π* transition of C=N group seems to get completely masked by high intensity of π → π* of C=N group and take place at 323 nm, (fig. 3-41).

For compound **[18],** high intensity bands of π → π* of C=N group take place at 305 nm, (fig. 3-42). Low intensity of n→ π* C=N group at λ_{max}

416 nm and low intensity n→ π* C=N group at λ_{max} 521 nm could be caused by solute-solvent interactions [94].

Compound **[19]**, the n → π* bands of C=N group seem to get completely masked by high intensity of π → π* of C=N group and take place at λ_{max} 434 nm, and red shift of π → π* bands of C=N group could be occurred and that caused by resonance effects of $-N(CH_3)_2$ group (fig. 3-43).

For compound **[20]**, high intensity of π→ π* bands of C=N group take place at λ_{max} 265 nm, low intensity n → π* of C=N group take place at 389 nm, (fig. 3-44).

For compound **[21]**, n → π* bands of C=N group seem to get completely masked by high intensity of π → π* of C=N group and take place at λ_{max} 323 nm, (fig. 3-45).

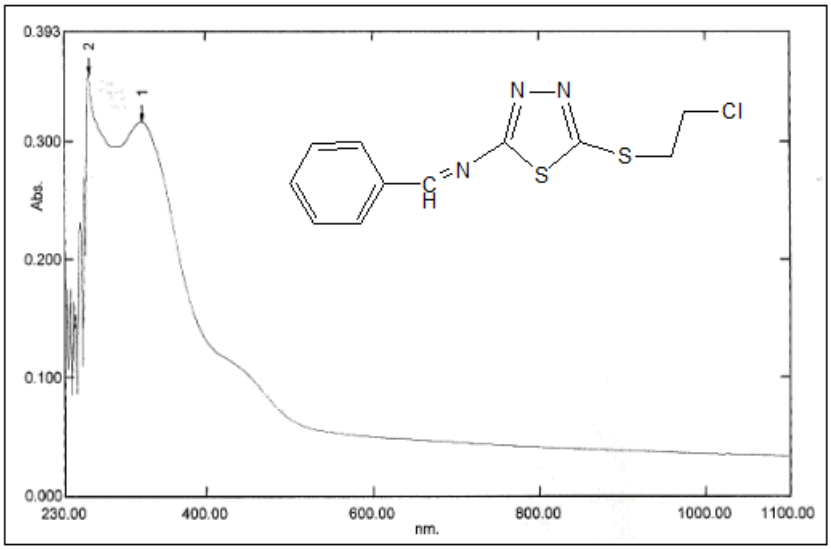

Figure (3-41). U.V. spectrum for compound [**17**].

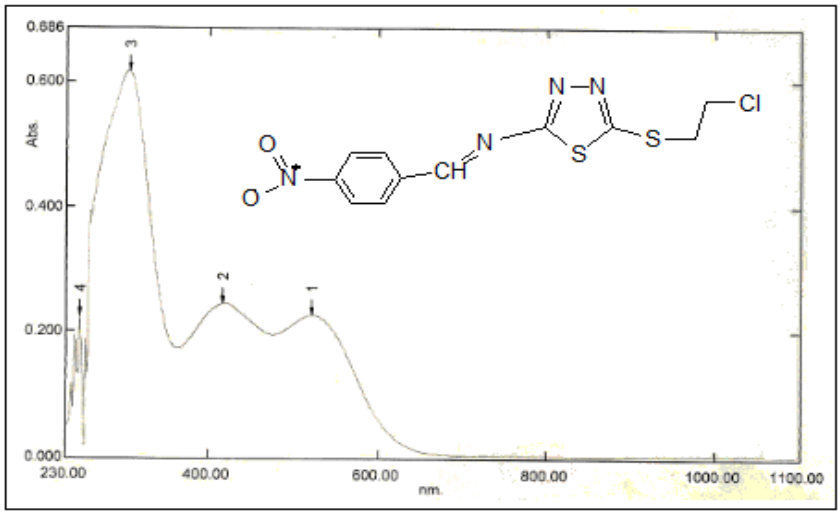

Figure (3-42) U.V. spectrum for compound [**18**].

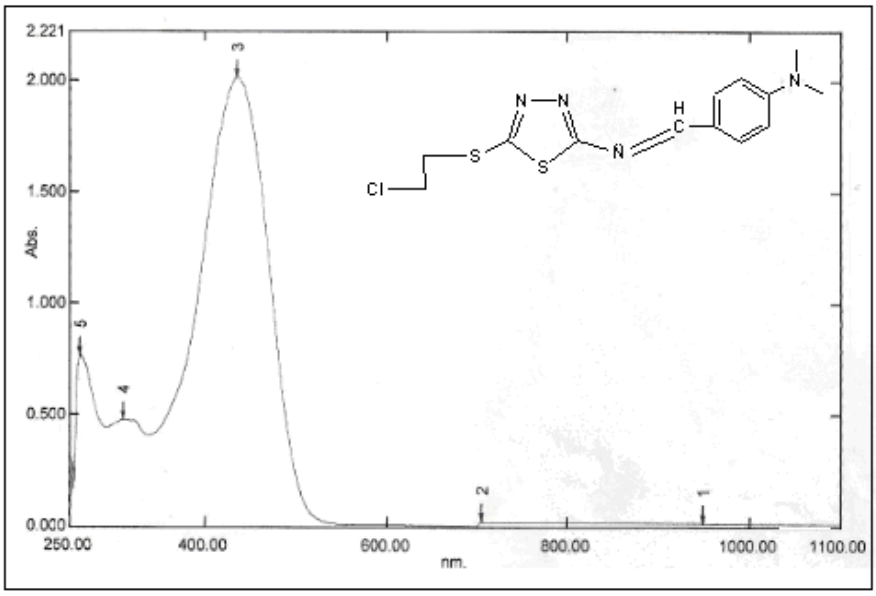

Figure (3-43). U.V. spectrum for compound [**19**].

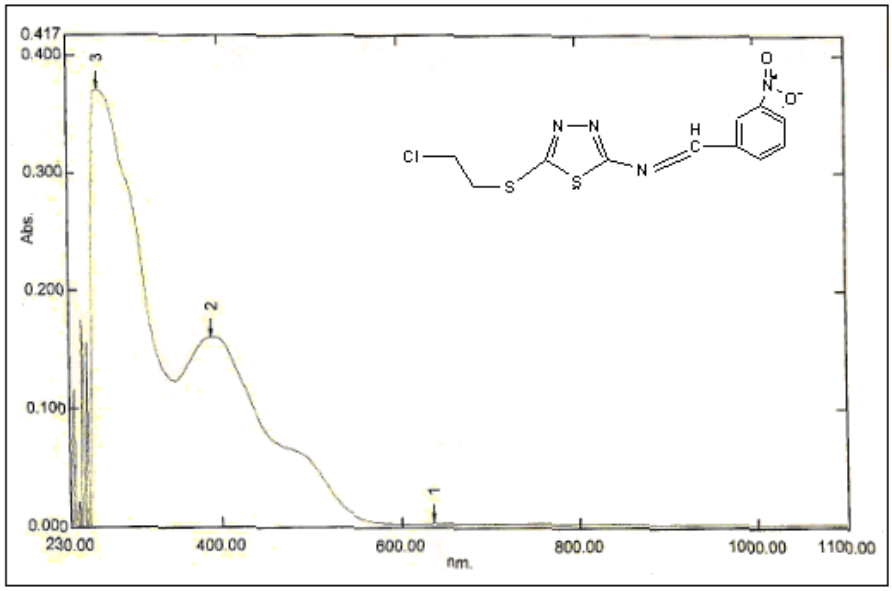

Figure (3-44). U.V. spectrum for compound [**20**].

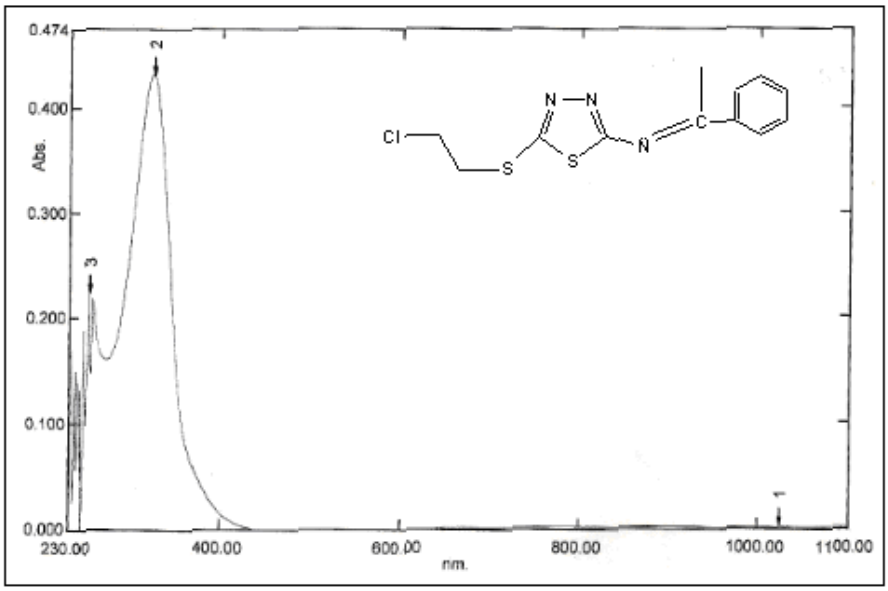

Figure (3-45). U.V. spectrum for compound [**21**].

3.6. Weight loss measurement and Theoretical calculations:

3.6.1. Weight loss measurement:

The prepared compounds [**1-5** and **12-21**] were used as inhibitors for the corrosion, the values of corrosion rate, surface coverage and inhibition efficiency from weight loss measurements at different concentrations of compounds [**1-5** and **12-21**] after 8 hours immersion of mild steel in 1M H_2SO_4 at 30^oC are summarized in Table (3-5) and Table (3-6), respectively.

First, the inhibition efficiency of compounds [**1-5**] as a function of concentration is shown in figure(3-46). The results of Table (3-5) and figure(3-46) show that as the inhibitor concentration increases, the corrosion rate decreases and therefore the inhibition efficiency increases. It can be concluded that this inhibitor acts through adsorption on mild steel surface and formation of a barrier layer between the metal and the corrosive media. The inspection of results of E (%) in Table (3-5) indicates that the protection efficiency E (%) increases with increasing the concentration of suggested inhibitors with the maximum inhibition efficiencies were achieved at 10^{-3} M. Thus, the comparative study reveals that order of maximum inhibition efficiency as follow: [**1**]> [**5**]> [**3**]> [**2**]> [**4**]. That order could be explain by the effect of molecular structure of organic inhibitors on inhibition efficiency, as well as adsorption process.

In order to confirm the adsorption of compounds [**1-5**] on mild steel surface, adsorption isotherms were studied. Adsorption isotherms can provide basic information on the interaction of inhibitor and metal

surface. Thus, the degree of surface coverage values (θ), at different inhibitor concentrations in 1 M H_2SO_4 was evaluated from weight loss measurements (θ= E (%)/100, Table (3-5)) at 30^oC and tested graphically for fitting to a suitable adsorption isotherm. The plot of (C/θ) against inhibitor concentration (C) (Figure 3-47) yields a straight line.

The negative values of ΔG^o_{ads} (as shown in Table 3-5) indicates spontaneous adsorption of [**1]-[5**] molecules on the mild steel surface and a strong interaction between inhibitor molecules and metal surface. The value of ΔG^o_{ads} is less than -40 kJ/mol, indicating electrostatic interaction between the charged metal surface, i.e., physical adsorption [95,96].

Table 3-5:Corrosion rate, inhibition efficiency, surface coverage (θ) and standard free energy of adsorption in the presence and absence of different concentrations of 2-[substituted-hydrazine] carbothioamides for the corrosion of mild steel in 1 M H_2SO_4 from weight loss measurements.

Inhibitor concentration (M)	1M H_2SO_4				
	ΔM(g)	Corrosion rate (mg cm^{-2} h^{-1})	E%	θ	ΔG^o_{ads} (KJ/mol)
Uninhibited	0.113	2.8775	-	-	
[1]					
0.001	0.0052	0.1324	95.39	0.9539	-32.45 (R^2=0.9658)
0.0001	0.0788	2.0066	30.26	0.3026	
0.00005	0.0839	2.1365	25.75	0.2575	
0.00001	0.0893	2.274	20.97	0.2097	
[2]					
0.001	0.0376	0.9574	66.72	0.6672	-35.50 (R^2=0.9984)
0.0001	0.0621	1.5813	45.04	45.04	
0.00005	0.0632	1.6093	44.07	0.4407	
0.00001	0.0653	1.6628	42.21	0.4221	
[3]					
0.001	0.0344	0.8759	69.55	0.6955	-41.68 (R^2=0.9999)
0.0001	0.0373	0.9498	66.99	0.6699	
0.00005	0.0383	0.9753	66.1	0.661	
0.00001	0.0396	1.0084	64.95	0.6495	
[4]					
0.001	0.0474	1.207	58.05	0.5805	-34.68 (R^2=0.9999)
0.0001	0.061	1.5533	46.01	0.4601	
0.00005	0.0721	1.8131	36.99	0.3699	
0.00001	0.0995	2.5337	11.94	0.1194	
[5]					
0.001	0.017	0.4329	84.95	0.8495	-31.43 (R^2=0.9956)
0.0001	0.0737	1.8767	34.78	0.3478	
0.00005	0.0941	2.3962	16.72	0.1672	
0.00001	0.1071	2.7273	5.22	0.0522	

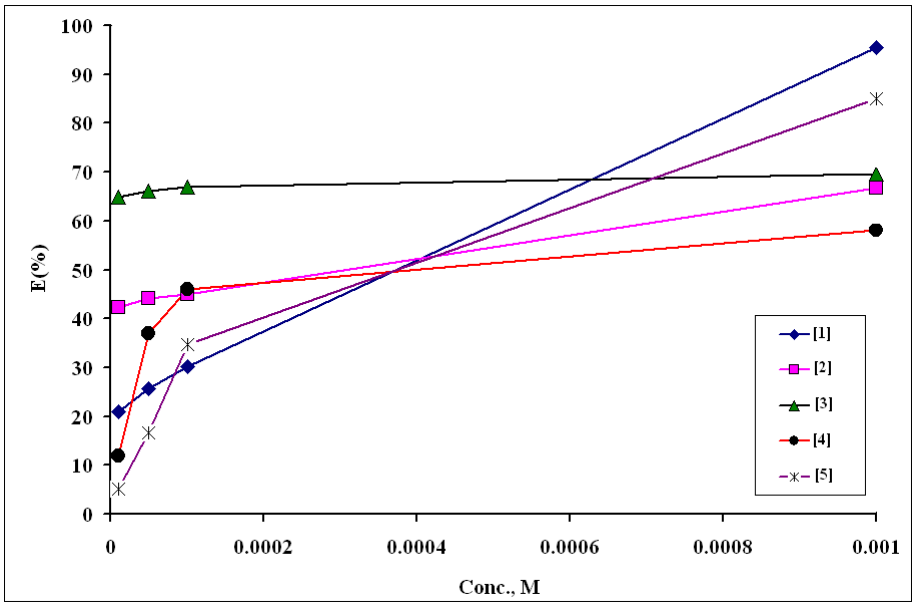

Figure (3-46). Effect of inhibitor concentration on the efficiencies of mild steel obtained at 30°C in 1 M H_2SO_4 containing different concentrations of prepared inhibitors [**1**]-[**5**].

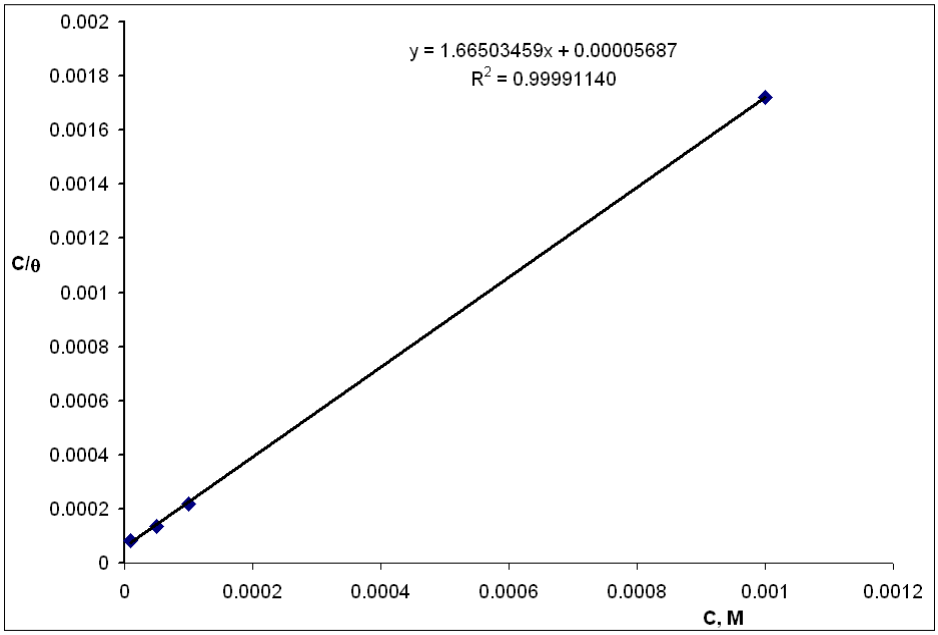

Figure(3-47). Langmuir adsorption isotherm plot for mild steel in 1M H_2SO_4 solution in the presence of various concentrations of inhibitor [**4**].

Second, the results of inhibition efficiency of compounds [**12-21**] in Table (3-6) show that as the inhibitor concentration increases, the corrosion rate decreases and therefore the inhibition efficiency increases. Also, the inhibition efficiency of compounds [**12-21**] as a function of concentrations is shown in Figure(3-48) and Figure(3-49). It can be concluded that this inhibitor acts through adsorption on mild steel surface and formation of a barrier layer between the metal and the corrosive media. The inspection of results of E (%) in Table (3-6) indicates that the protection efficiency E (%) increases with increasing the concentration of suggested inhibitors with the maximum inhibition efficiencies were achieved at 10^{-3} M. Thus, the comparative study reveals that order of maximum inhibition efficiency as follow: [**16**]> [**12**]> **[14**]> [**13]**> [**15**] and [**19**]> [**20**]> [**18]** > **[21**]> [**17**]. That order could be explain by the effect of molecular structure of organic inhibitors on inhibition efficiency, as well as adsorption process.

In order to confirm the adsorption of compounds [**12-21**] on mild steel surface, adsorption isotherms were studied. Adsorption isotherms can provide basic information on the interaction of inhibitor and metal surface. Thus, the degree of surface coverage values (θ), at different inhibitor concentrations in 1 M H_2SO_4 was evaluated from weight loss measurements (θ= E (%)/100, see Table (3-6)) at 30^oC and tested graphically for fitting to a suitable adsorption isotherm. The plot of (C/θ) against inhibitor concentration (C) (see Figure (3-50)) yields a straight line.

The negative values of ΔG^o_{ads} (as shown in Table 3-6) indicates spontaneous adsorption of [**12-21**] molecules on the mild steel surface

and strong interaction between inhibitor molecules and metal surface. The value of ΔG^{o}_{ads} is less than -40 kJ/mol, it's indicating that electrostatic interaction between the charged metal surface, i.e., physical adsorption [95,96].

Table (3-6):Corrosion rate, inhibition efficiency, surface coverage (θ) and standard free energy of adsorption in the presence and absence of different concentrations of 2-N-substituted benzylidene -5-(benzylthio)-1,3,4-thiadiazol-2-aminefor the corrosion of mild steel in 1M H_2SO_4 from weight loss measurements.

Inhibitor concentration (M)	1 M H_2SO_4				
	ΔM(g)	Corrosion rate(mg cm^{-2} h^{-1})	E%	θ	ΔG^{o}_{ads} (KJ/mol)
Uninhibited	0.113	2.8775	-	-	
[12]					
0.001	0.0115	0.2928	89.82	0.8982	-42.69 (R^2=0.9999)
0.0001	0.013	0.3310	88.50	0.8850	
0.00005	0.0188	0.4787	83.36	0.8336	
0.00001	0.0189	0.4812	83.27	0.8327	
0.000005	0.0404	1.0287	64.25	0.6425	
[13]					
0.001	0.0316	0.8046	72.04	0.7204	-35.28 (R^2=0.9983)
0.0001	0.0385	0.9804	65.93	0.6593	
0.00005	0.0715	1.8207	36.73	0.3673	
0.00001	0.0719	1.8309	36.37	0.3637	
0.000005	0.0759	1.9327	32.83	0.3283	
[14]					
0.001	0.0273	0.6951	75.84	0.7584	-35.30 (R^2=0.9972)
0.0001	0.0464	1.1815	58.94	0.5894	
0.00005	0.0771	1.9633	31.77	0.3177	
0.00001	0.0772	1.9658	31.68	0.3168	
0.000005	0.0959	2.4420	15.13	0.1513	
[15]					
0.001	0.0347	0.8836	69.29	0.6929	-25.20 (R^2=0.9990)
0.0001	0.0546	1.3903	51.68	0.5168	
0.00005	0.0699	1.7800	38.14	0.3814	
0.00001	0.0707	1.8003	37.43	0.3743	
0.000005	0.1034	2.6330	8.5	0.085	
[16]					
0.001	0.01	0.2546	91.15	0.9115	-37.96 (R^2=0.9989)
0.0001	0.0378	0.9625	66.55	0.6655	
0.00005	0.0384	0.9778	66.02	0.6602	

0.00001	0.0394	1.0033	65.13	0.6513	
0.000005	0.0609	1.5508	46.11	0.4611	
[17]					
0.001	0.0508	1.2936	55.04	0.5504	
0.0001	0.0655	1.6679	42.04	0.4204	-36.42 (R^2=0.9992)
0.00005	0.0697	1.7749	38.32	0.3832	
0.00001	0.0698	1.7774	38.23	0.3823	
0.000005	0.0824	2.0983	27.08	0.2708	
[18]					
0.001	0.0423	1.0771	62.57	0.6257	
0.0001	0.0675	1.7188	40.27	0.4027	
0.00005	0.0679	1.7290	39.91	0.3991	-35.40 (R^2=0.9979)
0.00001	0.0709	1.8054	37.26	0.3726	
0.000005	0.0959	2.4344	15.40	0.1540	
[19]					
0.001	0.0156	0.3972	86.19	0.8619	
0.0001	0.0175	0.4456	84.51	0.8451	
0.00005	0.0209	0.5322	81.50	0.8150	-40.52 (R^2=0.9999)
0.00001	0.0567	1.4438	49.82	0.4982	
0.000005	0.0686	1.7468	39.29	0.3929	
[20]					
0.001	0.0330	0.8403	70.80	0.7080	
0.0001	0.0367	0.9345	67.52	0.6752	-37.88 (R^2=0.9997)
0.00005	0.0433	1.1026	61.68	0.6168	
0.00001	0.0614	1.5635	45.66	0.4566	
0.000005	0.0995	2.5337	11.95	0.1195	
[21]					
0.001	0.0464	1.1815	58.94	0.5894	
0.0001	0.0498	1.2681	55.93	0.5593	-38.75 (R^2=0.9999)
0.00005	0.0605	1.5406	46.46	0.4646	
0.00001	0.0675	1.7188	40.27	0.4027	
0.000005	0.0679	1.7290	39.91	0.3991	

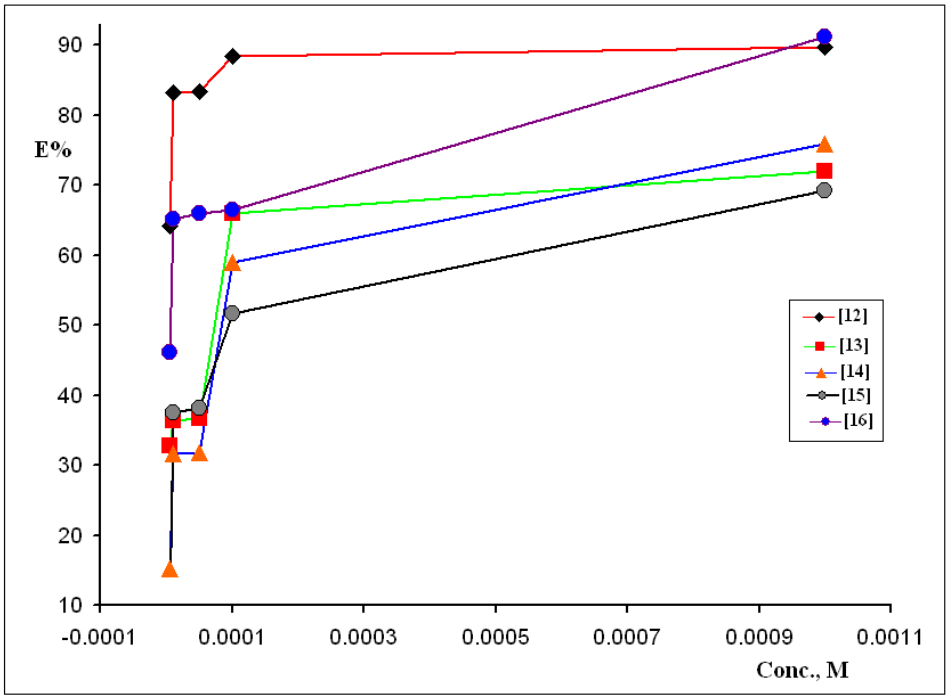

Figure (3-48). Effect of inhibitor concentration on the efficiencies of mild steel obtained at 30°C in 1 M H_2SO_4 containing different concentrations of prepared inhibitors [**12**]-[**16**].

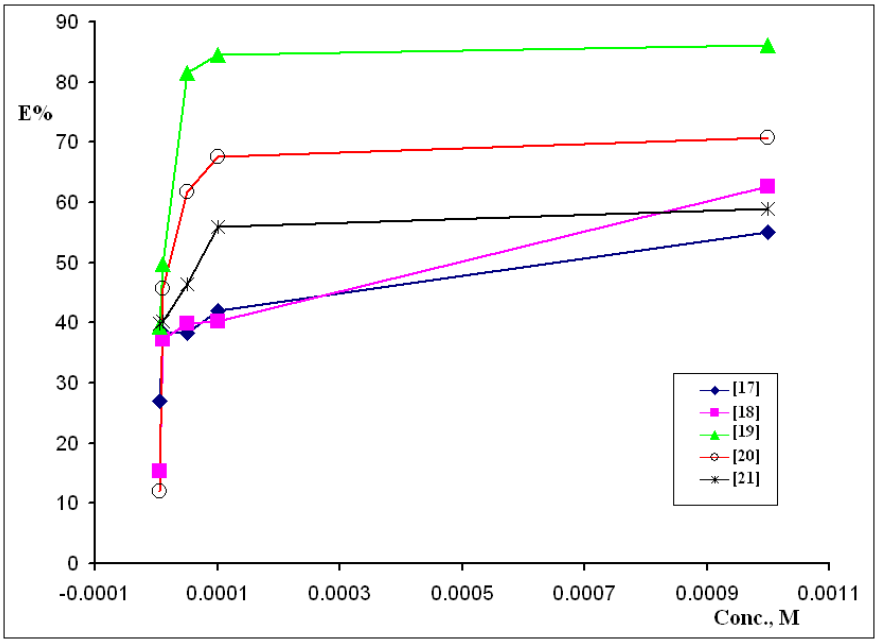

Figure (3-49). Effect of inhibitor concentration on the efficiencies of mild steel obtained at 30°C in 1 M H_2SO_4 containing different concentrations of prepared inhibitors [**17**]-[**21**].

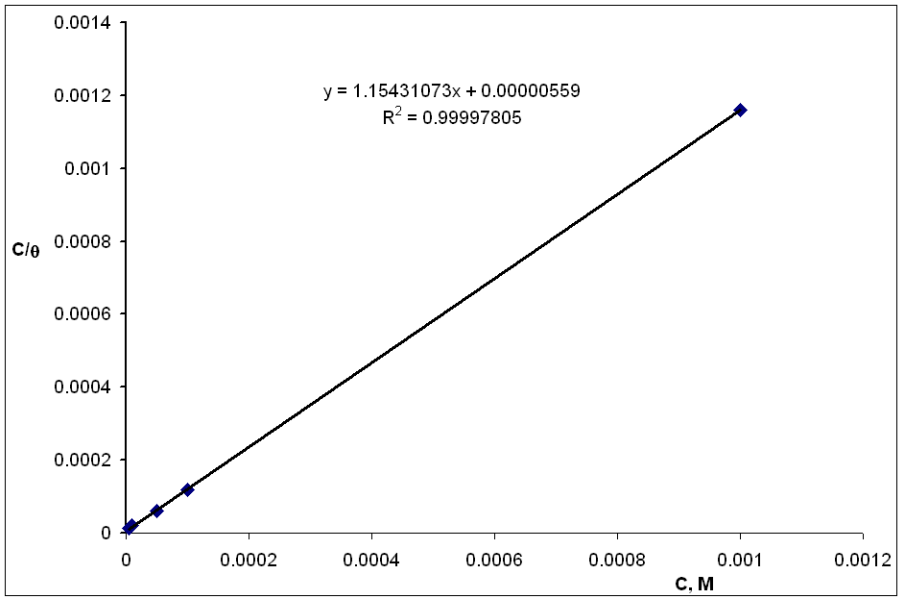

Figure (3-50). Langmuir adsorption isotherm plot for mild steel in 1M H_2SO_4 solution in the presence of various concentrations of inhibitor [**19**].

The anodic dissolution of iron in acidic media and the corresponding cathodic reaction has been reported as follows [97]:

$Fe \rightarrow Fe^{2+} + 2e^-$ (anodic reaction) (3-1)

$2H^+ + 2e^- \rightarrow H_2$ (cathodic reaction) (3-2)

As a result of these reactions, including the high solubility of the corrosion products, the metal loses weight in the solution. Corrosion inhibition of mild steel in 1 M H_2SO_4 by prepared compounds [**1-5**] and [**12-21**] can be explained on the basis of molecular adsorption. The compound inhibits corrosion by controlling both the anodic and cathodic reactions. In acidic solutions the prepared compounds [**1-5**] and [**12-21**]

exist as protonated species. These protonated species adsorb on the cathodic sites of the mild steel and decrease the evolution of hydrogen. The adsorption on anodic sites occurs through π-electron of aromatic ring and lone pair of electrons of nitrogen atom, which decreases anodic dissolution of mild steel [98].

3.6.2. Theoretical calculations:

The purpose of this work is to provide information about the electron configuration of several organic inhibitors by quantum chemical calculations and to investigate the relationship between molecular structure and inhibition efficiency. All the calculations for geometry optimization were performed using the semi-empirical calculations with PM3 method. For this purpose the Hyperchem Program with complete was used. This computational method has been proven to yield satisfactory results [71,72]. The easiest way to compare the inhibition efficiency of compounds [**1**]-[**5**] and compounds [**12**]-[**21**] is to analyze the energies of the highest occupied molecular orbital (HOMO) and the lowest unoccupied molecular orbital (LUMO). The calculated energies E_{HOMO}, E_{LUMO}, energy gap ($\Delta E=E_{LUMO}-E_{HOMO}$) and other indices are given in Tables (3-7) and (3-8).

Table (3-7): Calculated quantum chemical parameters of prepared compounds [**1-5**] as modeling systems by using PM3 method.

Comp. No.	HOMO (eV)	LUMO (eV)	$\Delta E(E_{HOMO}-E_{LUMO})$ (eV)	μ (Debye)	Formal charge		Planarity
					N_{atom} [a]	S_{atom}	
[1]	-8.6986	-1.0319	-7.6667	6.13	-0.138	-0.358	Planar
[2]	-8.5374	-0.9339	-7.6035	7.40	-0.168	-0.328	Semi-planar
[3]	-9.0797	-1.8667	-7.213	0.39	-0.107	-0.328	Planar
[4]	-8.9428	-1.6019	-7.3409	5.54	-0.116	-0.338	Planar
[5]	-8.7146	-0.9378	-7.7768	5.89	-0.167	-0.325	Semi-planar

[a] formal charge of N atom of imine group.

Table (3-8): Calculated quantum chemical parameters of prepared compounds [**12-21**] as modeling systems by using PM3 method.

Comp. No.	HOMO (eV)	LUMO (eV)	$\Delta E(E_{HOMO}-E_{LUMO})$ (eV)	μ (Debye)	Planarity
[12]	-8.9676	-1.6862	-7.2814	3.14	Planar
[13]	-9.2760	-2.1794	-7.0966	5.62	Planar
[14]	-8.4499	-1.5481	-6.9018	4.51	Planar
[15]	-9.2138	-2.0307	-7.1831	7.69	Planar
[16]	-8.8849	-1.6175	-7.2674	6.67	Planar
[17]	-9.1138	-1.7860	-7.3278	2.62	Planar
[18]	-9.4509	-2.2756	-7.1753	4.31	Planar
[19]	-8.4849	-1.6547	-6.8302	4.66	Planar
[20]	-9.4026	-2.1288	-7.2738	6.08	Planar
[21]	-9.0386	-1.7366	-7.3020	2.51	Planar

The energy gap (ΔE) between the HOMO and LUMO energy levels of the molecules is important factor, whereas, low absolute value of the energy gap (ΔE) gives good inhibition efficiencies [(99)]. The compound [**3**] showed lowest energy gap (Table 3-7) that in good agreement experimental results (Table 3-5) whereas, (E%)=70 and also showed chemisorption with value ΔG^{o}_{ads}=-41 kJ/mol [(100)].

Table (3-7) shows different dipole moments for suggested inhibitors [**1**]-[**5**]. The values of dipole moment due to non-uniform distributions of positive and negative charges on the various atoms (Figure(3-51)) and concentration of negative charges on N (C=N) and S atoms for all molecules. Non-uniform distribution of electronic density and planarity of molecule [101] are good factors to improve dipole–dipole interactions of organic molecules and mild steel surface.

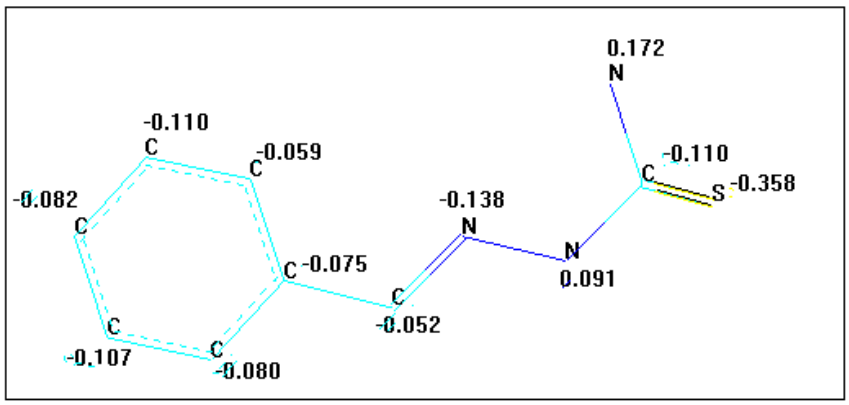

Figure (3-51). Formal charges of compound [**1**].

The compound [**19**] showed lowest energy gap (Table 3-8) that in good agreement experimental results (Table 3-6) whereas, (E%)=86 and also showed chemisorption with value ΔG^{o}_{ads}=-40 kJ/mol [100].

Non-uniform distributions of positive and negative charges on the various atoms (figures (3-52) and (3-53)) and concentration of negative charges on nitrogen atoms and carbon atoms of aromatic rings for all molecules. Non-uniform distribution of electronic density and planarity of molecule [101] are good factors to improve dipole–dipole interactions of organic molecules and mild steel surface.

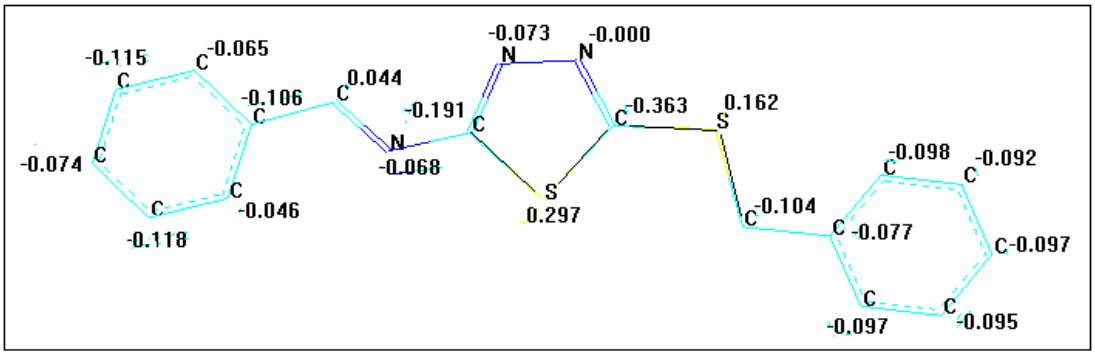

Figure (3-52). Formal charges of compound [**12**].

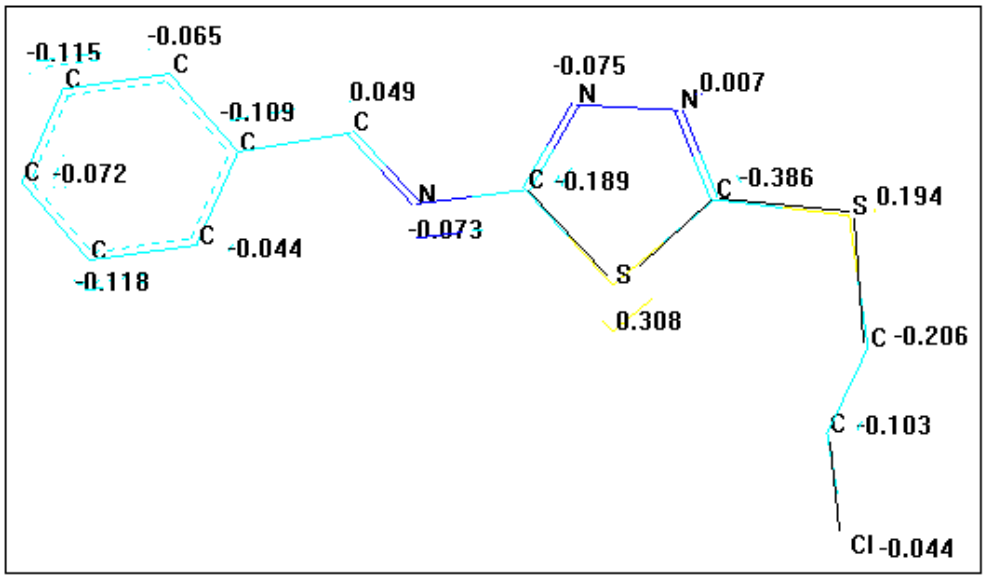

Figure (3-53). Formal charges of compound [**17**].

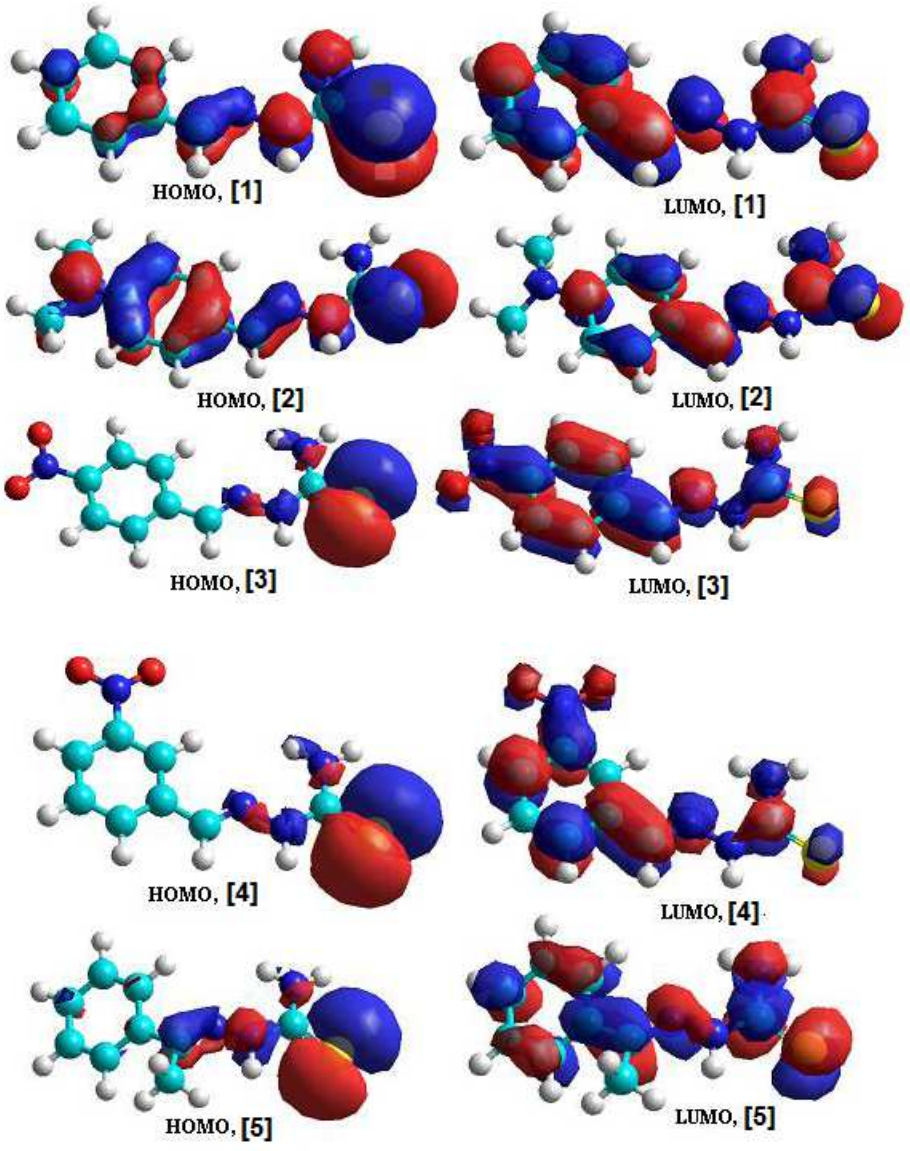

Figure (3-54).The frontier molecular orbital density distributions (HOMO and LUMO) by using PM3 method.

Finally, infinity corrected optical system (polarized microscope) of magnification (×20) of carbon steel specimens immersed in1M H_2SO_4 solution for 8 h (at 30 C˚) in the absence and presence of inhibitor system are shown in Figure (3-54) image (b) and image (c), respectively.


(a)

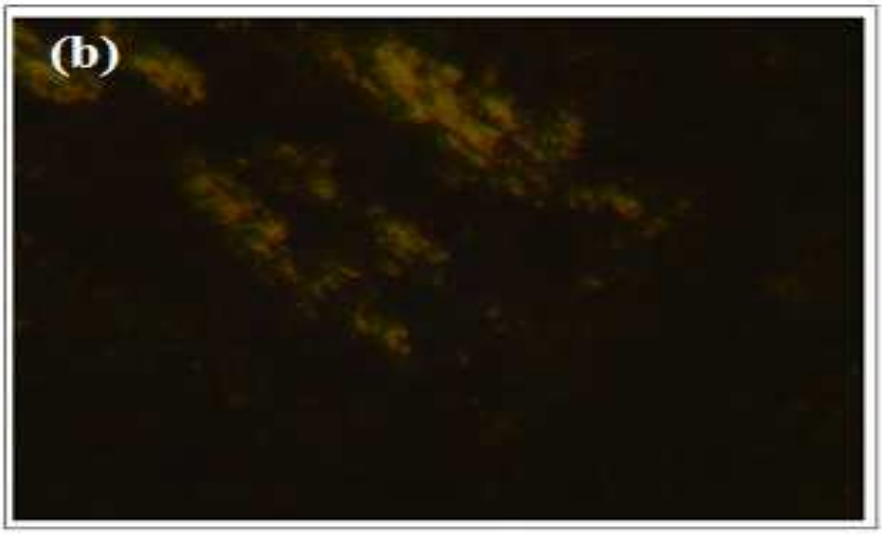
(b)

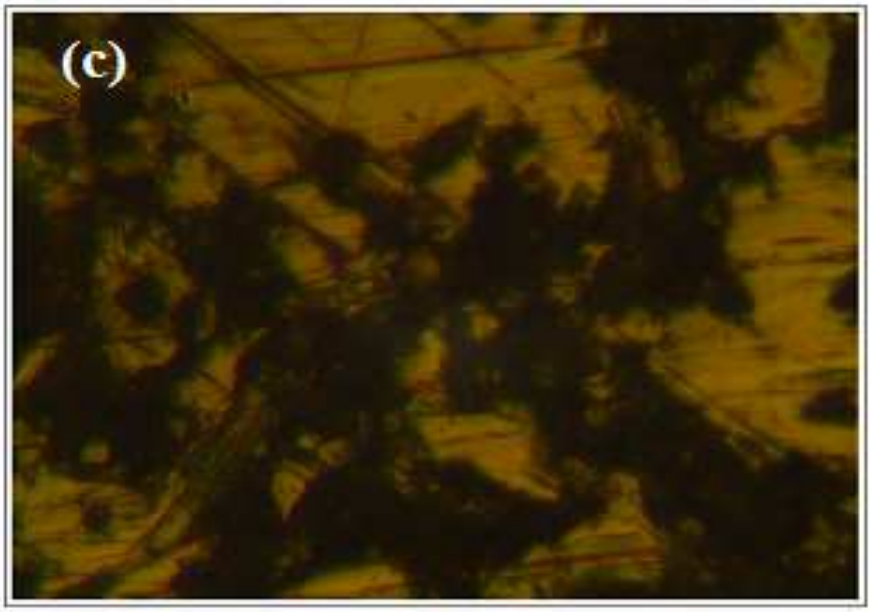

Figure (3-55). Two-dimensional polarized microscope images of the surface of (a) polished mild steel; (b) mild steel immersed in 1M H_2SO_4 solution; (c) mild steel immersed in 1M H_2SO_4 solution containing 1×10^{-3}M of inhibitor [**21**].

Figure (3-55) image (a) shows the smooth surface of the metal. This shows the absence of any corrosion products formed on the metal surface. Figure (3-55) image (b) shows the roughness of the metal surface which indicates the corrosion of mild steel caused by immersing in1M H_2SO_4 solution. Figure (3-55) image (c) indicates that in presence of inhibitor system mixture in1M H_2SO_4, the surface coverage increases which in turn results in the formation of a thin layer of insoluble complex [inhi-Fe^{+2}] on the surface of the metal.

4. Conclusion :

Some organic compounds contain hetero-atoms were prepared and identified by spectroscopic techniques. These organic compounds starting from (E)-2-benzylidene hydrazine carbothioamide [1] to (E)-5-(2-chloro ethyl thio)-N-(1-phenyl ethylidene)-1,3,4-thiadiazole-2-amine [21] contain (N and S atoms) revealed different inhibition efficiencies (physical and chemical adsorptions) for mild steel in 1M H_2SO_4 at 30^oC for 8 hours. Inhibition efficiencies (E%) increase with increasing concentration of inhibitor, while corrosion rate (W) decrease by increasing the concentration of the inhibitor. Theoretical calculations were used as a useful tools to investigate the relationship between molecular structure and inhibition efficiency by using semi-empirical molecular quantum calculations within the PM3 method.

5.Future Work :

1. Preparation of new hetero cyclic compounds derivatives .
2. Applying further methods to study the corrosion inhibitors for mild steel in acidic media and test the inhibition efficiency for these organic compounds.
3. Theoretical calculations will be used as a useful tools to investigate the relationship between molecular structure and inhibition efficiency by using semi-empirical molecular quantum calculations within the PM3 method.

6. References :

1- F. A. Carey, Organic Chemistry, McGraw-Hill, Inc. America, (1980).

2- R. M. Acheson,"An Introduction to the Chemistry of Heterocyclic Compounds", 3, 122,(1989).

3- T. Eicher, S. Hauptmann and A. Speicher,"The Chemistry of Heterocycles", 2nd Edition, Wiley-VCH Veriag GmbH & Co. (2003).

4-R. M. Acheson, An Introduction to the Chemistry of Heterocyclic Compounds, 2nd ed., Wiley International Edition, New York, London (1990).

5- P. V. Rague Schleyer , H. Jiao, Pure Appl. Chem., **1996,** 68, 209.

6- P. S. Fernandes and A. M. Raji, J. Ind. Chem. Soc., **1976**, LIII, 676.

7- M. M. Dutta and B. N. Goswami, J. Ind. Chem. Soc., **1987**, LXIV, 195 .

8- G. S. Gadginamath, S. A. Patil, Ind. J. Chem., **1996**, 35B, 1062 .

9. A. A. Hassan, A. E. Mourad, K. M. El-Shaieb, A. H. Abou-Zeid, J. Heterocycl. Chem., **2006**, 43, 471.

10., A. A. Hassan, N. K. Mohamed, A. M. Shawky, D. A. Döpp, ARKIVOC, **2003**,118-128(i).

11- M. M. Dutta, B. N. Goswami and J. C. S. Kataky, J. Heterocyclic Chem., **1986,** 23, 793.

12-A. K. Mansour, M. M. Eid and N. S. Khalil, Molecules, **1987**, 8, 744.

13- A. K. Sengupta and A. Bhatnagar, J. Ind. Chem. Soc., **1990**, LXIV, 616.

14- E. E. Ebenso, D. A. Isabirye and N. O. Eddy, Int. J. Mol. Sci., **2010**,11, 2473-2498.

15- S. D. Toliwal, J. Kalpesh, T. Pavagadhi, J. Appl. Chem. Research, **2010**, 12, 24-36.

16- J. S. Storm, Advanced in Heterocyclic Chemistry, CA. R. Katrizky and A. B. Bouttan, editors, **1966**, Vol. 9, Academic Press, Inc. New York.

17- C. Ainsworth , J. Am. Chem. Soc. , **1958**, 80 , 5201.

18- T. J. Kress, and S. M. Costantino, J. Heterocycl. Chem., **1980**, 17 , 607 .

19- B. F ö hlisch, R. Braun, and K. W. Schultze, Angew. Chem., Int. Ed. Engl. , **1967**, 6 , 361.

20. N. Demirbas, Euro. J. Med. Chem., **2004**, 39, 793.

21. N. Demirbas, Turk. J. Chem., **2005**, 29, 125-133.

22. A. A. Aly and R. EL-Sayed, Chem. Pap., **2006**, 60 (1), 56-60 .

23- V. Petrow, O. Stephenson, A. J. Thomas and A. M. Wild, J. Chem. Soc., **1958**, 1508.

24. A. A. H. Saeed, J. Chem. Eng. Data, **1984,** 29(3), 359.

25. A. A. H. Saeed and A. Y. Khedar, Canadian J. Appl. Spectroscopy, **1994,** 39(6), 173.

26. U. Casellato, P. Gerriero, S. Tamburini and P. A. Uigato, Inorg. Chem. Acta., **1986,** 75, 119 .

27. J. A. Goodiwn, L. J. Wilson, D. M. Stanbury and R. A. Scott, Inorg. Chem., **1989**, 28, 42.

28. A. A. H. Saeed, M. N. Al-Zagoum and M. H. WAtton, Can. J. Spectroscopy, **1980**, **25**, 137.

29. H. A. Staab and F. Vtigtle, Chem. Ber., **1965**, 98 ,2681.

30- G. G. Mohamed, M. M. Omar, A. M. Hindy, Turk. J Chem., **2006**, 30, 361- 382.

31- B. H. Nabeel and S. T. Farah, Research Journal of Chemical Sciences, June **2012**, Vol. 2(6), 43-49,.

32- Y. Prashanthi and S. Raj, J. Sci. Res., **2010**, 2 (1), 114-126.

33- J. Clayden, N. Greeves, S. Warren and P. Wothers, Organic Chemistry Oxford University Press, USA; 1 edition (2000).

34- T.W. Graham Solomons, C. B. Fryhle, Organic Chemistry, John Wiley & Sons, Inc (2011).

35- L.D. Wade Jr., Organic chemistry, 6th ed., Pearson Education, Inc., USA (2006).

36**.** Ijsseling FP. Survey of Literature on Crevice Corrosion (1979–1998). London: The Institute of Materials, (2000)**.**

37. P. Combrade, Crevice corrosion of metallic materials. In: P. Marcus, editor. Corrosion Mechanisms in Theory and Practice 2nd ed. New York–Basel, Marcel Dekker, (2002**).**

38- E. Ghali, V. S. Sastri and M. Elboujdaini, Corrosion Prevention and Protection, Practical Solutions, Wiley; 1 edition (2007).

39- P. R. Roberge, Handbook of Corrosion Engineering, New York: McGraw-Hill (1977).

40- E. Bardal, Corrosion and Protection (Engineering Materials and Processes), Springer, 1st Edition (2004).

41-D. D. Ebbing and S. D. Gammon, General Chemistry, Houghton Mifflin Company, USA (2009).

42- V. S. Bagotsky**,** Fundamentals of Electrochemistry, USA, John Wiley & Sons (2006).

43- R. C. Ayers Jr. and N. Hackerman, J. Electrochem. *Soc.*, **1963**, 110 , 507.

44- E. Norr, Corros. Sci., **2005**, 47, 33.

45- M. Lagrenee, B. Mernari, M.Bouanis, M. Traisnel, and F. Bentiss, Corros. Sci., **2002**, 44 , 573.

46- F. Bentiss, M. Lagrenee, M. Traisnel, and J.C. Hornez, Corros. Sci., **1999**, 41,789.

47- M. A. Quraishi, and R. Sardar, Corrosion, **2002**, 58 ,748.

48- M. Abdallah, Corros. Sci., **2004**, 46,1981.

49- A. M. Abdel-Gaber, B. A. Abd-El-Nabey, I. M. Sidahmed, A. M. El-Zayady and M. Saadawy, Corros. Sci., **2006**, 48(9), 2765-2779.

50- E. E. Ebenso and U. J. Ekpe, W. Afri, J. Biol. Appl. Chem., **1996**, 41, 21-27.

51- E. Chaieb, A. Bouyanzer, B. Hammouti and M. Benkaddour, J. Appl. Surf. Sci., **2005**, 246, 199-206.

52- M. N. Desai, M. B. Desai, C. B. Shah, S. M. Desai, Corros. Sci., **1986**, 26, 827.

53- H. Shokry, M. Yuasa, I. Sekina, R. M. Issa, H.Y.El. Baradie, G.K. Gomma, Corros. Sci., **1998**, 40, 2173.

54- G. K. Gomma, M. H. Wahdan, Mater. Chem. Phy., **1995**, 39, 209.

55- S. Li, S. Chen, S. Lei, H. Ma, R. Yu and D. Liu, Corros. Sci., **1995**, 41, 2173.

56- S. L. Li., Y.G. Wang, S.H. Chen, R. Yu, S.B. Lei, H.Y. Ma and D.X. Liu., Corros. Sci., **1991**, 41 , 1769.

57- Z. Quan, S. Chan, Y. Li and X. Lui, Corros. Sci., **2002**, 44 ,703.

58- H. Ma, S. Chen, L. Niu, S. Shang, S. Li, S. Zhno and Z. Quan, J. Electrochem., Soc., **2001**, 148, 132.

59- A. K. Singh, M. A. Quraishi, Int. J. Electrochem. Sci., **2012**, 7, 3222 – 3241.

60- S. Chitra , K. Parameswari1and A. Selvaraj , Int. J. Electrochem. Sci., **2010**, 5, 1675 – 1697.

61- K. F. Khaled, A. El-mghraby, O. B. Ibrahim, O. A. Elhabib and M. A. M. Ibrahim, J. Mater. Environ. Sci., **2010**, 1(3), 139-150.

62- M. Z. A. Rafiquee, S. Khan, N. Saxena and M. A. Quraishi, Portugaliae Electrochimica Acta, **2007**, 25, 419-434.

63- G. F. Mars, Corrosion Engineering, 3rd ed., McGraw-Hill, New York (1986).

64- A. W. Adamson, and A. B. Gast, Physical Chemistry of surfaces, 6th ed., Wiley-interscience, New York (1997).

65-L. Ferrari, J. Kaufmann, F. Winnefeld, and J. Plank, J. Colloid Interface Sci., **2010**, 347 (1), 15–24.

66- J. Y. N. Philip, J. Buchweishaija and L. L. Mkayula, Tanzania J. Sci., **2002**, 28(2),105-116.

67- F. Jensen, Introduction to Computational Chemistry, Wiley, New York (1999).

68- J. Stewart. J. Comp. Chem., **1989**, 10, 209.

69- G. Bereket, C. Ogretir, A. Yurt, J. Mol. Struct. (THEOCHEM), **2001**, 571, 139.

70- G. Bereket, C. Ogretir, E. Hur, J. Mol. Struct. (THEOCHEM), **2002**, 578, 79.

71- N. O. Eddy, B. I. Ita and E. E. Ebenso, Int. J. Electrochem. Sci., **2011,** 6, 2101-2121.

72- S. M. Quraishi, M. A. Quraishi, and R. Quraishi, Open Corros. J., **2009**, 2, 83-87.

73- R. M. Issa, A. M. Khedr and H. Rizk, J. Chin. Chem. Soc., **2008**, 55, 875-884.

74- A. I. Vogel, A. R. Tatchell, B. S. Furnis, A. J. Hannaford and P. W. G. Smith, Vogel's Textbook of Practical Organic Chemistry, Prentice Hall, 5 edition, pp.1160 (1996).

75- ASTM G 31 – 72, “Standard Practice for labortary Immersion Corrosion Testing of Metals”, West Conshohocken, PA, ASTM (1990).

76- M. Ajmal, A. S. Mideen and M. A. Quraishi, Corros. Sci., **1994**, 36, 79.

77- R. Agrawal, T.K.G. Namboodhiri, Corros. Sci., **1990**, 30, 37.

78- Stewart, J. P. James, J. Comput. Chem., **1989**, 10 (2), 209.

79- HyperChem, version 7.5, z Hypercube, Inc.: Gainesville, FL, USA, 2002.

80- L. G. Wade, Organic chemistry, Pearson Education, Inc., Pearson Prentice Hall (2006).

81- D. L. Pavia, G. M. Lampman and G. S. Kriz, Introduction to Spectroscopy, Brooks Cole; 3rd edition (2000).

82- H. K. Adli, W. M. Khairul and H. Salleh, Int. J. Electrochem. Sci., **2012**, 7, 499 – 515.

83- S. Bige, Z. Kilici, Z. Hayvali, T. Hokelek and S. Safran, J. Chem. Sci., **2009**, Vol. 121 , 989–1001.

84- C. N. R. Rao, UV and Visible Spectroscopy Chemical Applications, London, Butterworths (1961).

85- M. R. Christie, Color Chemistry, Royal Society of Chemistry (2001).

86- P. S. Kalsi, Spectroscopy of Organic Compounds, John Wiley & Sons (Asia) Pte Ltd. (1995).

87- R. J. Cremlyn, An Introduction to Organosulfur Chemistry, John Wiley & Sons Ltd. (1996).

88- K. M. Daoud, A. W. Al-Obaydi and M.J. Mohammed, Nat. J. Chemistry, **2008**, Volume 31, 531-542.

89. A. K. Gupta and H. K. Mishra, J. Indian Chem. Soc., **1981,** LVIII , 508.

90. N. S. Cho and G. N. Kim, J. Heterocyclic Chem., **1993,** 30, 397.

91. S. G. AL-Bajalany, Ph.D.Thesis, University of Tikrit (2005).

92. J. P. Henichart, H. Rymond and L. Brigite, J. Heterocyclic Chem., **1977**, 14(4), 615-619.

93- L. D. Field, S. Sternhell and J. R. Kalman, Organic Structures from Spectra ,fourth edition , John Wiley & Sons Ltd. (2007).

94- M. S. Zakerhamidi, A. Ghanadzaheh and M. Moghadam, Chem. Sci. Transactions, **2012**, 1(1)**,** 1-8.

95- S. A. Umoren , I. B. Obot, E.E. Ebenso, N.O. Obi-Egbedi, Port. Electrochim. Acta, **2008**, 26, 199.

96-S. A. Umoren, I.B. Obot, E.E. Ebenso and P.C. Okafor, Port. Electrochim. Acta, **2008,** 26, 267.

97- M. A. Amin, K. F. Khaled, , Corros. Sci., **2010,** 52**,** 1762–1770.

98- S. K. Shukla, I. Ahamad, M. A. Quraishi, Materials Letts., **2009**, Vol. 63, 819–822.

99- M. M. El-Naggar, Corros. Sci., **2007**, 49, 2226-2236 .

100- F. Bentiss , M. Lebrini, M. Lagren´ee, M. Traisnel, A. Elfarouk, H. Vezin, Electrochim. Acta, **2007**, 52, 6865-6872.

101- I. B. Obot, N.O. Obi-Egbedi, Surf. Rev. Lett., **2008**, 15(6), 903-910.

Summary

1- This work involves preparation of some organic compounds contain hetero-atoms, that starting from (E)-2-benzylidene hydrazine carbothioamide [**1**] to (E)-5-(2-chloro ethyl thio)-N-(1-phenyl ethylidene)-1,3,4-thiadiazol-2-amine [**21**], are summarized below:

- First set of organic compounds was prepared in one step by a condensation reaction between the carbonyl group of aldehydes or ketones and the amino group of Thiosemicarbazide derivatives to produce the compounds:

[**1**]- (E)-2-benzylidene hydrazine carbothioamide.

[**2**]- (E)-2-(4-nitro benzylidene) hydrazine carbothioamide.

[**3**]- (E)-2-(4-(dimethyl amino) benzylidene) hydrazine carbothioamide.

[**4**]- (E)-2-(3-nitro benzylidene) hydrazine carbothioamide.

[**5**]-(z)-2-(1-phenyl ethylidene) hydrazine carbothioamide.

- Second set of organic compounds was prepared by reaction of 5-amino-2-thiol-1,3,4-thadiazole in two steps: i) a condensation reaction between the carbonyl group of aldehydes or ketone and the amino group; ii) an alkylation reaction between (benzyl chloride or 1,2-dichloro ethane) and thiol group to yield the following compounds:

[**12**]-(E)-N-benzylidene-5-(benzyl thio)-1,3,4-thiadiazol-2-amine.

[**13**]-(E)-5- (benzylthio)-N-(4-nitro benzylidene)-1,3,4-thiadiazol-2-amine.

[**14**]-(E)-5-(benzylthio)-N-(4-(dimethyl amino) benzylidene)-1,3,4-thiadiazol-2-amine.

[**15**]-(E)-5- (benzylthio)-N-(3-nitro benzylidene)-1,3,4-thiadiazol-2-amine.

[**16**]-(E)-5-(benzylthio)-N-(1-phenyl ethylidene)-1,3,4-thiadiazol-2-amine.

[**17**]-(E)-N-benzylidene-5-(2-chloro ethylthio)-1,3,4-thiadiazol-2-amine.

[**18**]-(E)-5-(2-chloro ethylthio)-N-(4-nitro benzylidene)-1,3,4-thiadiazol-2-amine**.**

[**19**]-(E)-5-(2-chloro ethylthio)-N-(4-(dimethyl amino) benzylidene)-1,3,4-thiadiazol-2-amine.

[**20**]- (E)-5-(2-chloro ethylthio)-N-(3-nitro benzylidene)-1,3,4-thiadiazol-2-amine.

[**21**]-(E)-5-(2-chloro ethylthio)-N-(1-phenyl ethylidene)-1,3,4-thiadiazol-2-amine.

2- The prepared compounds were identified by melting points, F.T.I.R, UV-visible and ^{1}H-NMR spectroscopy and the result obtained are compatible the structures assigned to these compounds.

3- The above organic compounds which contain hetero-atoms were used as corrosion inhibitors for mild steel in 1M H_2SO_4 at 30^{o}C. Weight loss regards as evaluation method to test the inhibition efficiency of the above compounds. Tables (3-5) and (3-6) indicates that the protection efficiency E (%) increases with increasing the concentration of suggested inhibitors with the maximum inhibition efficiencies were achieved at 10^{-3} M.

4- Theoretical calculations to investigate the relationship between molecular structure and inhibition efficiency by using semi-empirical

molecular quantum calculations within the PM3 method as implemented in HyperChem package.

The preparation steps of the compounds [1-21] can be represented as shown in the following scheme:

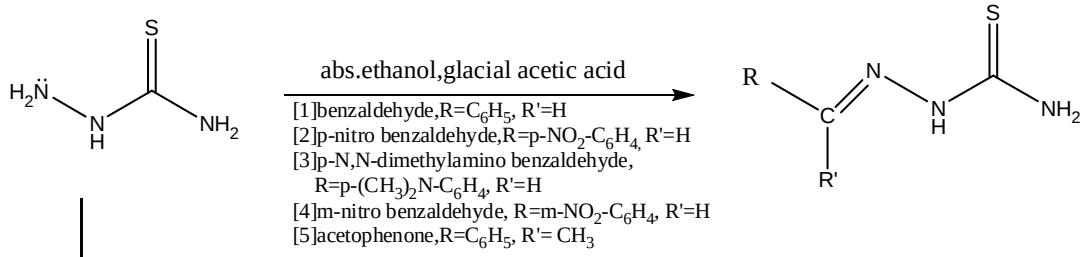

[1]benzaldehyde,R=C_6H_5, R'=H
[2]p-nitro benzaldehyde,R=p-NO_2-C_6H_4, R'=H
[3]p-N,N-dimethylamino benzaldehyde,
R=p-$(CH_3)_2$N-C_6H_4, R'=H
[4]m-nitro benzaldehyde, R=m-NO_2-C_6H_4, R'=H
[5]acetophenone,R=C_6H_5, R'= CH_3

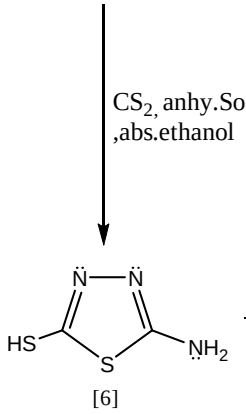

[6]

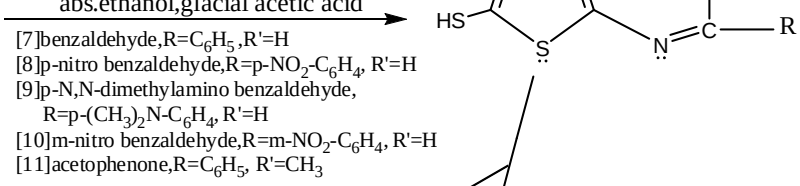

[7]benzaldehyde,R=C_6H_5,R'=H
[8]p-nitro benzaldehyde,R=p-NO_2-C_6H_4, R'=H
[9]p-N,N-dimethylamino benzaldehyde,
R=p-$(CH_3)_2$N-C_6H_4, R'=H
[10]m-nitro benzaldehyde,R=m-NO_2-C_6H_4, R'=H
[11]acetophenone,R=C_6H_5, R'=CH_3

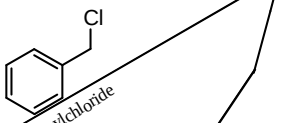

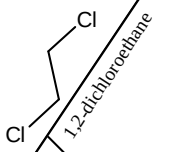

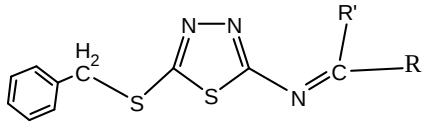

[12]benzaldehyde,R=C_6H_5, R'=H
[13]p-nitro benzaldehyde,R=p-NO_2-C_6H_4,R'=H
[14]p-N,N-dimethylamino benzaldehyde,
R=p-$(CH_3)_2$N-C_6H_4, R'=H
[15]m-nitro benzaldehyde,R=m-NO_2-C_6H_4, R'=H
[16]acetophenone, R=C_6H_5, R'=CH_3

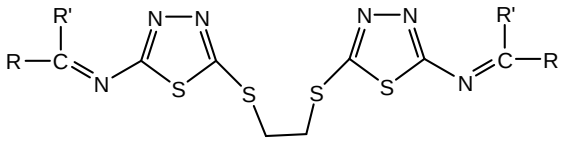

[22]benzaldehyde,R=C_6H_5, R'=H
[23]p-nitro benzaldehyde,R=p-NO_2-C_6H_4,R'=H
[24]p-N,N-dimethylamino benzaldehyde,
R=p-$(CH_3)_2$N-C_6H_4, R'=H
[25]m-nitro benzaldehyde,R=m-NO_2-C_6H_4, R'=H
[26]acetophenone, R=C_6H_5, R'=CH_3

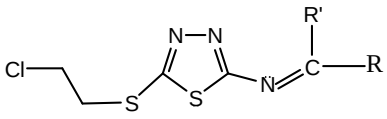

[17]benzaldehyde,R=C_6H_5, R'=H
[18]p-nitro benzaldehyde,R=p-NO_2-C_6H_4,R'=H
[19]p-N,N-dimethylamino benzaldehyde,
R=p-p-$(CH_3)_2$N-C_6H_4, R'=H
[20]m-nitro benzaldehyde,R=m-NO_2-C_6H_4, R'=H
[21]acetophenone, R=C_6H_5, R'=CH_3

الإهداء

إلى نور الهدى... ومقلة العيون الحبيب المصطفى (ص)

إلى من أوقد لي شموع الحياة لينير لي دربي والدي العزيز

إلى نبع حياتي ومن ترسم لي الأمل كلما وهن العزم والدتي العزيزة

إلى ابتسامة حياتي ومعنى وجودي أخي وأخواتي

إلى الأختين اللتين لم تلدهما لي أ مي تماره وزمن

إلى رفاقي في كل دروب العلم المتباينة زملائي الاعزاء

إلى كل قلب خفق حبا وخوفا علي أهدي ثمرة جهدي هذا

بان ٢٠١٣

CHAPTER ONE

INTRODUCTION

CHAPTER TWO

EXPERIMENTAL
Part

CHAPTER THREE

RESULTS AND DISCUSSION

REFERENCES

Republic of Iraq
Ministry of Higher Education and Scientific Research
Al-Nahrain University
College of Science
Department of Chemistry

Preparation of some Organic Compounds contain Hetero- atoms as Corrosion Inhibiters for Mild Steel in Acidic Media.

A Thesis submitted to the College of Science Al-Nahrain University in partial Fulfillment of the requirements for the Degree Of Master of Science in Chemistry
By

Ban Ameen Abd-al-Jabbar
B.Sc.2010
(Al-Nahrain University)

Supervised By
Dr. Mahdi S. Shihab

2013 *1434*

Acknowledgement

First of all, I thank Allah for helping me to overcome difficult that stood in my way during the research.

I would like to address my sincere gratitude to the persons who have accompanied me along the course and those who have been there by the side to support me.

My supervisor ***Dr. Mehdi S. Shihab*** *for his supervision, continuous encouragement, advice, discussion and suggestions throughout my study.*

I would like to express my special thanks to my ***parents****, my* ***sisters*** *and my* ***brother*** *for their invaluable support and encouragement.*

Also I would like to direct my deep thanks to ***Dr. Ahmed Abd al-Razzaq****,* ***Dr. Nasreen R. Jber, Mrs. Rasha Saad Jwad*** *(Al-Nahrain university, college of science, department of chemistry) for their very helpful discussion and corporation and for their invaluable support to achieve this research and* ***Dr. Adnan Ibrahim*** *(Karbala University, college of science, department of chemistry), for his efforts.*

Also, my gratitude to all my friends, especially, Tamara Sami, Marwa Hameed, Hanan Hussain, Alaa Adnan, Mohammed Muayed.

I am most grateful for assistance given to me by the staff of Chemistry Department of Al- Nahrain University.

Ban 2013

Contents

List of Abbreviations

FTIR	Fourier Transform infrared
^{1}H-NMR	Proton Nuclear Magnetic Resonance
M.P.	Melting point
M.W.	Molecular weight
W	Corrosion rate
ΔM	Mass Loss
S	Area
T	immersion period
E%	percentage inhibition efficiency
θ	degree of surface coverage
K_{ads}	equilibrium constant of the adsorption/desorption process
C	inhibitor concentration (M) in the test solution.
ΔG^{o}_{ads}	standard free energy of adsorption
E_{HOMO}	energy of the highest occupied molecular orbital

E_{LUMO}	energy of the lowest unoccupied molecular orbital
ΔE	energy gap between LUMO and HOMO
DMSO	Dimethyl Sulfoxide
EtOH	Ethanol

List of Tables

List of Figures

بِسْمِ ٱللَّهِ ٱلرَّحْمَٰنِ ٱلرَّحِيمِ

نرفع درجات من نشاء
وفوق كل ذي علم عليم

صدق الله
العظيم

سورة يوسف
- جزء من الآية ٧٦

العراق
وزارة التعليم العالي والبحث العلمي
كلية العلوم /جامعة النهرين
قسم الكيمياء

تحضير بعض المركبات العضوية الحاوية على ذرات غير متجانسة ودراسة كفاءتها على تثبيط تأكل الحديد الصلب في الاوساط الحامضية

رسالة
مقدمة إلى كلية العلوم -جامعة النهرين
وهي جزء من متطلبات نيل درجة الماجستير في الكيمياء

من قبل

بان أمين عبدالجبار

بكلوريوس 2010 (جامعة النهرين)

بأشراف

د. مهدي صالح شهاب

1434 *2013*

الخلاصة

١-هذا العمل يتضمن تحضير بعض المركبات العضوية الحاوية على ذرات غير متجانسة ابتداء من المركب ٢- بنزلدين هايدرازين كاربون ثايو امايد[١] و انتهاء بالمركب ٥-(٢- كلورو اثيل ثايو)-N-(١- فنيل اثيليدين)- ١، ٣،٤- ثايادايازول -٢- امين [21] كما موضح في ما يلي :

- المجموعة الاولى من هذه المركبات العضوية تم تحضيرها بخطوة واحدة من خلال تفاعل التكثيف بين مجموعة الكاربونيل للالديهايدات او الكيتون ومجموعة الامين للثايوسيمي كارباز ايد حتى تنتج المركبات التالية :

[١]-٢- بنزلدين هايدرازين كاربوثايوامايد.

[٢]-٢-(٤- نايتروبنزلدين) هايدرازين كاربوثايوامايد.

[٣]-٢-(٤- (داي مثيل امينو) بنزلدين) هايدرازين كاربوثايوامايد.

[٤]-٢-(٣- نايتروبنزلدين) هايدرازين كاربوثايوامايد.

[٥]-٢-(١- فنيل اثيليدين) هايدرازين كاربوثايوامايد.

- المجموعة الثانية من هذه المركبات العضوية تم تحضيرها من خلال تفاعل ٥- امينو - ٢- ثايول -١، ٣، ٤ - ثايادايازول بخطوتين :

i) تفاعل تكثيف بين مجموعة الكاربونيل للالديهايدات او الكيتون ومجموعة الامين .

ii) تفاعل الكلة بين (بنزيل كلورايد او ١، ٢ – داي كلورو ايثان) ومجموعة الثايول لتكوين المركبات التالية :

[١٢]- N - بنزلدين –٥ – (بنزيل ثايو) -١ ، ٣ ، ٤ – ثايادايازول - ٢ - امين.

[١٣] -٥ - (بنزيل ثايو) -N-(4 - نايترو بنزلدين)-١، ٣، ٤- ثايادايازول- ٢ - امين.

[١٤]-٥ - (بنزيل ثايو) -N-(4 -(داي مثيل امينو) بنزلدين)-١، ٣، ٤- ثايادايازول - ٢ – امين.

[١٥]-٥ - (بنزيل ثايو) -N-(3 - نايترو بنزلدين)-١، ٣، ٤- ثايادايازول - ٢ - امين.

[١٦]-٥ - (بنزيل ثايو) –N-(١- فنيل اثيليدين) -١ ، ٣ ، ٤ – ثايادايازول - ٢ - امين.

[١٧] -N- بنزلدين –٥ – (٢-كلورواثيل ثايو) -١ ، ٣ ، ٤ – ثايادايازول - ٢ – امين.

[١٨]-٥ - (٢-كلورو اثيل ثايو) -N-(٤- نايترو بنزلدين)١، ٣ ، ٤ – ثايادايازول - ٢ - امين.

[١٩]-٥ - (٢- كلورو اثيل ثايو) N-(4 -(داي مثيل امينو)بنزلدين) -١ ، ٣ ، ٤ – ثاياديازول-٢-امين.

[٢٠]-٥ -(٢- كلورو اثيل ثايو)- N-(٣- نايترو بنزلدين) -١ ، ٣ ، ٤ – ثاياديازول - ٢ –امين.

[٢١]-٥ - (٢-كلورواثيل ثايو) -N -(١- فنيل اثيليدين) -١ ، ٣ ، ٤ – ثاياديازول - ٢ - امين.

٢- تشخيص المركبات اعلاه من خلال قياس درجات الانصهار ، طيف الاشعة فوق الحمراء وتقنية الاشعة المرئية والغير مرئية.

٣- المركبات العضوية اعلاه الحاوية على ذرات غير متجانسة تم استخدامها كمثبطات لتأكل الحديد الصلب في محلول حامض الكبريتيك بتركيز ١ مولاري وبدرجة حرارة ٣٠ مئوية . الخسارة بالوزن تعتبر طريقة تقييم لأختبار كفاءة التثبيط للمركبات اعلاه .

٤- الحسابات النظرية تم حسابها لغرض البحث عن العلاقة بين التركيب الجزيئي وكفاءة التثبيط من خلال استعمال حسابات ميكانيك الكم التجريبية PM3 ضمن برنامج HYPERCHEM.

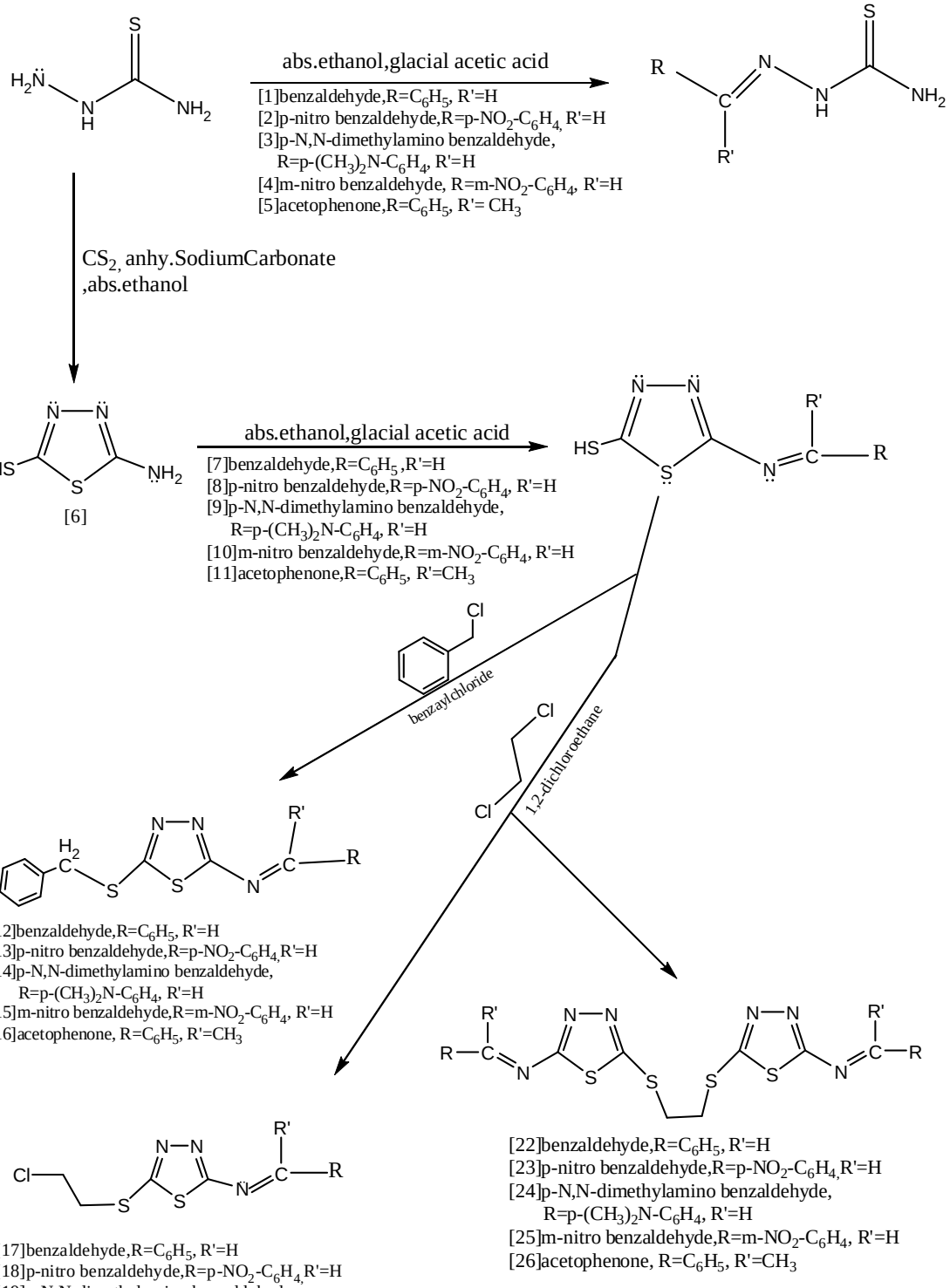
abs.ethanol,glacial acetic acid
[1]benzaldehyde,R=C6H5, R'=H
[2]p-nitro benzaldehyde,R=p-NO2-C6H4, R'=H
[3]p-N,N-dimethylamino benzaldehyde,
R=p-(CH3)2N-C6H4, R'=H
[4]m-nitro benzaldehyde, R=m-NO2-C6H4, R'=H
[5]acetophenone,R=C6H5, R'= CH3
CS2, anhy.SodiumCarbonate
,abs.ethanol
[6]
abs.ethanol,glacial acetic acid
[7]benzaldehyde,R=C6H5,R'=H
[8]p-nitro benzaldehyde,R=p-NO2-C6H4, R'=H
[9]p-N,N-dimethylamino benzaldehyde,
R=p-(CH3)2N-C6H4, R'=H
[10]m-nitro benzaldehyde,R=m-NO2-C6H4, R'=H
[11]acetophenone,R=C6H5, R'=CH3
benzaylchloride
1,2-dichloroethane
[12]benzaldehyde,R=C6H5, R'=H
[13]p-nitro benzaldehyde,R=p-NO2-C6H4,R'=H
[14]p-N,N-dimethylamino benzaldehyde,
R=p-(CH3)2N-C6H4, R'=H
[15]m-nitro benzaldehyde,R=m-NO2-C6H4, R'=H
[16]acetophenone, R=C6H5, R'=CH3
[17]benzaldehyde,R=C6H5, R'=H
[18]p-nitro benzaldehyde,R=p-NO2-C6H4,R'=H
[19]p-N,N-dimethylamino benzaldehyde,
R=p-p-(CH3)2N-C6H4, R'=H
[20]m-nitro benzaldehyde,R=m-NO2-C6H4, R'=H
[21]acetophenone, R=C6H5, R'=CH3
[22]benzaldehyde,R=C6H5, R'=H
[23]p-nitro benzaldehyde,R=p-NO2-C6H4,R'=H
[24]p-N,N-dimethylamino benzaldehyde,
R=p-(CH3)2N-C6H4, R'=H
[25]m-nitro benzaldehyde,R=m-NO2-C6H4, R'=H
[26]acetophenone, R=C6H5, R'=CH3